

AD-A172 287

END-POINT CONTROL OF FLEXIBLE MANIPULATORS(U) STANFORD

1/2

UNIV CA DEPT OF AERONAUTICS AND ASTRONAUTICS

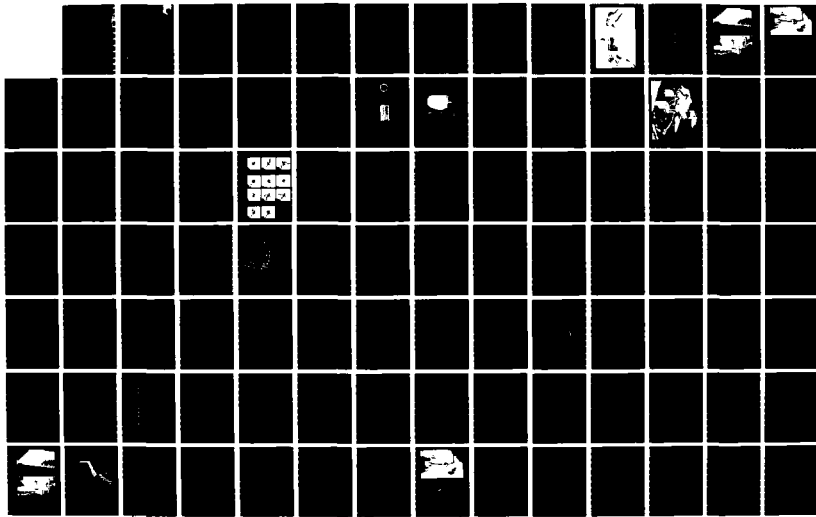
R H CANNON ET AL. SEP 86 AFWL-TR-86-4051

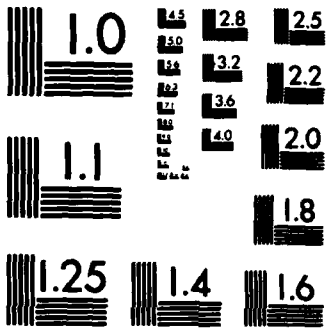
UNCLASSIFIED

F33615-82-K-5108

F/G 5/8

NL



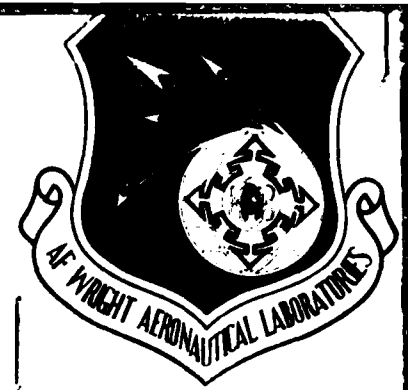


105

AD-A172 287

AFWAL-TR-86-4051

①



END POINT CONTROL OF FLEXIBLE MANIPULATORS

Robert H. Cannon  
Thomas O. Binford

Stanford University  
Department of Aeronautics and Astronautics  
Durand 250  
Stanford, California 94305

September 1986

Final Report for Period September 1984 - August 1985

Approved for public release; distribution is unlimited

DTIC  
ELECTE  
SEP 29 1986  
S D  
B

DTIC FILE COPY

MATERIALS LABORATORY  
AIR FORCE WRIGHT AERONAUTICAL LABORATORIES  
AIR FORCE SYSTEMS COMMAND  
WRIGHT-PATTERSON AIR FORCE BASE, OHIO 45433-6533

86 9 25 0 31

NOTICE

When Government drawings, specifications, or other data are used for any purpose other than in connection with a definitely related Government procurement operation, the United States Government thereby incurs no responsibility nor any obligation whatsoever; and the fact that the government may have formulated, furnished, or in any way supplied the said drawings, specifications, or other data, is not to be regarded by implication or otherwise as in any manner licensing the holder or any other person or corporation, or conveying any rights or permission to manufacture, use, or sell any patented invention that may in any way be related thereto.

This technical report has been reviewed and is approved for publication.



TED J. BRANDEWIE  
Project Manager  
Computer Integrated Mfg Branch

12 Sept 86

FOR THE COMMANDER



WALTER H. REIMANN  
Acting Chief  
Computer Integrated Mfg Branch

If your address has changed, if you wish to be removed from our mailing list, or if the addressee is no longer employed by your organization please notify AFWAL/MLTC, Wright-Patterson AFB OH 45433-6523 to help maintain a current mailing list.

Copies of this report should not be returned unless return is required by security considerations, contractual obligations, or notice on a specific document.

UNCLASSIFIED

SECURITY CLASSIFICATION OF THIS PAGE

AD-A172287

## REPORT DOCUMENTATION PAGE

1a. REPORT SECURITY CLASSIFICATION <b>UNCLASSIFIED</b>		1b. RESTRICTIVE MARKINGS	
2a. SECURITY CLASSIFICATION AUTHORITY		3. DISTRIBUTION/AVAILABILITY OF REPORT	
2b. DECLASSIFICATION/DOWNGRADING SCHEDULE		Approved for public release; distribution is unlimited.	
4. PERFORMING ORGANIZATION REPORT NUMBER(S)  SP0 Reference 13389-01-00		5. MONITORING ORGANIZATION REPORT NUMBER(S)  AFWAL-TR-86-4051	
6a. NAME OF PERFORMING ORGANIZATION  Stanford University	6b. OFFICE SYMBOL (If applicable)	7a. NAME OF MONITORING ORGANIZATION Air Force Wright Aeronautical Laboratories Materials Laboratory (AFWAL/MLTC)	
6c. ADDRESS (City, State and ZIP Code) Dept. of Aeronautics and Astronautics Durand 250 Stanford, CA 94305		7b. ADDRESS (City, State and ZIP Code)  Wright-Patterson AFB, OH 45433-6533	
8a. NAME OF FUNDING/SPONSORING ORGANIZATION  DARPA	8b. OFFICE SYMBOL (If applicable)	9. PROCUREMENT INSTRUMENT IDENTIFICATION NUMBER  F33615-82-K-5108	
8c. ADDRESS (City, State and ZIP Code) Air Force Wright Aeronautical Lab Materials Laboratory Wright-Patterson AFB OH 45433-6533		10. SOURCE OF FUNDING NOS.	
11. TITLE (Include Security Classification) End Point Control of Flexible Manipulators		PROGRAM ELEMENT NO. 61102F	PROJECT NO. 2306
12. PERSONAL AUTHOR(S) Professor Robert H. Cannon, Professor Thomas O. Binford		TASK NO. A3	WORK UNIT NO. Completed
13a. TYPE OF REPORT Final	13b. TIME COVERED FROM 9/1/84 TO 8/30/85	14. DATE OF REPORT (Yr., Mo., Day) September 1986	15. PAGE COUNT 128
16. SUPPLEMENTARY NOTATION			
17. COSATI CODES		18. SUBJECT TERMS (Continue on reverse if necessary and identify by block number)	
FIELD	GROUP	SUB. GR.	Intelligence, manipulators, sensing, control, end-point, sensors, flexible manipulators, force control, control, algorithms, adaptive control.
13	08		
09	02		
19. ABSTRACT (Continue on reverse if necessary and identify by block number)			
<p>This document reports progress for the third and final year of the DARPA Contract. Objectives of this research were:</p> <ul style="list-style-type: none"> <li>- First, to increase the speed and precision of performing "slew and touch" tasks for a flexible robot arm.</li> <li>- Second, to develop a universal robot end effector, capable of performing generic manipulation functions.</li> </ul> <p>This research focuses on the following advances toward the next generation of intelligent robots, force sensing and control, enhanced motion capability, improved performance in moving heavy loads at high speed and high level language command of generic motions.</p> <p>We have achieved essentially all of the contract's formal Statement-of-Work goals, and additional ones as well.</p>			
20. DISTRIBUTION/AVAILABILITY OF ABSTRACT UNCLASSIFIED/UNLIMITED <input type="checkbox"/> SAME AS RPT. <input checked="" type="checkbox"/> DTIC USERS <input type="checkbox"/>		21. ABSTRACT SECURITY CLASSIFICATION  UNCLASSIFIED	
22a. NAME OF RESPONSIBLE INDIVIDUAL  T. Brandewie		22b. TELEPHONE NUMBER (Include Area Code)  (513) 255-7371	22c. OFFICE SYMBOL  AFWAL/MLTC

Block 19 Continued

An experimental system was built around a dextrous three-finger hand, sensors, computer interfaces, and control system. The hand enables generic motions: stable grasping, delicate force control, fine motion and repositioning of objects. An initial analysis of force control was implemented in a hierarchical control system. Generic task operations were decomposed into generic motions of objects, elemental rotations and translations. These elemental motions form a complete set which will be implemented in the course of the research. Coordinated, three-finger motion was implemented for one of these elemental rotations. Tendon tension sensors support force control. An 8 X 8 array of tactile sensors was developed to provide force and location sensing for each finger. Touch sensor technology is based on a continuum mechanics analysis of force measurement. A multi-microprocessor system is under construction to provide increased computation power, improved real-time response, and improved communication.

Using a very flexible manipulator arm, we have accomplished rapid slew-and-touch, without pause, to a moving target. We have established the absolute physical limits on slew velocity and control speed, and have achieved performance near these limits; and we have demonstrated smooth switching through end-point position control and end-point force control. To do this we developed both a simple end-point force sensor and an optical position-sensing system for both the end-point of the manipulator and the target.

Next, using the flexible arm with a fast attached wrist (a two link system) we have also demonstrated fast slew and touch, and have shown that the high-speed wrist control makes possible quite exquisite control of the force at the fingertip; despite rapid speed of contact, force level can be maintained precisely at the specified value, without force overshoot.

Our first lightweight two-link arm with flexible tendons has now been controlled using both conventional collocated joint-angle sensors and using new end-point position control; and the superiority of the latter has been shown. We are now in a position to develop end-point force control for this two-input two-output system.

Proceeding from our experience with the single two-link arm, we have completed design of a system of two cooperating two-link arms, each fitted with a three-axis wrist and gripping system. We will begin construction of this experimental system (in new laboratory space) in the next phase of our DARPA-supported research.

Distribution Statement A is correct for this report.

Per Mr. T. Brandewie, AFWAL/MLTC



This is the final version of this report.  
Per Mr. T. Brandewie, AFWAL/MLTC

Accession No.	
NTIS	<input checked="" type="checkbox"/>
DTIC	<input type="checkbox"/>
DAVIDSON	<input type="checkbox"/>
ADONIS	<input type="checkbox"/>
By _____	
Distribution _____	
Availability _____	
Dist	Spec
A-1	

**Table of Contents --**

~~Abstract~~ . . . . . ~~ii~~

**Introduction . . . . . 1**

**Summary . . . . . 1**

**Rationale . . . . . 2**

**Overview of Results . . . . . 2**

**Technical Report Part I. Dextrous Hands : . . . . . 8**

**Dexterity: Summary of Project Accomplishments . . . . . 8**

**Overview, . . . . . 10**

**Hand Construction & Improvement, . . . . . 11**

**Sensor Progress, . . . . . 12**

**Force Control Capability, . . . . . 19**

**Manipulation Strategy, . . . . . 19**

**Computation Power, . . . . . 30**

**Plans . . . . . 32**

**Technical Report Part II. Force Control of Very Flexible Manipulators : . . . . . 33**

**Summary of Project Accomplishments . . . . . 33**

**II-1. Force Control of a Single, Very Flexible Manipulator, . . . . . 36**

**II-2. Flexible Arm with Quick Wrist for Precision Force Control, . . . . . 75**

**II-3. Two Link Arm Control, . . . . . 81**

**II-4. Design for a Two-Cooperating-Arm System, . . . . . 87**

**II-5. Tight Control of Joint Torque.. . . . . 98**

**II-6. Technology Assessment . . . . . 111**

**List of References . . . . . 115**

**Appendix A. Statement of Work . . . . . 117**

LIST OF ILLUSTRATIONS

<u>Figure</u>		Page
1.	The Stamps K-JPL...	3
2.	~ ~ ~ ~ ~	4
3.	~ ~ ~ ~ ~	5
etc		

## INTRODUCTION

### Summary

This is our Final Report on a three year contract to conduct research on intelligent sensory control of end effectors and manipulators. This is a joint research program between the Robotics Laboratory of the Stanford Artificial Intelligence Laboratory (SAIL) and the Aerospace Robotics Laboratory (ARL) of Stanford's Aeronautics and Astronautics Department. The joint program operates within the Center for Automation and Manufacturing Science (CAMS).

SAIL reports progress on fabrication of a three finger hand with sensors, on sensory control of the hand, on intelligent task execution with the hand, and on sensor technology. ARL describes progress in force control and fast-slew-and-touch with very flexible manipulators, and on planning for a two-cooperating-arm research facility.

These elements of task execution can be termed intelligence, skill, dexterity, and control, going from high-level planning strategy to servo-level control. The research addresses four major advances in robots; first, precision force control, second, dexterity, third, slewing a flexible arm rapidly and precisely to force contact *without pause*, and fourth, dynamic cooperation of two manipulators.

The next major development in industrial robots is likely to be force control, especially in assembly. Robots in industry and in most research laboratories have position control of gross motion, not force control for fine motions in parts mating. The two programs in this joint effort study different aspects of force control of robots, in making contact with objects, in exerting controlled forces on objects, and in making rapid motions of parts for assembly.

This rather major initial assault on the force control problem was conceived jointly with our DARPA sponsors with a set of Goals — contained in the Statement of Work (SOW) that were designed to achieve a new technology level from which the next advances can begin. It is now clear that these future advances will include achievement of high-level dextrous hand skills using feedback from tactile fingertip arrays, and the experimental achievement of dynamic cooperation between two nonrigid manipulator systems. The Goals of the present contract have indeed positioned us, as we had hoped.

It is satisfying to report that not only were all the specific Contract Goals essentially met, but there have been achievements beyond the original goals, typically of an unanticipated nature, as there should be in a university research program. In particular, the concept of dynamic cooperation between manipulators — and the central role that force control must play in it — were not anticipated three years ago. We have now developed this concept to where we are ready to begin building our experimental equipment.

For convenience, the detailed Contract SOW is provided as Appendix A of this report. Here, by way of introduction, we describe quantitatively the rationale for how we have proceeded, followed by an overview of our activities. Then we present our research results to date in the formal Report on Research that is the body of this Final Report.

## Rationale

Industrial robots and most robots in research laboratories have hands like pliers, i.e., two jaws without sensors with only a single degree of freedom. They cannot grip many objects in many positions, or make stable grasps, or adapt to incomplete information about position and orientation in grasping. Three fingers with the necessary freedoms and with force sensing support are now capable of grasping curved objects in many positions, grasping them stably, adaptive grasping, re-orienting objects, and fine motion for parts mating and force control.

We study intelligence in grasping strategies and in parts identification by grasping.

We also study control methods that can contribute to lowering the cost of using robots by making them much faster and more precise and thereby increasing their payload despite limited strength and despite flexibility. Current robots are made stiff enough and strong enough to ignore loads. A Unimation PUMA weighs 120 pounds and carries a payload of five pounds. Unavoidable flexibility in drive trains of robots and in their mounts make precise end-point control of flexible robots an issue of central importance.

## Overview of Results

To advance the technology of dextrous hands we have completed construction of the Stanford-JPL three-finger hand (Fig. 1), including electronic and software interfaces, and we have mounted the hand on a PUMA 560 robot arm. We have designed and designed, built, and demonstrated three classes of force sensors for the hand: tendon-tension sensors, three-component-force sensing fingers, and 8x8 tactile arrays for finger tips (six versions). We have implemented a three-hierarchical-level force control system. We have demonstrated one- and three-finger object manipulation. We have developed a multi-microprocessor system ("NYMPH") for hand control.

To advance the technology for force control of manipulators we have developed a series of experimental systems which require that increasingly more-advanced control capability be achieved to successfully control them. In each case flexibility has been greatly exaggerated, to force us to solve the control problem in a fundamental way. And in each case we have striven to achieve not only force control *per se*, but also smooth, rapid switching — without pause — *from* a rapid slew toward a target object *to* firm contact with precisely controlled forces level against the object.

Specifically, during the three year span of this contract, we have conceived, designed and built the following three experimental systems, and carried out control system research on each:

- a) A very flexible robot-manipulator arm (Fig. II-1(a) and (b) and Fig. 2.) having both end-point position (optical) and end-point force sensors to be used by the control system for tight control.
- b) A second very flexible arm with a separately-driven fast "wrist" mounted at its end (Fig. II-1(c) and (d) and Fig. 3). The wrist tip has its own position (optical) and force (load cell) sensors.



**Figure 1. The Stanford-JPL Three Finger Hand.**

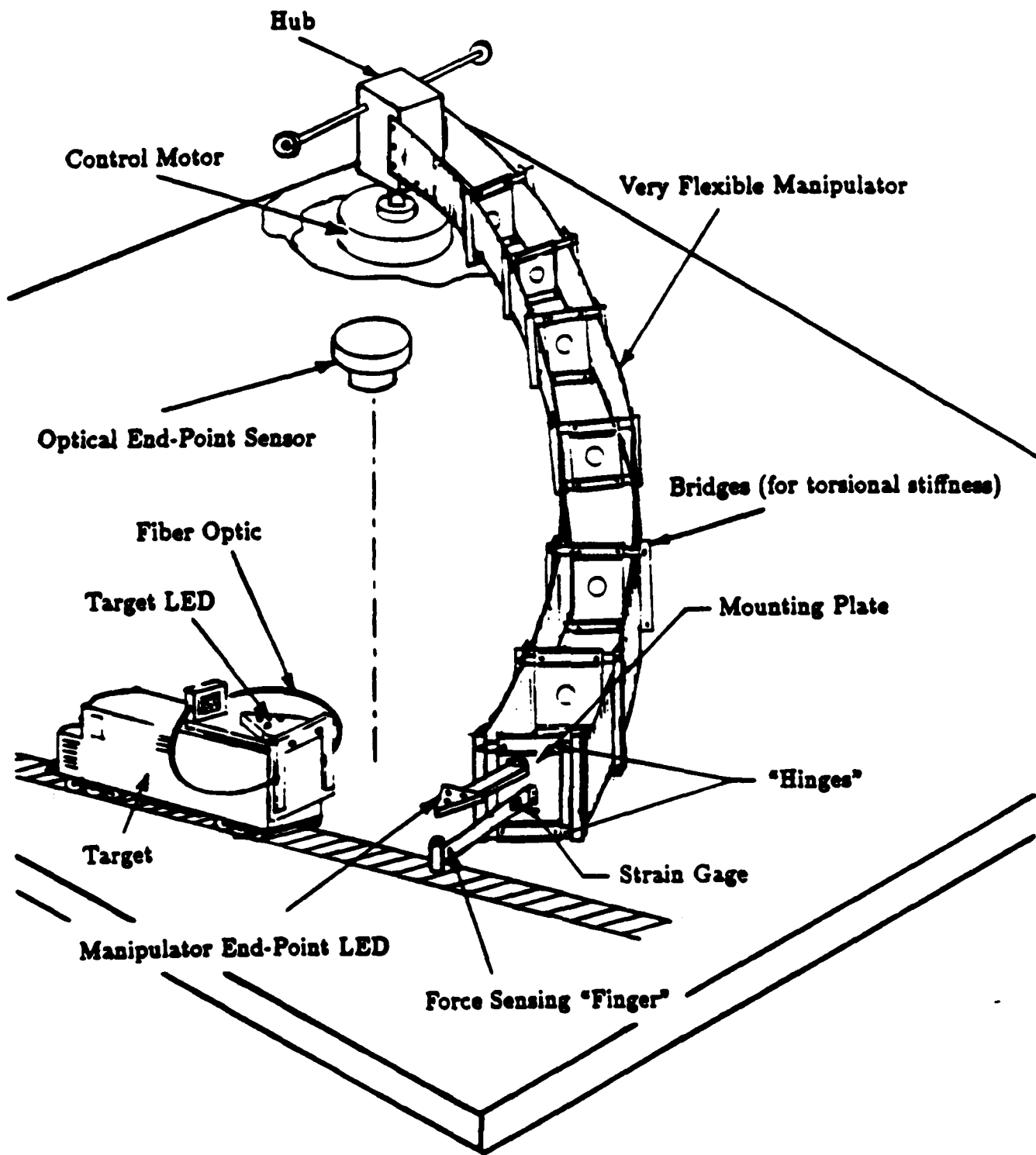


**Figure 2. Apparatus for Force Control of Very Flexible Manipulator.**

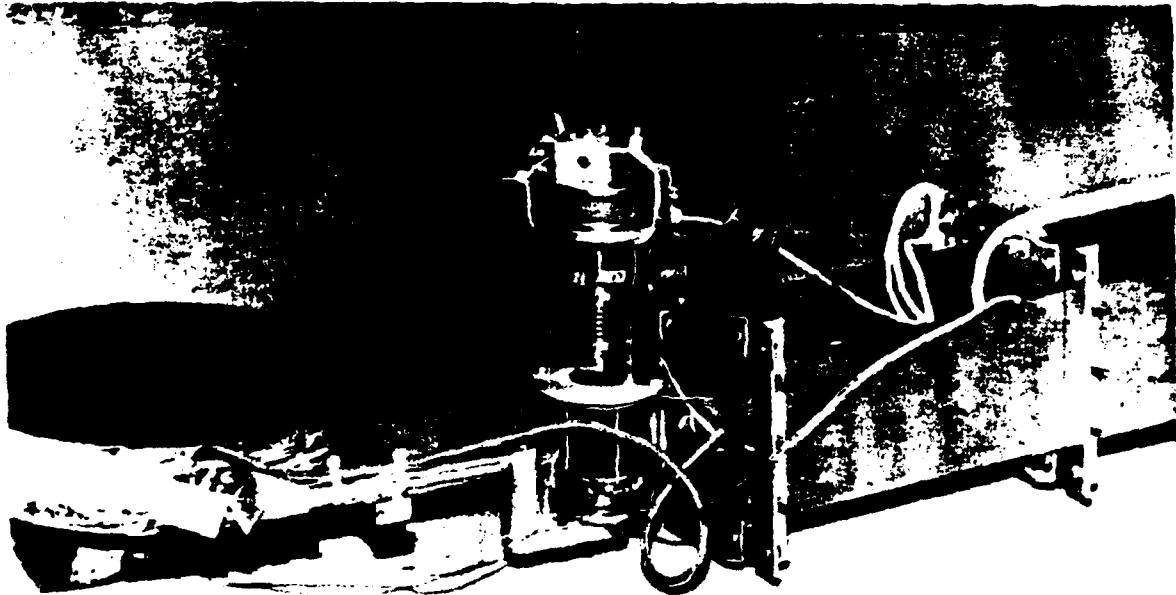
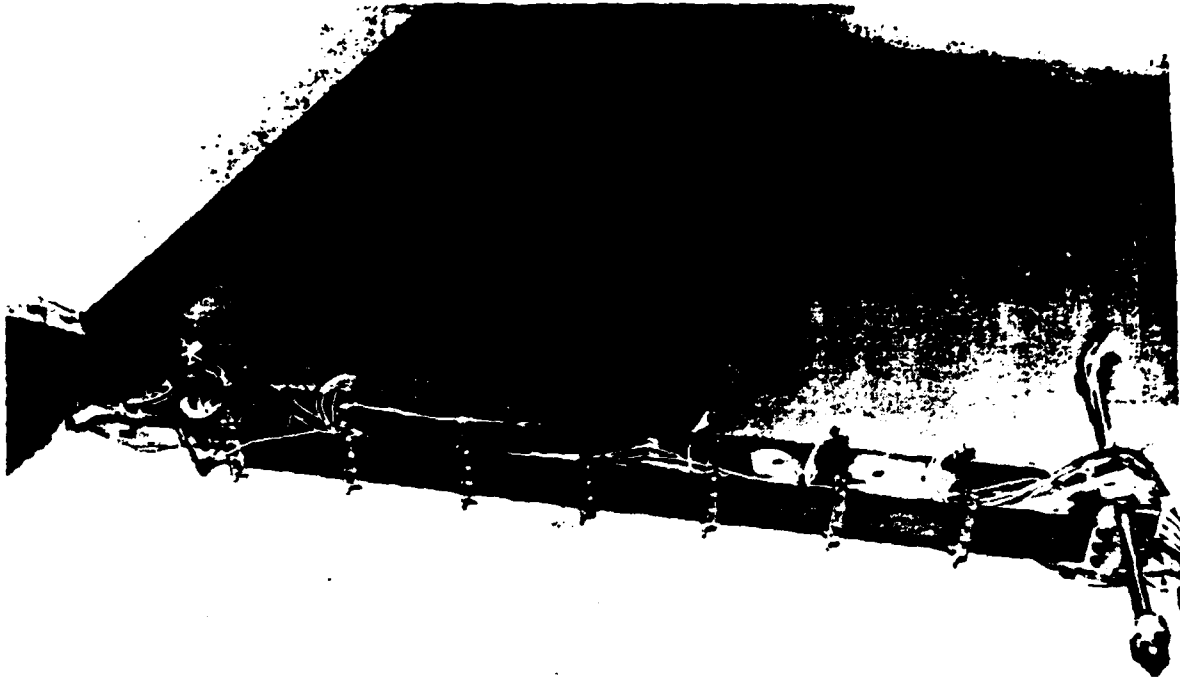


**Figure 3. Photographs of flexible arm with quick wrist in contact with stationary target.**  
**Top: System overview, Bottom: Detail of wrist and sensors.**

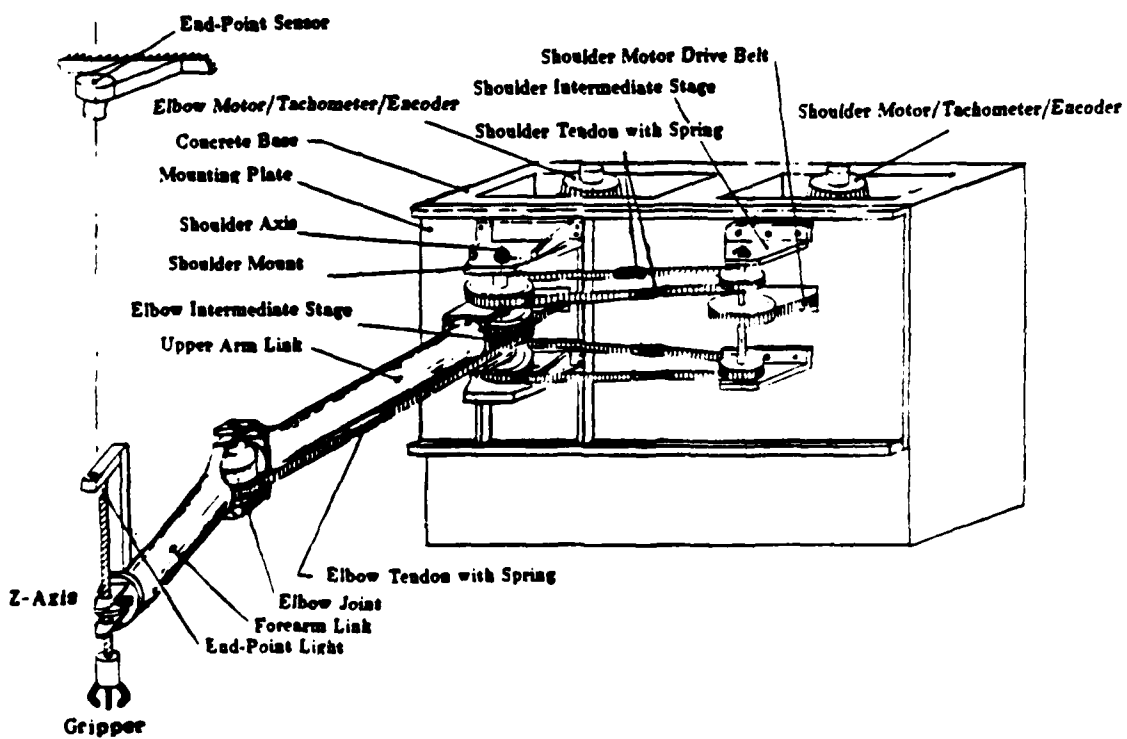
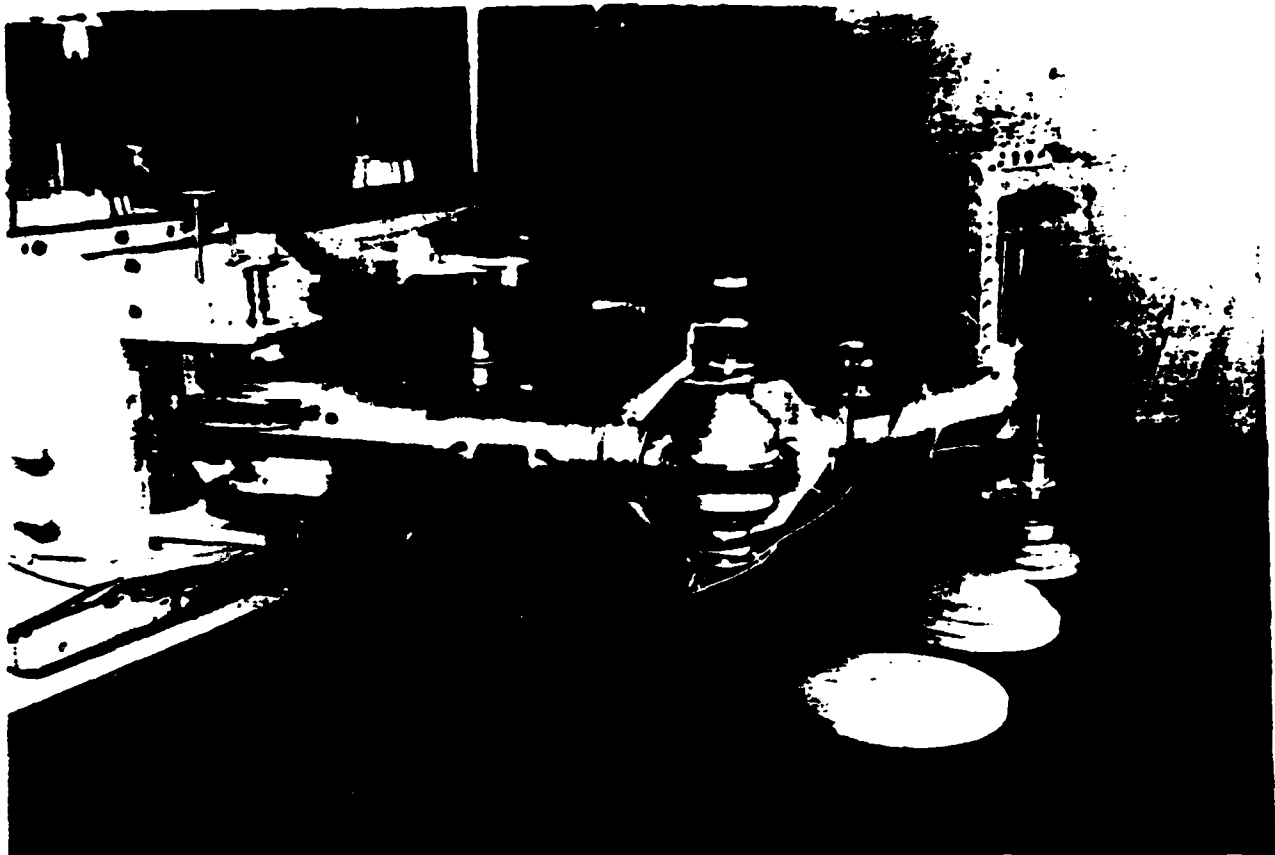


**Figure 4. The Stanford Two-Link Manipulator with Flexible Tendons.**  
 a) Photograph b) Schematic

- c) A two-link arm (Fig. II-1 (e) and Fig. 4) whose links (bones) are light and rigid, but whose drive train (tendon system) is very flexible. (This system was developed jointly with both DARPA and AFOSR support, and is used for different experiments in the two programs.)

With the single very flexible arm Jim Maples has now accomplished rapid slew-and-touch, without pause, to a moving target. He has established the absolute physical limits on slew velocity and control speed, and has achieved performance near these limits; and he has demonstrated smooth switching between end-point position control and end-point force control. To do this he developed both a simple end-point force sensor and an optical position-sensing system for both manipulator end point and target.

Using the flexible arm with fast wrist (a two link system), Scott Tilley and Ray Kraft have also now demonstrated fast slew and touch, and have shown that the high-speed wrist control makes possible quite exquisite control of the force at the fingertip: despite rapid speed of contact, force level can be maintained precisely at the specified value, without force overshoot. Ray Kraft adopted a new load-cell force sensor for this work.

Our first lightweight two-link arm with flexible tendons has now been controlled by Michael Hollars using both conventional colocated joint-angle sensors and using new end-point position control; and the superiority of the latter has been shown. We are now in a position to develop end-point force control for this two-input two-output system, which Brian Anderson will lead.

Proceeding from our experience with the single two-link arm, a group led by Larry Pfeffer has completed design of a system of two cooperating two-link arms, each fitted with a three-axis wrist and gripping system. Sensing and control computing systems are being designed by Stan Schneider and Chris Ulick. Pfeffer, working with Oussama Khatib in SAIL, has also developed and demonstrated on a Puma arm, a special servo for achieving very tight control of joint torque. We will begin construction of this experimental system (in new laboratory space) as soon as funding for this next phase of our DARPA-supported research arrives.

# TECHNICAL REPORT

## PART I: DEXTROUS HANDS

### Dexterity: Summary of Project Accomplishments

SAIL reports on progress in intelligent sensory control of a three finger hand:

1. Mechanical construction of the Stanford-JPL three finger hand was completed. Electronic and software interfaces were implemented to control computers. The hand was mounted on a PUMA 560 arm. Mechanical modifications to the hand were made.
2. Sensors were implemented for the hand. Sensors were designed and built to measure tension in the tendons which drive the hand. Force-sensing fingers which measure three components of force were designed and fabricated. An analysis was made of tactile sensing mechanisms, analyzing force measurement using continuum mechanics for sensors embedded in a flexible medium. Six versions of finger tips with 8x8 touch sensing arrays were designed and fabricated to evolve sensors which are now usable for task execution on the hand.
3. Analysis was made to design a hierarchical force control system for manipulating objects. A force control system was implemented for the hand with a three level hierarchy, the hand level coupling three force-controlled fingers, the finger level coupling four tension-controlled tendons, and tendon tension control level.
4. A task decomposition was made into task operations which decompose into fundamental motions controlling position, velocity, and force/torque. Position and velocity were resolved into fundamental rotations and translations. One elemental rotation was implemented, first as rolling objects with one moving finger, then twirling a baton with three fingers. Adaptive grasping of objects with and without models was analyzed. A modeling system intended for recognition of objects from models was implemented as a step toward identification of objects from models.
5. A multi-microprocessor system ("NYMPH") was designed and largely implemented in order to provide improved compute power, real time response, and simplified software development.

Following paragraphs summarize the progress in each of the three years. When the project began, the hand was designed partially built. In the first year, we completed fabrication of the end effector, made mechanical modifications, obtained a twelve channel electronic interface, and made a software interface the end effector to a control computer. We analyzed and implemented a hierarchical force control for the hand, fabricated tendon tension sensors and force-sensing fingers, and analyzed rolling an object. We analyzed force measurement by sensors embedded in elastic media.

In the second year, we demonstrated simultaneous motion of three fingers, analyzed decomposition of tasks into component motions, and demonstrated rolling an egg between two fingers, one of the fundamental motions. We brought a PDP11/60 online to double computation power. We implemented improved force control. We fabricated and tested several versions of an 8 x 8 tactile sensor array. We designed, built, and integrated a 12 channel interface for the hand which provided improved performance.

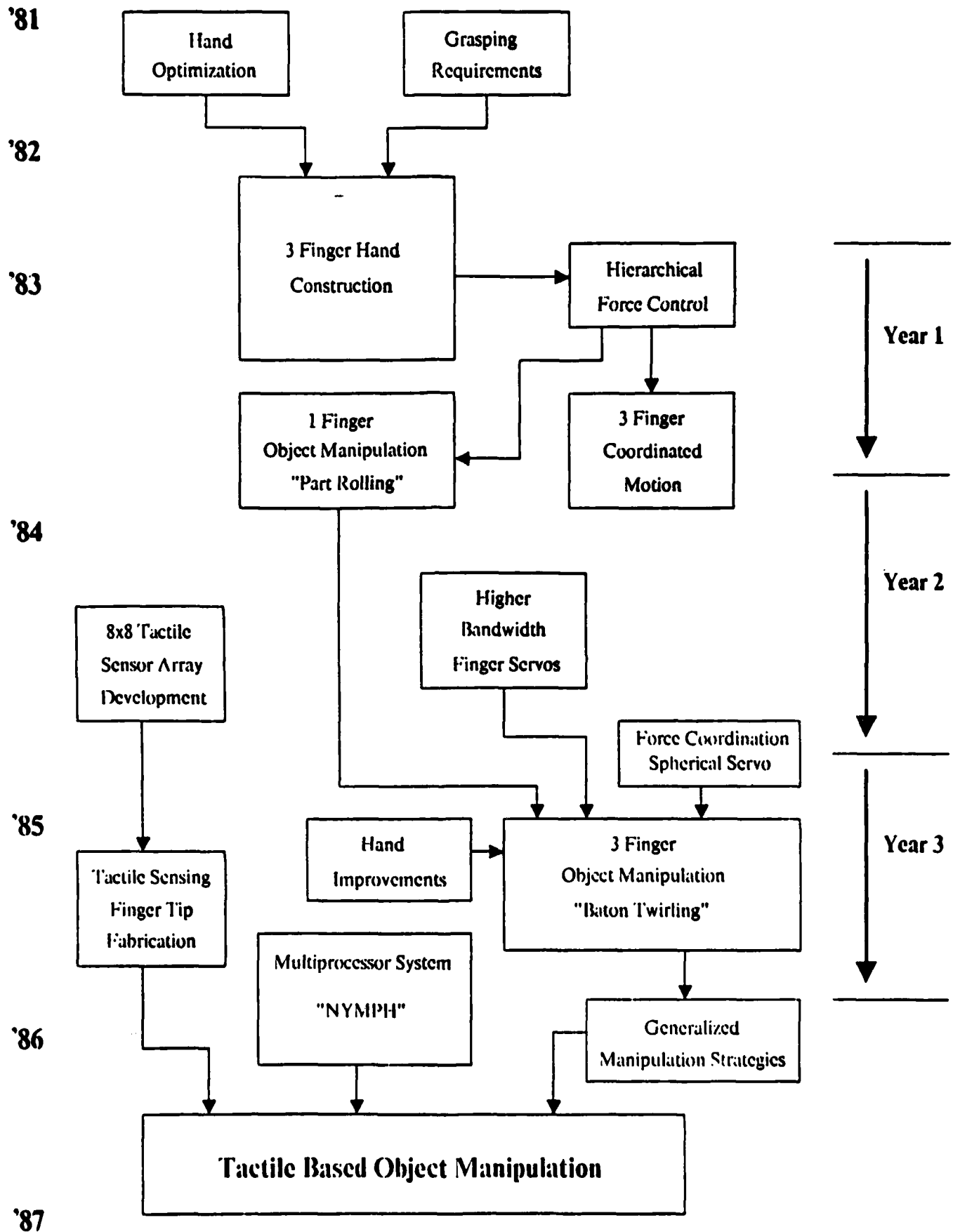


Figure I-1. Overview of progress.

In the third year, we have demonstrated twirling an object. We have mounted the hand on a PUMA arm and have proceeded toward implementing combined hand and arm force controlled motions. We implemented a succession of tactile sensor arrays on fingers, achieving an 8x8 array on curved finger tips which will be adequate to support future research. We designed, tested, and began construction of a multi-microprocessor system, and began implementation of software for it.

Figure I-1 provides an overview of progress during the last 3 years.

## Overview

Salisbury made a careful analysis which went into the design of the universal end effector, the Stanford-JPL hand, to have the necessary and sufficient degrees of freedom to re-position objects arbitrarily. To achieve the necessary dexterity, it has three fingers and nine degrees of freedom. Five of the hand parameters were chosen to optimize a measure of the range of three finger grasp positions. The hand was designed and partially fabricated under a grant from JPL and with support from NSF. Each finger has three degrees of freedom (humans have a fourth which is quite valuable). Fingers were powered with pull-pull tendons in order to reduce friction and enhance controllability. With two tendons per freedom, 18 motors and tendons would have been necessary. The number of motors and tendons was reduced by coupling tendons to use only  $n+1$  tendons instead of  $2n$ , hence four tendons per finger, a total of 12 tendons and 12 motors.

Under this contract, the hand was assembled. Mechanical modifications were included. Subsequent modifications have improved the sensitivity of force control at the fingertip by a factor of four. Continuing modifications are aimed at reducing the effect of motor friction and further improving the sensitivity of force exertion. The hand was mounted on a PUMA 560 arm in order to experiment with combined coarse and fine motion.

Thus far, force control is based on sensors for tendon tension. Fearing has designed an 8x8 array of capacitive sensors for fingertips. He built the multiplexer electronics to reduce the number of signal wires to bring the signals to the computer. A series of improved sensors has led to a sensory fingertip which will be replicated for the three fingers.

Force control was designed to control position, velocity, and internal forces exerted on objects, rather than control joint variables. This level of control is natural for commands in a high language to communicate with the control module, i.e. specifying motions of objects rather than motions of hand joints. It provides a level of device independence. Incorporation of hand commands in AL has been investigated by Cai and Fearing. The force control module is a hierarchy of hand level, finger level, and tendon level. Finger motions are specified in a spherical coordinate system to express opposition of fingers.

Force strategies for global motions are formulated in terms of fundamental motions. The research program is to implement a complete set of three rotations and three translations. (Ref. 3) analyzed open loop finger force strategies like rolling an object; these strategies are insensitive to object size and mass. Rolling a grasped object about a finger is possible by superimposing a tangentially directed force on a radially directed force that keeps the object grasped.

## **Hand Construction and Improvements**

Construction of the hand and modifications were completed under this contract. An electronic interface was constructed and software was completed for interfacing the hand to the laboratory's PDP11 minicomputers. A PDP11/60 computer was debugged and brought into use as a control computer.

### **Hand Improvements:**

A continuing problem with achieving adequate force control with the three finger hand has been a need to run the low level motor servo at low gains because of large motor inertias, friction, and the complicated dynamic couplings of the  $n+1$  tendon control scheme. For instance, because of the coupling, applying a torque of 1000 gm-cm about joint 1 gives a reflected torque of 500 gm-cm about the other two joints, just due to the intrinsic mechanical coupling and motor stiction.

Micha Bar reduced the gear ratio to 9.4:1 from 28:1. While this reduces our peak force at the end of the finger to 1 Kg from about 3 Kg previously, the improved dynamic performance makes it worthwhile. With the new gears, the old simple motor tension servo was tried again. Because of lower reflected motor inertia and brush stiction, much improved joint torque and finger force control was achieved. We can now run with a tendon tension error gain of 10, and still have a stable tension servo. Previously, the maximum gain was about 2.5. The motor stiction seen as tendon stiction is reduced to about 500 gm from the previous 1500 gm. Theoretically, we can now control tendon tension with an accuracy of 50 gm, or only about 5 gm at the end of the finger with the finger extended. Because of other friction sources, the observed force resolution is probably  $\pm$  20 gm.

The hand is running now on worn tendon sheaths that wore out prematurely due to improper routing. Lubrication has been added inside between the tendon and its sheath to reduce wear and friction. A complete new set of tendons will be ordered along with a replacement motor for one that has an out of alignment shaft. This should optimistically reduce overall friction by a factor of two. Further friction reduction may come from substituting brushless motors for the current DC servo motors.

Micha Bar developed new compliant, cylindrical finger tips that provide a much better surface for rolling motions of objects, and much better contact area than the original oblong hard rubber finger tips. They improve the useful workspace of the hand by allowing more space where the finger tips contact each other, rather than the links of the finger colliding together. The compliant finger tips provide greater resistance to disturbance torques for corners and edges of objects. These finger tips have helped performance considerably. These are the same size as the tactile sensing finger tips which will be substituted soon.

The hand has been mounted on a PUMA 560 arm, but adequate computation cycles have not been available to drive the hand and arm simultaneously. The disk drive to bring up VAL-II for the arm on the Mark II controller has been purchased. This will allow position control of the arm, while the hand provides force control and fine motion control. Eventually, it is intended to couple Khatib's force control of the arm with hand force control.

The hand was first operational at the end of the first year of this contract using a

PDP 11/45 and two Unimation 260 controllers operating as torque output and optical shaft encoder input devices. This was sufficient to servo all 12 tendons simultaneously to control joint torques for simultaneous 3 finger motion. During the second year, the PDP 11/60 was brought on stream, with about twice the floating point power of the 11/45. At the start of the third year, the custom-designed 12 channel controller was substituted for the Unimate controllers. The Unimate controllers had caused much trouble; they were unreliable and their slow interface to the PDP-11 reduced servo rates. The 12 channel interface has rapid response, and a very useful feature that if the computer crashes, the hand motors will gracefully turn off, rather than run at full torque as the Unimate controllers were prone to do. This results in many fewer broken tendons.

### **Sensor Progress**

The hand has a tension sensor for each tendon. Fearing has been at work to build a touch sensor array which measures force and contact location over each fingertip. Initially, an analysis was made of measuring forces from the continuum mechanics of a deformable medium enclosing an array of sensors (Ref. 3) Six versions of an 8 x 8 tactile array have been fabricated and tested. The first version of the sensor was on a flat surface. The array of the sensor has been encapsulated in a compliant, cylindrical finger tip slightly larger than human. A cylindrical finger tip is necessary for reorientation operations, which require parts to roll on the finger tips. Construction of calibration apparatus has started. The sensor shows enough sensitivity to enable more reliable and robust experiments than has been possible without sensing. Currently, sensitivity is about 20 grams. There is one usable finger now. We intend to fabricate tactile arrays for each finger and mount them on the hand by November 1985. Sensor development continues to achieve greater sensitivity and other improvements. We are also alert to incorporate suitable sensors which may be developed by groups working on sensors at Stanford or elsewhere. A key element of the sensory system is a multiplexing sensor processor which switches and amplifies low level capacitance signals to interface to computers. The sensor processing electronics has been in operation for a year.

Micha Bar encapsulated the 8 x 8 capacitive sensor array developed in '84 in a cylindrical finger tip of 25 mm radius and 40 mm length. This array covers the circumference of the finger uniformly, which is important since during re-orientations, objects will roll about most of the finger. The coating is 5.4 mm of polyurethane over a 15 mm diameter Delrin core. The finger is made by molding the core with its conductors. The molding operation is important for assuring mechanical integrity of the sensing layers, and uniformity of the covering layer. Rami Rise improved the sensor by adding a ring at the top to give the tip some sensitivity. This will be very helpful for rotations that use finger tip contact. Figure I-2 shows the construction of this finger tip. Construction has also been started on calibration apparatus for the finger that will allow accurate application ( within 25 um) of forces with accurate directions and magnitudes. Figure I-3 shows a completed finger tip with cables attached.

Much work has been done in trying to maximize sensitivity and minimize hysteresis by choice of polyurethane foam covering hardness, and the dielectric hardness. To date, the best sensor shows short term hysteresis of about 5% and sensitivity threshold (just

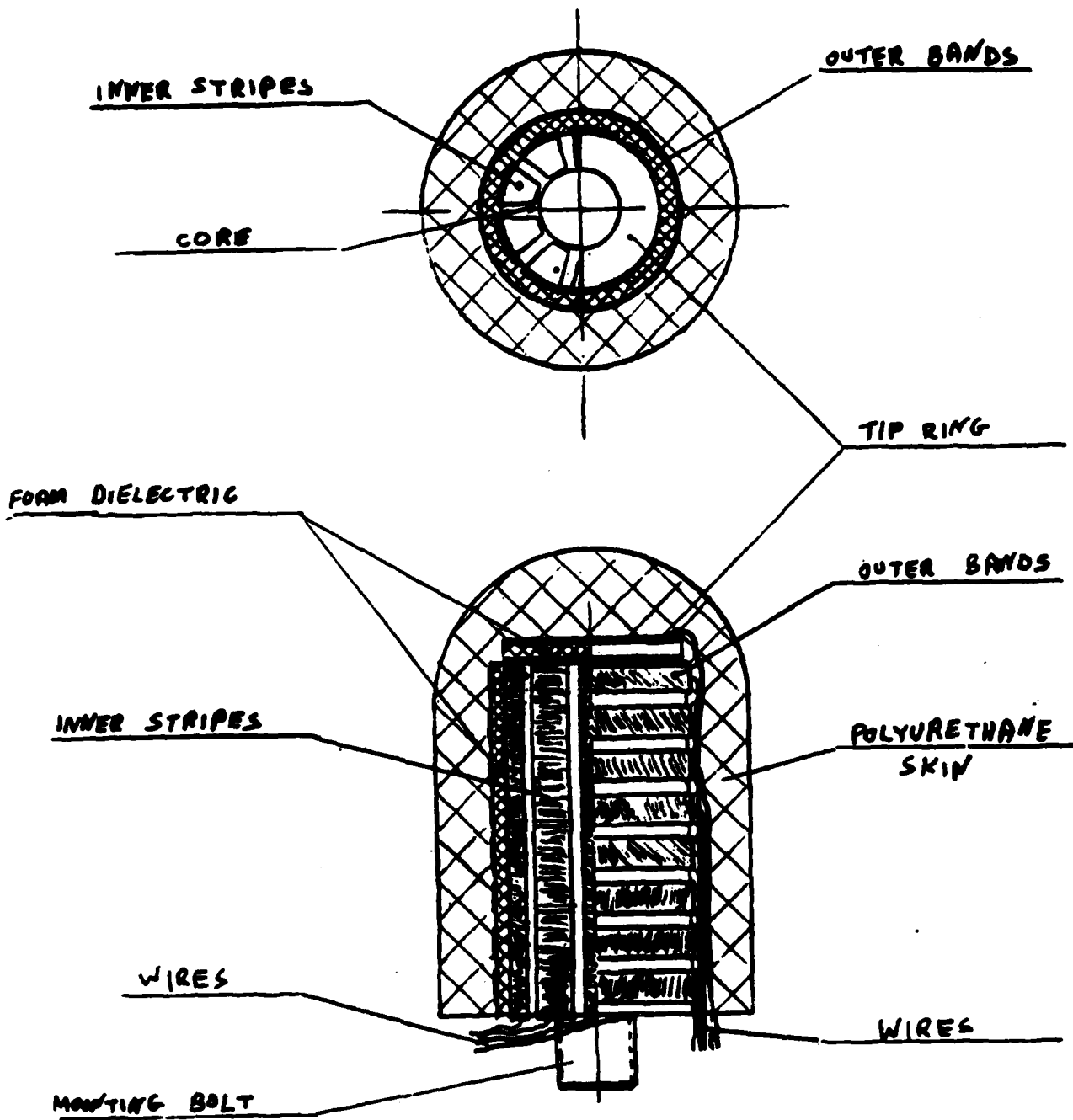
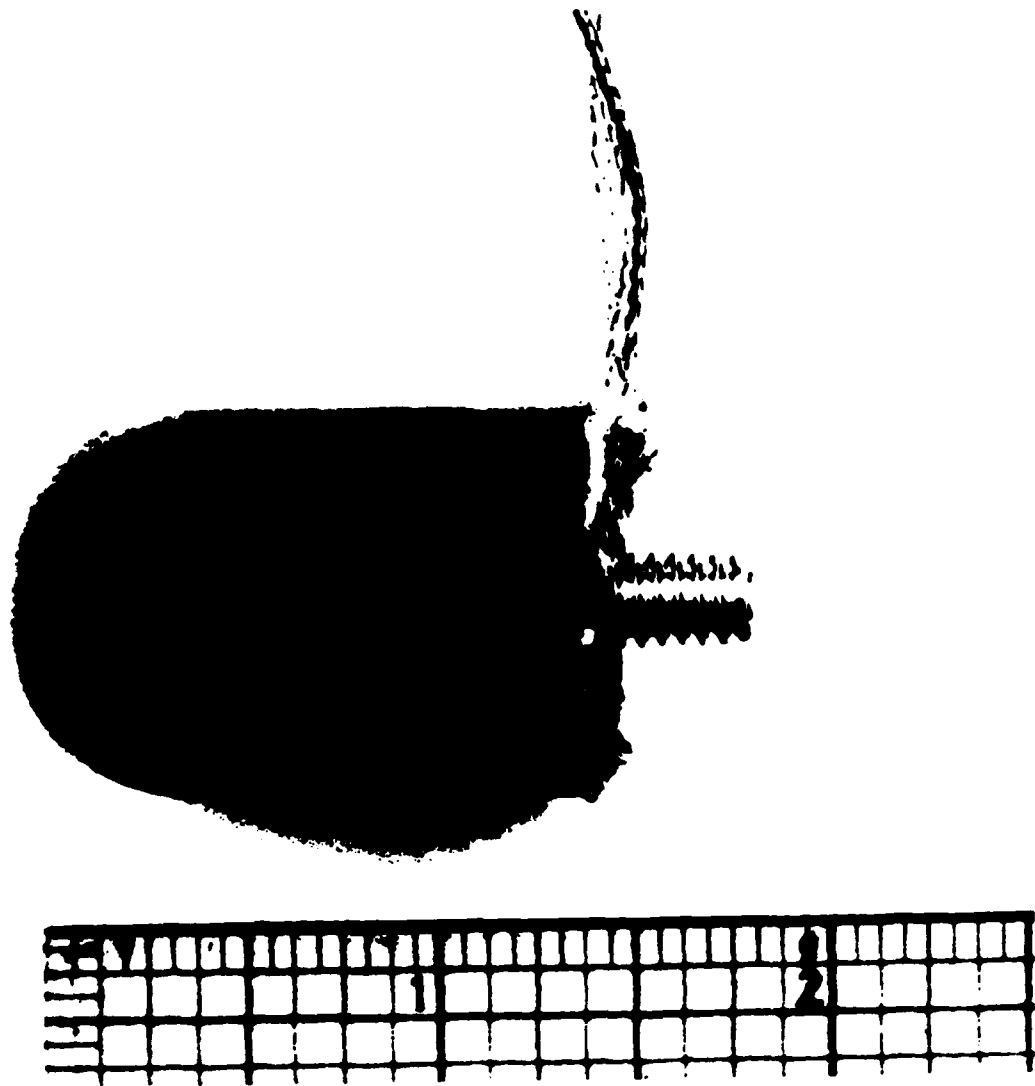


Figure I-2. Fingertip construction.



**Figure I-3. Tactile Sensing Finger Tip.**

noticeable contact) of about 20 grams. Figure I-4 shows the output of a capacitive cell versus applied force. Note the greater pressure sensitivity with greater contact area. Through creative signal processing, we expect to get lower contact thresholds, and to live with this slight amount of hysteresis. The prototype flat sensor developed last year showed greater sensitivity, so we anticipate being able to improve the cylindrical sensor also. For typical grasping forces in the 200 - 500 gram range, the present sensitivity will be initially adequate.

An important property of a tactile sensor is its impulse response. This response indicates the sensitivity of the sensor, and its spatial frequency response. If the sensor is linear, then from the superposition principle, the sensor response for any desired pressure on the surface can be predicted. Conversely, we hope that from the subsurface deflection response, conclusions about the contact condition on the surface can be made. For example, angle of force, indicating potential slip could be determined from these measurements.

Figure I-5 shows the impulse response of a typical cell as a probe with constant force is moved along the surface. Note that the width of the probe is significant compared to the width of the response. Using a very crude plane stress model (linear elastic half plane), the predicted strains at 5.4 mm depth are shown in Figure I-6 for a point force applied above the origin. Note the rough agreement between the two, which is somewhat hidden by the blurring due to the wide probe width. The testing apparatus under construction will allow much finer determination of this response. Because of the wide impulse response, spatial resolution will be poor, however good localization is more important for good force control. With sensor spacing on the order of 3 mm, deep sensors are needed to avoid aliasing when the deflection pattern is reconstructed from its samples.

Although capacitive sensors are inherently high impedance devices, susceptible to noise pick up, improved cable shielding has given substantial improvement over last year's prototype flat sensor. The standard deviation of the noise due to stray field pickup is now less than 1.0 when the sensor is first calibrated. (Due to hysteresis effects, the constant offset capacitance can change, disturbing the statistics).

During the second year of this contract, a flat prototype 8x8 sensor had been developed, and the electronics had been designed. The sensing mechanism is based on the deflection of capacitor plates, that are formed at the intersection of crossed copper strips. Using multiplexers, one row is excited by a 10 volt 100 kHz sinusoidal drive signal. The output is read from one column, amplified and detected to give a DC output signal inversely proportional to the capacitor deflection. The entire 64 elements of the array are read at 10 Hz. For an important component of the finger force control loop, a 30 - 50 Hz rate would be preferable, if adequate computation speed is available. The 10 Hz rate should suffice for making corrections to manipulation operations, as when parts leave desired trajectories.

Analytic studies have been started aimed at predicting contact forces from subsurface strain measurements. One preliminary result is that 3 strain sensor measurements beneath the surface are usually sufficient to recover the angle, location, and magnitude of a line force using the plane strain model. Comparison of simple linear elastic models and the actual composite cylindrical finger tip will start shortly, when adequate measurement apparatus is available.

Figure I-7 shows two 3 axis force sensing fingers that were fabricated for a two

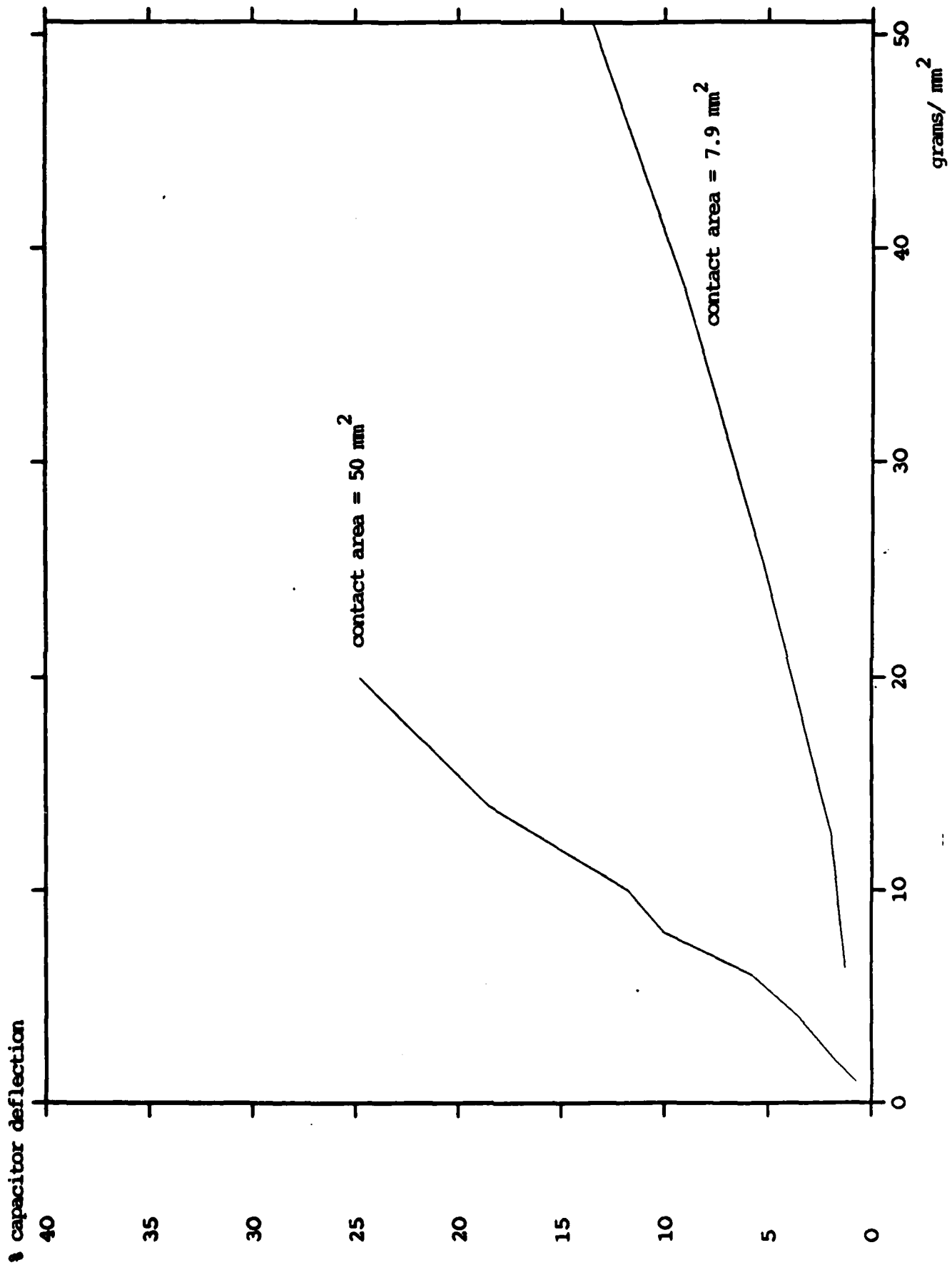
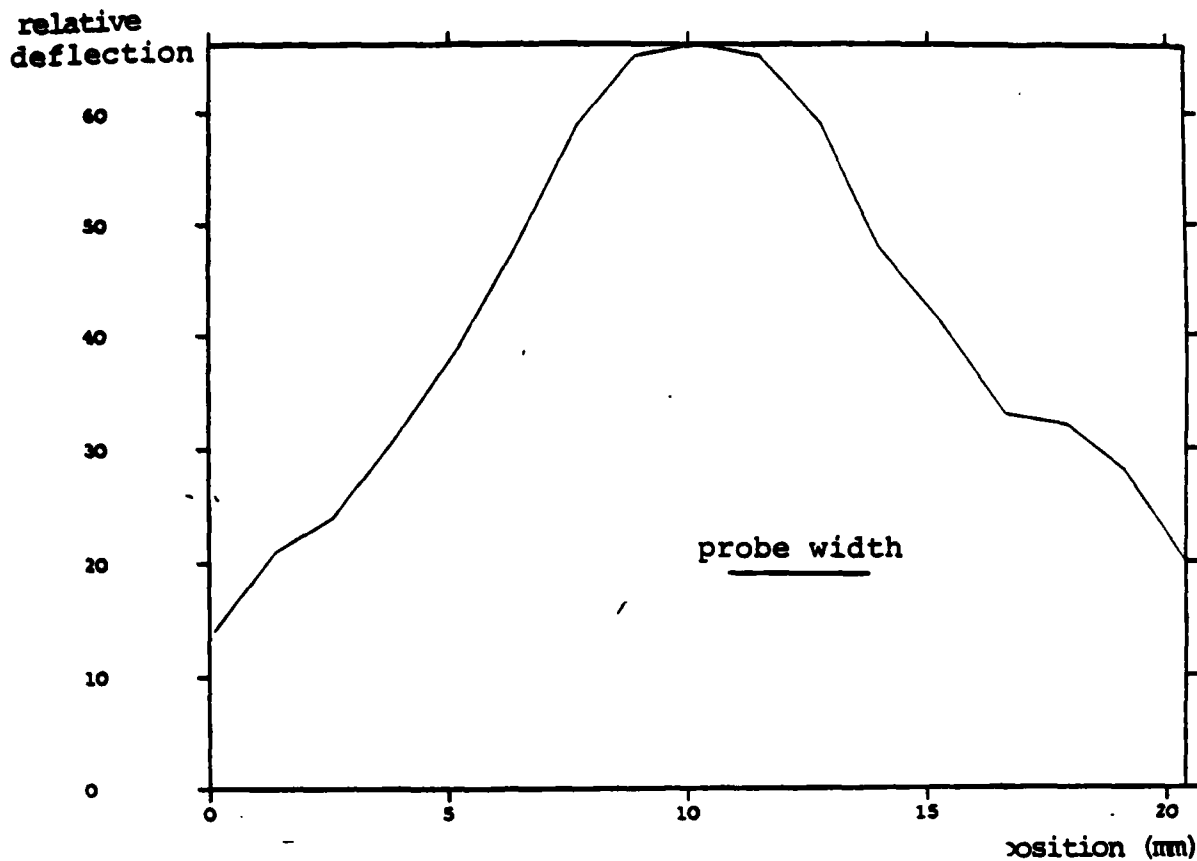
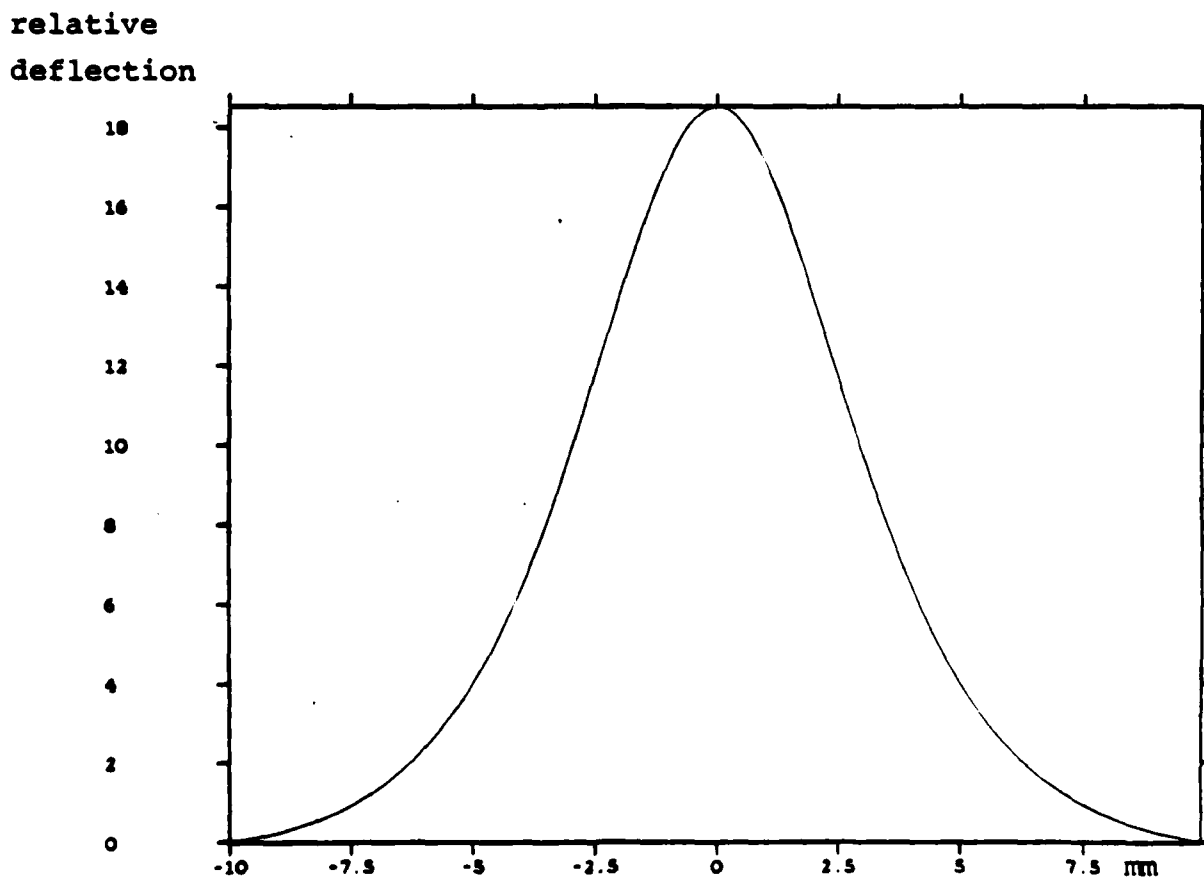


Figure I-4. Output vs. applied force.



**Figure I-5. Actual impulse response.**



**Figure I-6. Predicted impulse response.**



Figure I-7. Force sensing fingers on Hand.

finger parallel jaw type hand. The sensor measures x,y,z components of force, and was designed for high sensitivity, about 1 gram. It has an interesting design of three nested parallelograms, each of which measures one component of force. The fingers were used in experimentation in force control. They have shown sensitivity of a few grams; additional care in handling their sensor signals should increase the sensitivity to their designed value.

## **Force Control Capability**

### **Spherical Servo**

Fearing built a spherical coordinate finger force control system that is very useful for object manipulation. The purpose of this geometry is that a force can always be directed in the radial direction towards another finger. This gives force and moment equilibrium automatically if friction angles are not violated. The previous implementation, used for demonstrating part rolling, approximated a spherical geometry over a small range by generating a non-diagonal 3x3 Cartesian stiffness matrix that provided radial and two orthogonal force directions. The new system updates a transformation matrix from spherical to Cartesian coordinates at the same servo rate as the Jacobian calculations.

The spherical coordinate system allows forces to be applied in three directions  $r$ ,  $\theta$  and  $\phi$ . There is a singularity of representation when the  $r$  vector coincides with the  $z$  axis (one of the angles becomes unspecified), but this has been avoided by aligning the spherical coordinate system with the finger so that the mechanical singularity (finger straight out), corresponds to the representation singularity. Our motion directions correspond to lines of latitude and longitude on a globe.

Figure I-8 shows how the spherical control loop is built onto a Cartesian control system which calculates the desired joint torques. In the implementation on the PDP 11/60, the spherical servo runs at a rate of 33 Hz for all three fingers simultaneously. Much work went into optimizing the Pascal code for the hand to achieve this rate.

### **Joint Servo**

A second servo running at 100 Hz takes as input the desired joint torques from the spherical servo, and controls motor torques. Figure I-9 shows the joint torque control scheme, based on individual tendon tension controllers. In the future, the dynamics of the inter-tendon interactions will need to be considered at this level to get rapid changes in joint torques, and more stable operation. A mathematical model of the dynamics of the pulley motor system has been derived that considers the 4 motor masses, 4 tendon equivalent springs, and the coupling between them. This is at least an eight order system, even neglecting finger load dynamics; it represents a challenging control problem.

Previously, for the implementation of three finger coordinated motion, the tendon level and joint level servos were run at different rates. An integrator was in each tendon tension controller to help overcome static friction. Its removal has improved dynamic performance.

## **Manipulation Strategy**

Tasks for robots can be decomposed into generic task elements: tool using, parts acquisition (grasping), parts transfer, and parts mating. Generic task operations can be

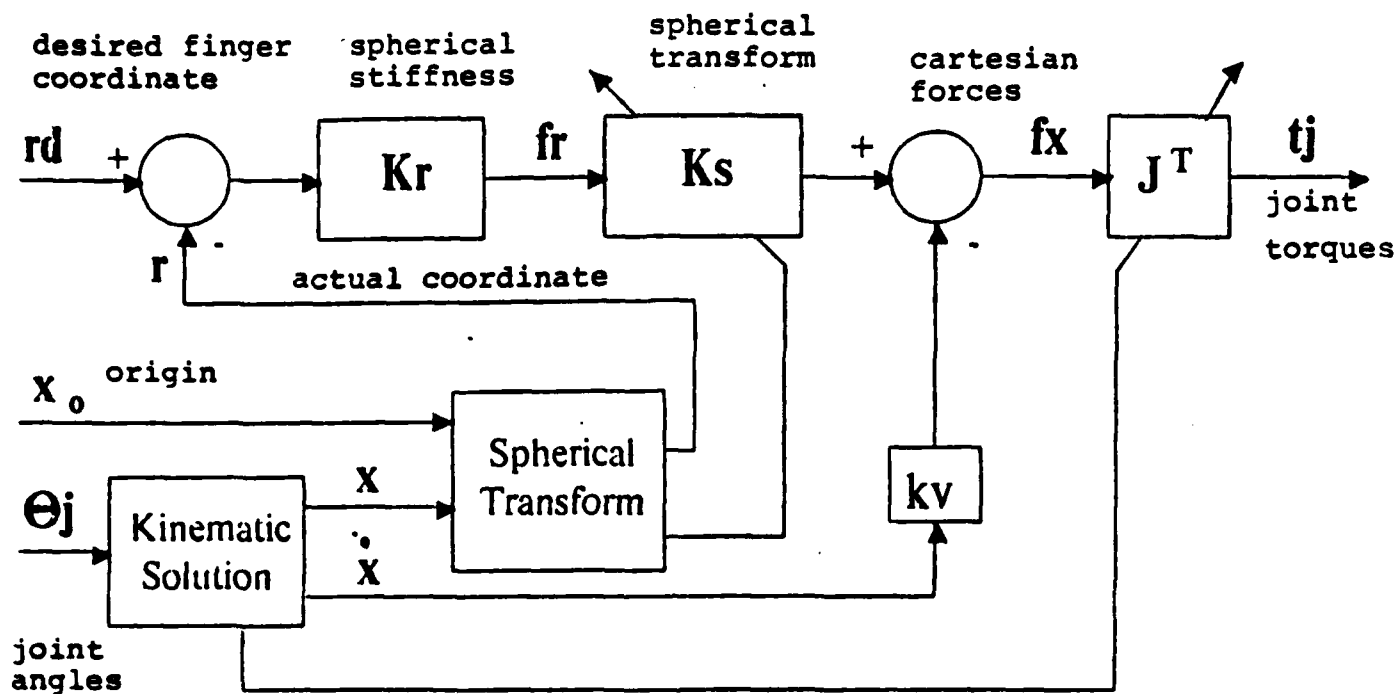
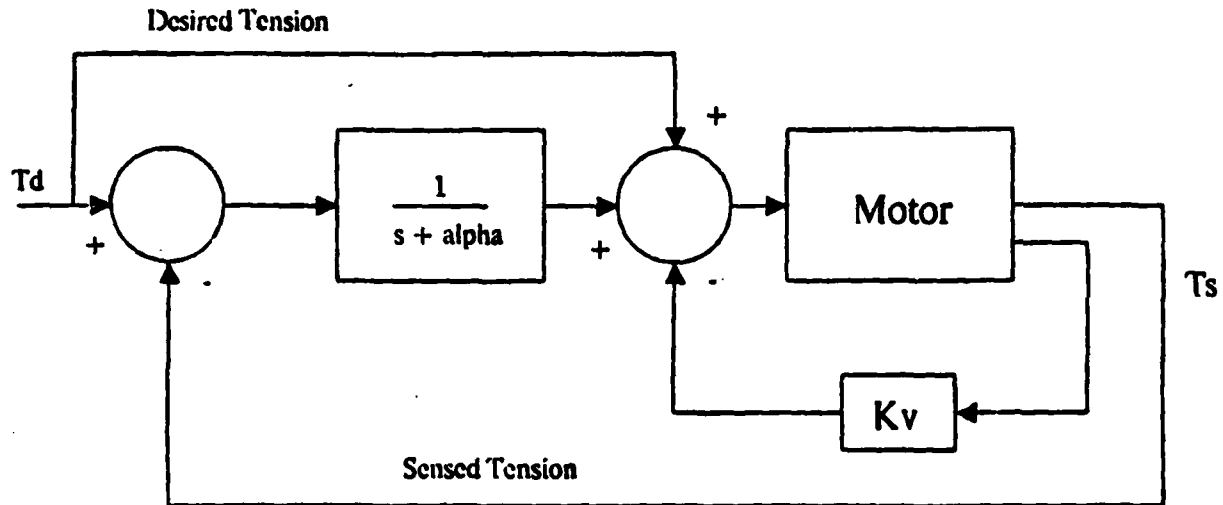


Figure I-8. Spherical servo block diagram.

## Tendon Tension Controller (TC)



## Finger Joint Controller

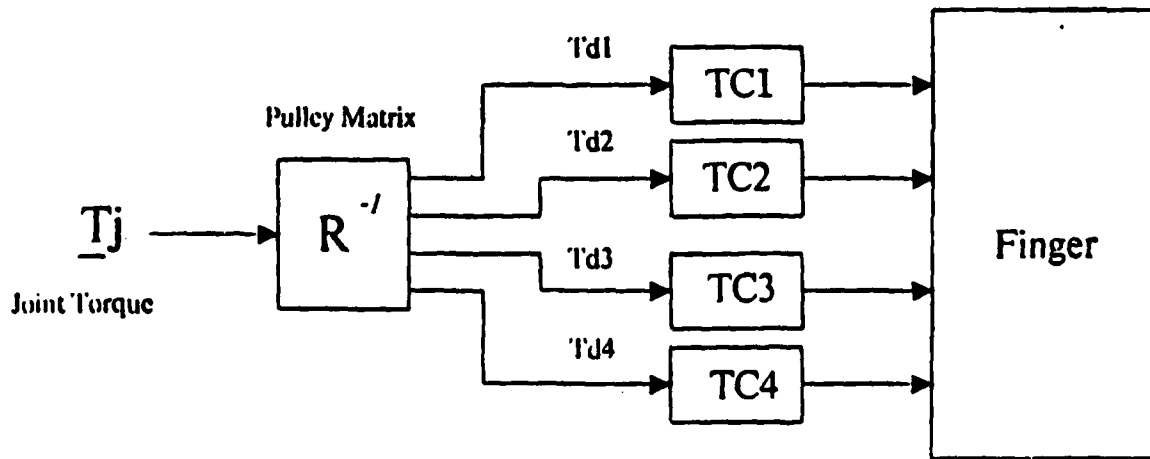


Figure I-9. Low level hand servo.

constructed from generic motions: controlling coarse position and velocity; sensing and controlling forces and torques exerted on parts; and sensing and controlling fine motion corrections to gross motion. The dextrous hand enables stable grasping, delicate force control, fine motion; it provides the degrees of freedom necessary to re-position objects. Tool using, parts acquisition (grasping), parts transfer, and parts mating all involve re-positioning. Those task elements decompose into fundamental motions controlling position, velocity, and force/torque. Re-positioning was decomposed into three fundamental rotations about axes related to finger motions and three basic translations along these axes. This analysis into object position, velocity, and forces exerted on the object forms the basis for programming hand operation in a high level language, e.g. AL.

Several studies were made of strategies for grasping and parts acquisition. A part rolling operation was accomplished first, moving only one finger under force control. A videotape was made of it. A twirling operation has been completed which involves coordinated three finger force control strategies. It implements one of the component rotations needed for reorientation, not as a small motion but as a global motion involving repeated regrasping. Twirling has been recorded on videotape.

### **TWIRL implementation**

Two of the main proposed uses for multi-fingered articulated hands are fine positioning of objects in the hand, and large motion reorientation and regrasping operations of objects within the hand. Our efforts have been aimed at first achieving gross object re-orientation ability before trying for fine accurate motions. Fine motion techniques for hands have generally not been extensible to large motions with rolling and slip at the finger contacts, while our methods are intended for both fine motion and large motions.

Fearing, (Ref. 3), showed that open loop finger force strategies can be developed to cause object motions which are insensitive to object size and mass. These operations give the ability to reorient an object in the hand while maintaining a quasi-stable grasp, that is, with limited slip.

Figure I-10 shows the force strategy applied to cause object reorientation. A sequential plan of applied forces is used to reorient and regrasp an object with the three fingers of the Stanford/JPL hand in an operation called "twirling". Rolling of a grasped object about a finger is possible by superimposing a tangentially directed force on to the radially directed force that keeps the object grasped. If an object is stably grasped by two fingers using a radially directed force at one finger, the object will remain stably grasped when a third finger applies a disturbance force. By cyclically rolling and regrasping, "twirling" can be achieved with only open loop force and position control.

Because of limited grasp stability with point contacts, line contacts were chosen for the twirling operation, This considerably reduces the available workspace of the fingers. Figure I-11 shows the reorientation of a bar through 180 degrees by this method. Best results so far were 8 complete revolutions of a wooden bar before it was dropped. Typical performance is about 2 full revolutions for an aluminum bar or rod. An analysis has been started to determine why objects shift within the hand during reorientation, and are thus subsequently dropped.

The forces for a cylindrical finger contacting an object were analyzed when the contact location is uncertain. With the present spherical servo scheme, we calculate desired forces for a point in the center of the finger tip. By using the inverse Jacobian transpose, we can find out what our actual applied force is as the contact location varies. The result was calculated for a 3 DOF finger with the same dimensions as on the hand. An example was evaluated for a downward force (such as would be used to grasp an object). As the contact location moves around the circumference of the cylinder, the force stays the same (Figure I-12). But as the contact moves along the length of the finger, its direction changes significantly (Figure I-13). Different finger orientations have stable or unstable contact forces. That is, in some orientations, a displacement of the contact causes a restoring force that would tend to push the contact back towards the desired location. Another interesting result of this analysis is that it points out that singularities of the mechanism will appear at certain contact locations on the finger, depending on the finger joint angles. The force control strategy will need to change to avoid these contact locations.

We think that appropriate force strategies for object re-orientation should be demonstrated before attempting to close the loop with tactile or visual feedback. Open loop strategies are very good at exposing problems with assumptions and execution that would be complicated by tactile sensing in the loop. Now that we have some experience with open loop performance, we can feel confident that object manipulation is possible with the 3 finger hand, and will not be failing due to inadequate quantity or quality of sensor data.

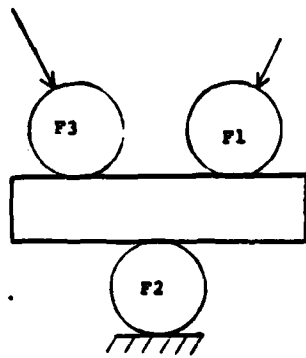
Twirling is just one of three orthogonal gross reorientations that are useful with three fingers. Figure I-14 shows all three basic rotations. Note that all three of these rotations require slip between the fingers which gives the object extra mobility beyond that provided by 3 DOF fingers without slip. The use of slip principles can be extended to control translation of an object with just three fingers. (With four fingers, two fingers can maintain a grasp while the other two are transferred down the object). A three finger translation technique is shown in Figure I-15. In this figure, finger 3 is used to change the force balance so that the object will slide at only finger one, causing rotation about finger two, and the translation of finger one. When finger one has translated, the object can be securely grasped between fingers 1 and 3. This allows finger one to move back to position for the next cycle of translation.

When the basic rotations and translations have been developed, it will be possible to implement a high level description of desired object behavior for repositioning. This will be incorporated into a system with tactile sensing for sensory driven object control.

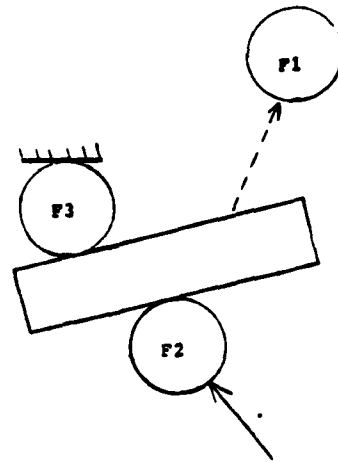
In two dimensions, we have previously shown that all 2 D objects are graspable with two fingers with very small friction, given appropriate grasping locations. We have also shown the greater contact stability with stiffness controlled fingers for grasping when the radius of curvature of the object contour is greater than the interfinger distance, due to potential energy considerations.

Part rolling, our preliminary object reorientation example was first implemented in Nov. 1983. This showed the capability of the hand for fine, though not necessarily certain motion. This example, run on the PDP 11/45 used a crude approximation to spherical coordinates by using a constant transformation matrix.

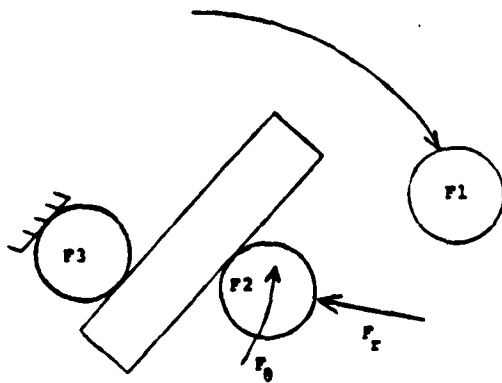
Goering built an object modeling system in order to investigate the recognition of



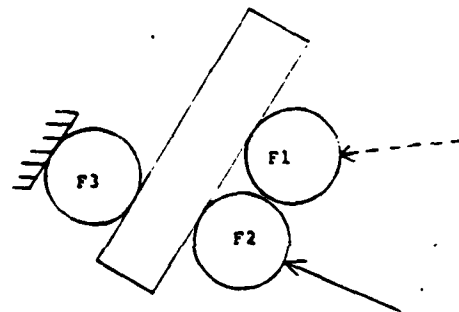
STABLE GRASP



REMOVE FINGER



ROLL



REGRASP

Figure I-10. Twirling sequence.

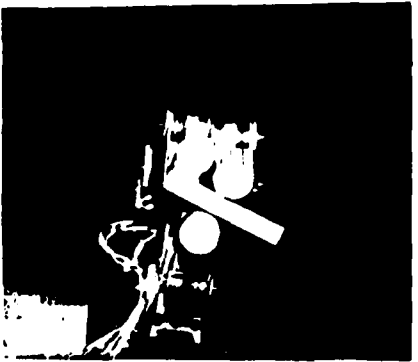
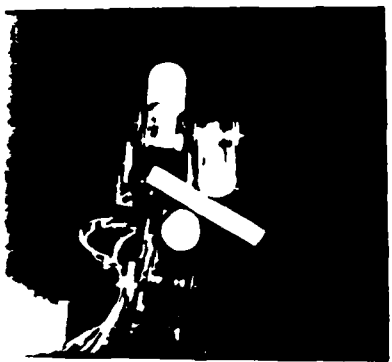
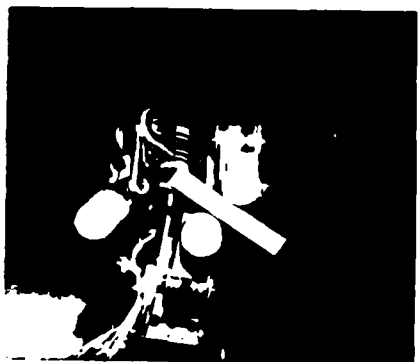
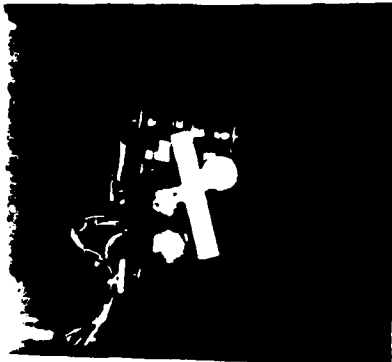
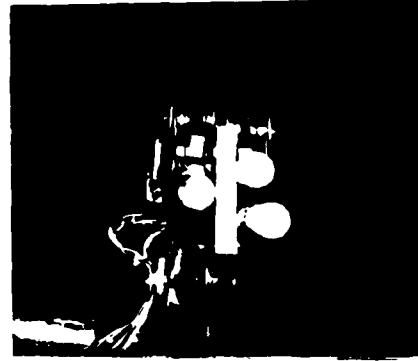
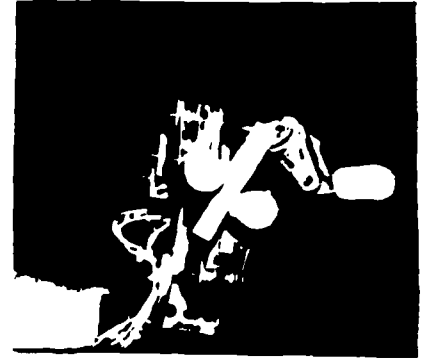
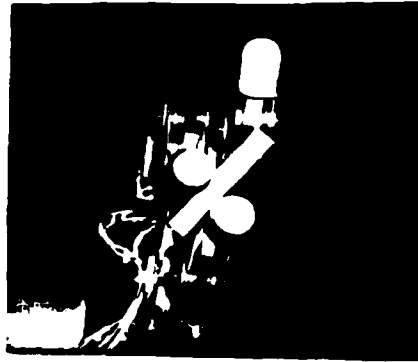
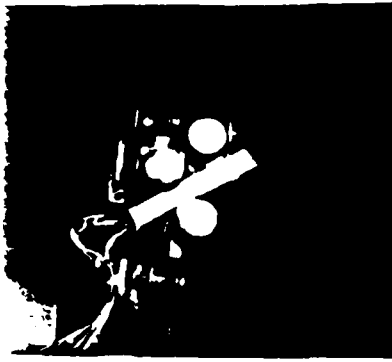


Figure I-11.

Twirling demonstration.

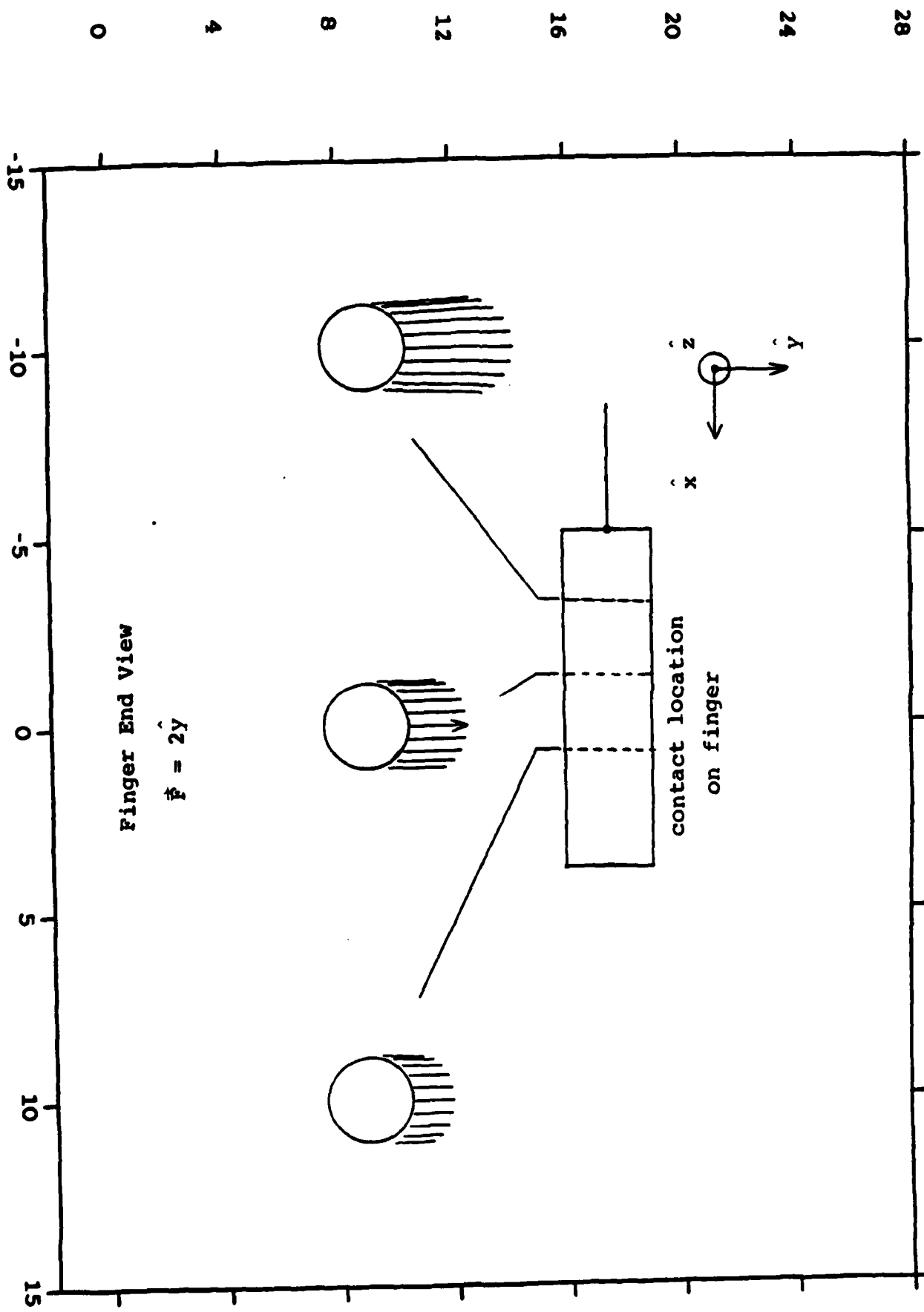
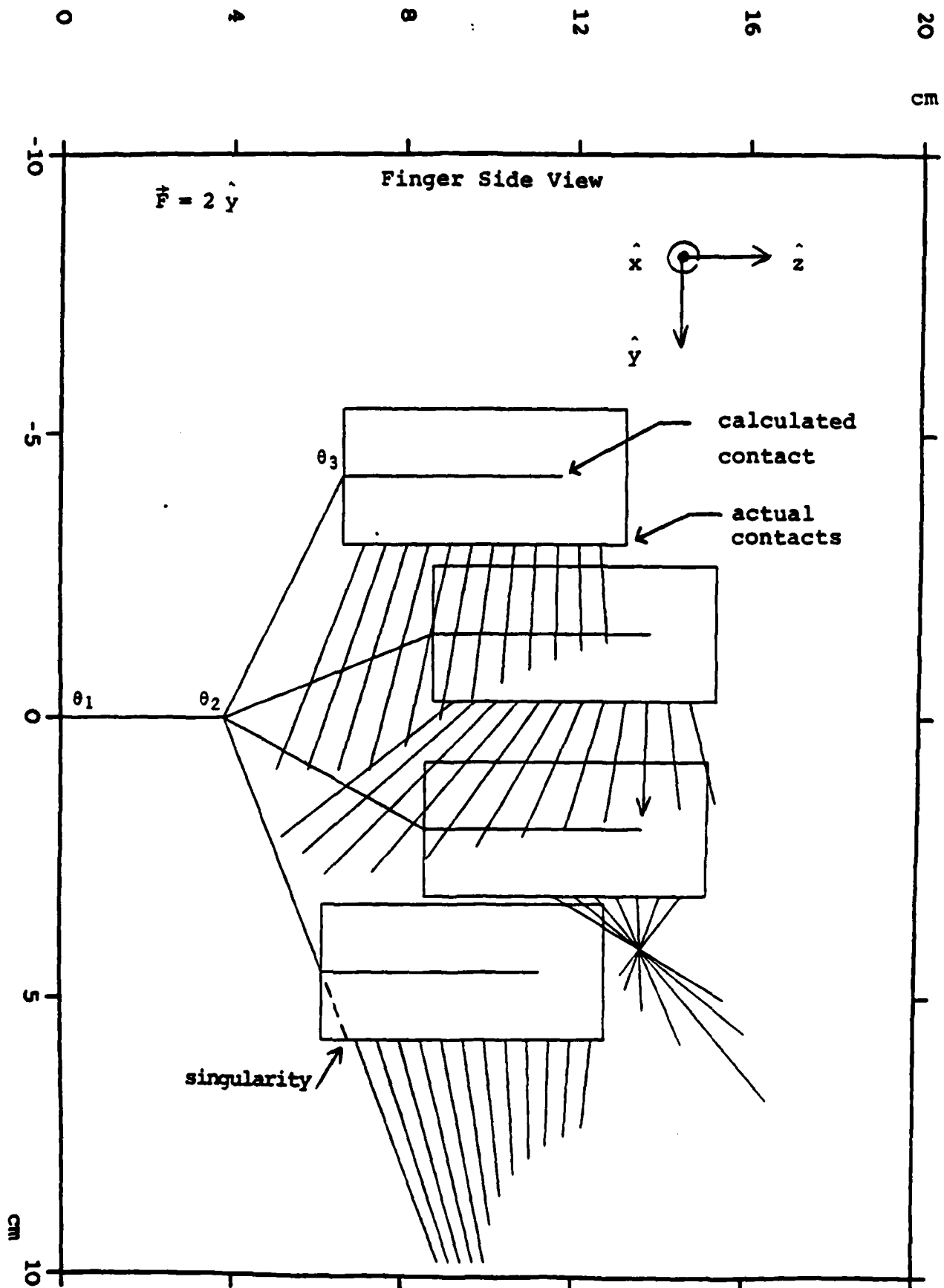
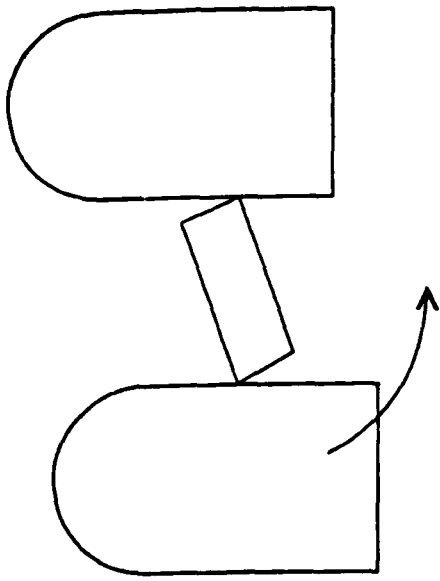


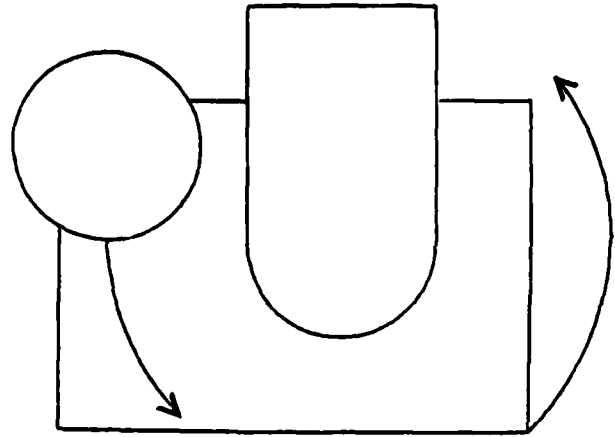
Figure I-12. Force errors around finger circumference.



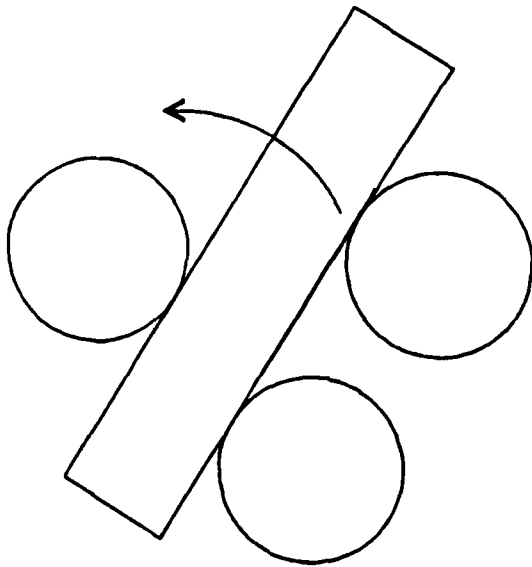
**Figure I-13. Force errors along finger length.**



Pitch



Yaw



Roll ("Twirl")

**Figure I-14. Three basic object rotations.**

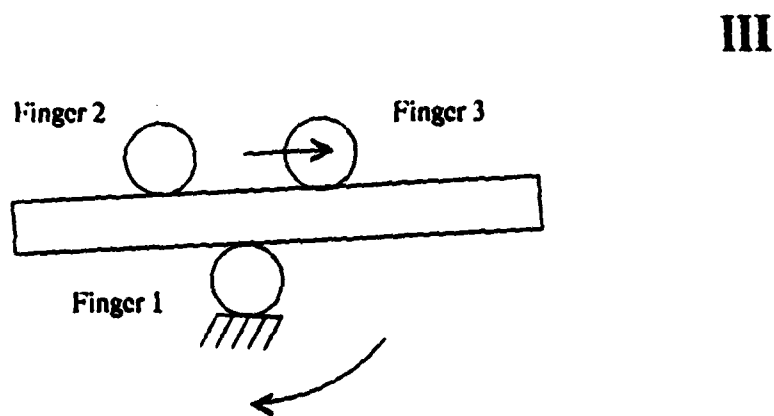
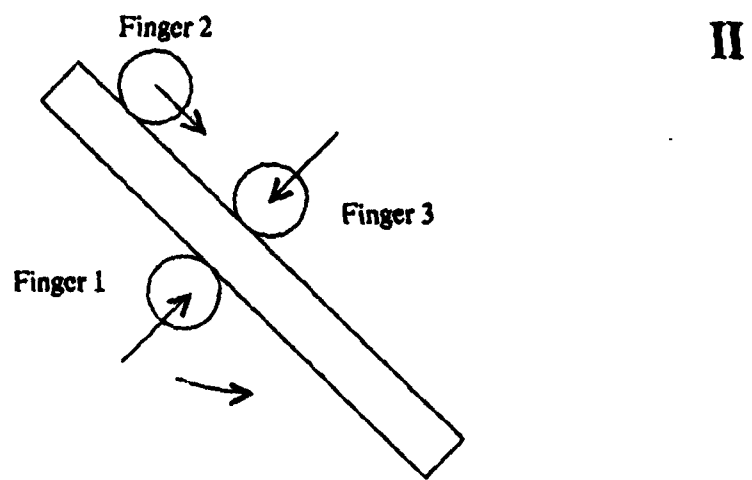
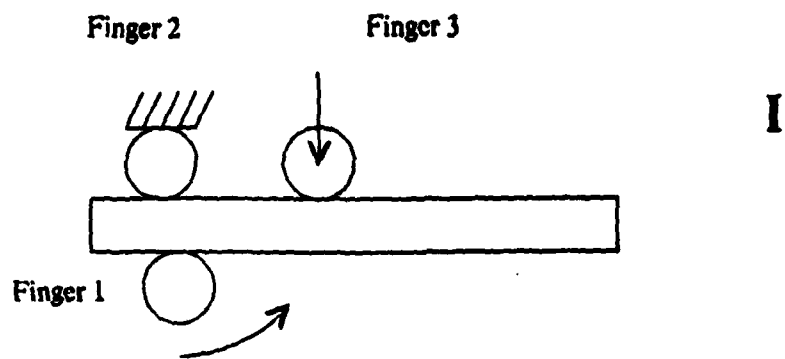


**Figure I-15. Translating object with three fingers.**

objects from sparse information provided by a few contacts of sensory fingers. Position, surface orientation, and curvature of object surface obtained from touch sensing of each of three fingers provide the sensory input. The recognition regime is based on analyzing models of known objects to determine a database of grasp parameters of stable grasps. This work was aimed at extending work by Lozano-Perez and Grimson.

### **Computation Power**

New capabilities developed for hand task programs now consume all of the PDP11/60 computer. Construction of a multi-microprocessor system was undertaken to provide increased computation power. It was designed, then a two processor experimental version was tested to verify the design, and components were ordered for a seven processor system which is now under construction. Benchmark programs were run which indicate that its performance will be a factor of five times that of the PDP11/60. In addition, it will have vastly superior real-time response and communication bandwidth for interfacing to sensors and mechanical devices. Software development is underway. Software development includes task decomposition, communication and synchronization, display, debugging, file handling, editing, and system utilities. A single processor version of the hand program is expected to run in October 1985. The multi-processor system NYMPH is expected to be first operational in November.

Running on the PDP 11/60, the hand was limited to a 33 Hz servo rate for the spherical force servo level, and 100 Hz for the joint and motor level servo that controls joint torques. Using simple control schemes such as tendon tension regulators on each motor, these servo rates give a very marginally stable force control system. To improve performance, either higher servo rates, or improved dynamic control algorithms are required. Both options require significant computational power. In addition, incorporating tactile sensing data and high level object control descriptions requires more computation power.

After evaluating the options which included a larger minicomputer like a VAX 11/780, and 32 bit microcomputers, we chose the National Semiconductor 32016 CPU for its speed, availability, and ease of use. This processor has a measured performance of 40% of a VAX 11/780 on identical C programs. As of the end of summer '85 all hardware pieces of the NYMPH system were in place, and development had started on partitioning the 3 finger hand code to run on 7 processors as shown in Figure I-16. Each processor has 512K bytes of local dual ported memory (four times that of the 11/60), so there will be ample room for fast lookup tables for trigonometric functions, which will give even more performance improvement over the PDP 11/60.

With the multiprocessor configuration shown, we expect to run the joint servo at 200 Hz, and the spherical force servo at about 70 Hz. Adequate computation power should remain at this level to adjust force control strategies based on the object's attitude in the hand. The tactile information processor will be determining contact type, location, and net forces at some rate between 10 - 30 Hz.

An important consideration is the latency between detecting a change at the finger contacts, and effecting a change at the finger joints. With this proposed structure, the primary delay will be due to the tactile processing. Another limit on throughput can be the bandwidth of the Multibus, which will limit the addition of more processors. Estimates

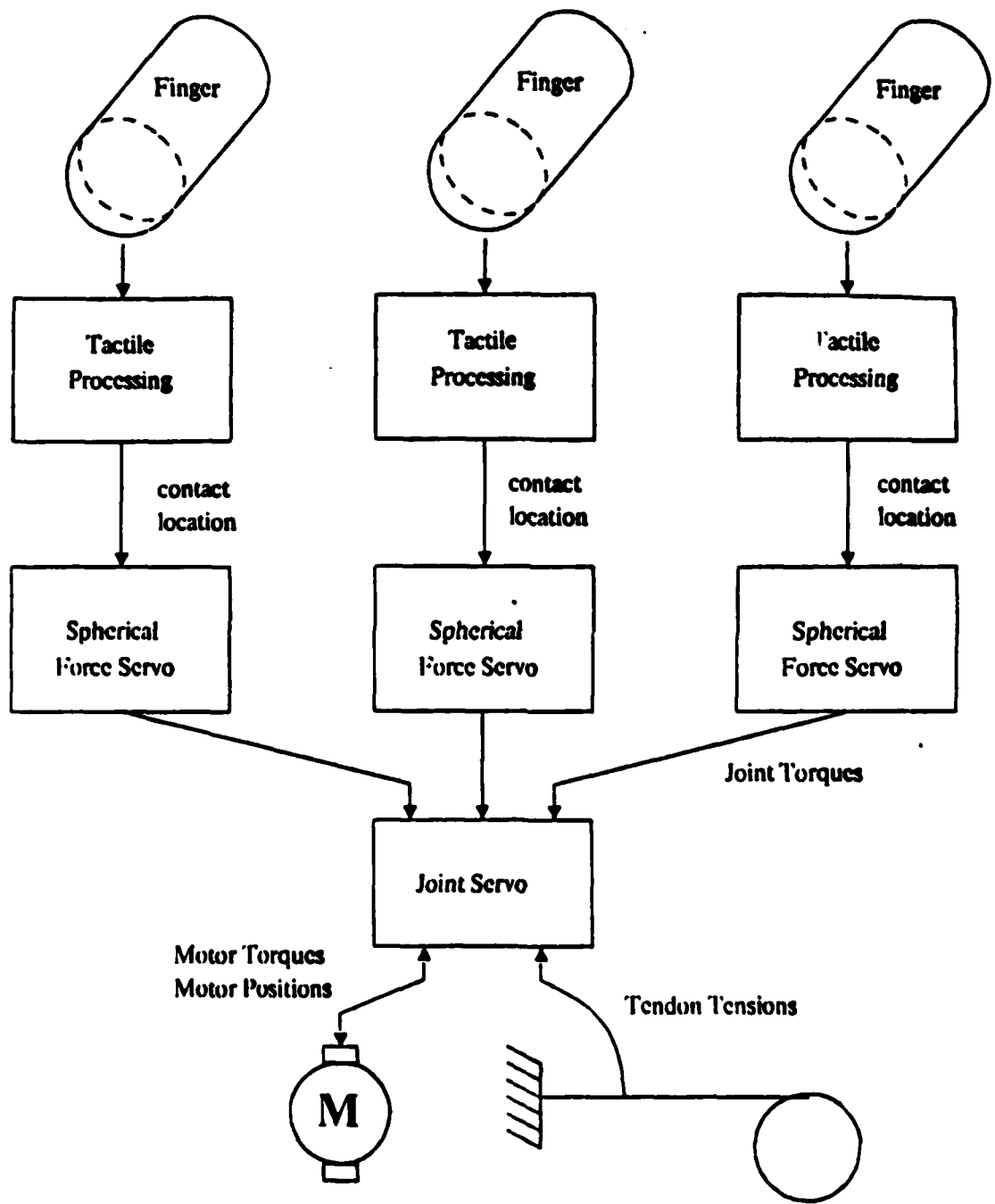


**Figure I-16. Multiprocessor system for Stanford/JPL Hand.**

indicate that the Multibus will be about 10% occupied, which is comfortable.

J. Bradley Chen developed a software message processing protocol to provide terminal IO and network file transfer to the multiprocessor system with a Sun-2 processor. The Sun, running under the V kernel (a distributed message based operating system), provides a powerful window-based user interface for development of programs that simultaneously execute on various processors. A window is opened for terminal IO to each 32016 CPU board, so debugging information is visible from all processors at once.

## **Plans**

**85-86:**

During the next year, we plan to:

1. Continue developing open loop force strategies for object re-orientation, developing the complete set of fundamental rotations, getting rotations in two directions mutually perpendicular to the "twirling" plane. This will give roll, pitch, and yaw control to grasped general cylinders of constant cross section and normal spine. We hope to develop gross translation capability, such as sliding a bar along between 3 fingers; alternately translating and regrasping it. This type of motion should easily fit into our current force control strategies.
2. Develop tactile processing capability — determine contact location and magnitude from the 8 x 8 tactile array finger tip. Accurately determine transduction characteristics of the sensors we have in order to improve their design.
3. Mount the tactile sensor electronics on the hand.
4. Complete hardware and software development of the multi-microprocessor system and convert hand software.
5. Implement closed loop grasping using 3 8x8 tactile sensing finger tips. This will need the full processing power of the NYMPH system.

## TECHNICAL REPORT

### PART II: FORCE CONTROL OF VERY FLEXIBLE MANIPULATORS

#### Summary of Project Accomplishments

This DARPA-supported research is focused on demonstrating new capabilities for touch and force control, on slew-and-touch control, and on the extensions of control theory necessary to achieve them.

During the three years of this contract we accomplished essentially all of our objectives, as guided by Section 4.1 (Technical Requirements) of our DARPA Contract:\* and in addition, we established and met some valuable new objectives that had not been thought of three years ago.

First, we conceived, designed, and built three experimental systems:

- a) A very flexible robot-manipulator arm (Fig. II-1(a) and (b) and Fig. II-2) having both end-point position (optical) and end-point force sensors to be used by the control system for tight control.
- b) A second very flexible arm with a separately-driven fast "wrist" mounted at its end (Fig. II-1(c) and (d) and Fig. II-24(a)). The wrist tip has its own position (optical) and force (load cell) sensors.
- c) A two-link arm (Fig. II-1 (e) and Fig. II-27) whose links (bones) are light and rigid, but whose drive train (tendon system) is very flexible. (This system was developed jointly with both DARPA and AFOSR support, and is used for different experiments in the two programs.)

After building the experimental systems, we carried out experiments and performed demonstrations which are documented below and (more at length) in separate reports, and which are also recorded on video tape. The experiments/demonstrations include the following:

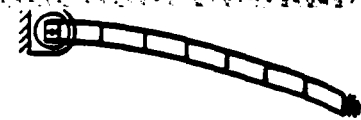
1. Flexible Arm (Task 1 and Tasks 4, 5, 6, 7 of the DARPA Contract). Performance by the very flexible arm (a above), in a slew-and-touch maneuver to a moving target (Task 1). The absolute physical limits on slew velocity, control speed (time delay and bandwidth), and force envelope were determined as part of this research, and control near these limits was demonstrated (for the first time), as reported in Section II-1 below. These demonstrations also fulfill specifically the requirements of Tasks 5,\*\* 6, and 7, as will be discussed in detail in what follows.
2. End Point Sensors (Task 2). Position, force, and (surrogate) proximity sensors were developed in conjunction with Task 1, and were an integral part of the demonstrations described above.

---

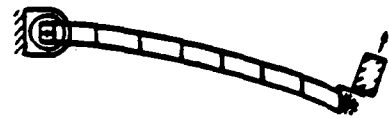
\* For convenience, this section of the Contract Statement of Work is provided as Appendix A hercof.

\*\* We are, however, remiss in that DD form 1423 was not submitted beforehand.

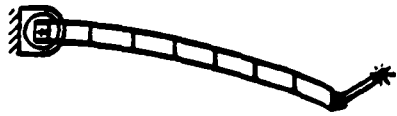
(a) **Very Flexible One-Link Manipulator**  
(Rapid pick and place.)



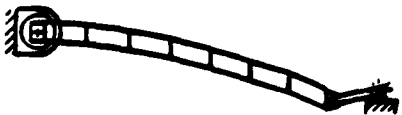
(b) **Very Flexible Manipulator with Force Control**  
(Slew and Touch moving target.)



(c) **Flexible Manipulator with Fast Wrist**  
(Precise snatch and place.)



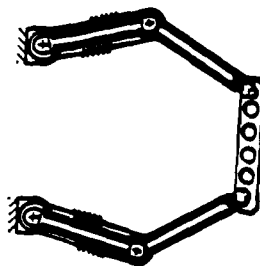
(d) **Flexible Manipulator with Fast Wrist**  
(Slew and Precision touch.)



(e) **Two-Link Arm with Elastic Tendons**  
(2D pick and place; slew and position touch.)



(f) **Cooperating Two-Link Arms**  
(Long-part handling.)



(g) **Two-Link Arm with Double Wrist**  
(Very fast precise 2D tasks.)



(h) **Two-Flexible-Link Arm**



**Figure II-1. Sequence of Experimental systems,  
(A through E built and tested; F through H under development)**

3. **Three New Robotic Arm System Designs (Task 3.)** These designs have been carried out, and two of them, — systems *b* and *c* above — have also been built (not required by the work statement); and preliminary tests have been run, with some very interesting results reported in Sections II-2 and II-3 below. The first demonstration (also not required for these systems) was of slew-and-touch control for Flexible Arm With Wrist System *b* (a two-revolute-joint system), in which a tenfold improvement in force-control speed and precision has already been achieved, with a minimization of target impulse force. (Report Section II-2 below). The second demonstration was of end-point position (but not yet force) feedback control of the two-revolute-joint two-link System *c*. This last demonstration was accomplished — using the DARPA-Air Force two-link facility — as part of our AFOSR supported research: but it has important implications for our DARPA work on force control, and is therefore described briefly, for reference, in Report Section II-3 below.
4. **Two Cooperating Arms.** The most advanced system designed under Task 3 of this contract is a pair of cooperating arms to be controlled as a system. Each arm has two main links (driven by tendons as in System *c* above), supporting a three-axis wrist and gripper, for a total of 5 revolute joints. Thus the entire system, which is to be controlled by a single digital controller, has 10 revolute joints. This system is to be built, and extensive research carried out with it, under a new DARPA contract. The design's features are described in Section II-4 below.
5. Another important development that was not part of our original task statement is an experimental inner-loop system for tight control of robot joint torques. This capability — reported on in Section II-5 below — will contribute importantly to all of our future manipulator control research.

Before presenting our report on each research and demonstration activity (Section II-1 through II-5), we address further Statement of Work Task 3.

#### **New Arm Designs (Task 3)**

Several different aspects of our research concerned new robotic designs, the subject of Task 3 in the statement of work. The three main areas were the design and testing of a fast wrist for force control, design of an improved flexible drive system for the two link manipulator, and the analysis and design of a pair of full six-degree-of-freedom manipulators for research on endpoint force control and cooperative manipulation. These designs have the common characteristics of decreased mass and rapid tip motion, as specified in Task 4.1.3.1. All three have at least two revolute joints: the cooperative arm design has five revolute joints in each of the manipulators.

Impulsive force transients on targets were minimized by a variety of techniques (SOW 4.1.3.1.2.) These included the use of compliant structure and sensors (Ref. 8), the use of a low-mass minimanipulator in both position and force control, the use of compliant drive systems, and the use of joint-torque control to improve transient response.

A study of the mass distribution of minimanipulators was performed, to provide understanding of the effect of mass distribution on dynamic performance. This led to an understanding of both manipulator design criteria and sensor placement for optimum response.

## SECTION II-1: FORCE CONTROL OF A SINGLE, VERY FLEXIBLE MANIPULATOR

This Section describes work now completed by James Maples — that completes Task 1, 4, 5, 6, and 7 of the DARPA Contract. The work is reported fully in Ref. 8, of which 20 copies are forwarded with this Final Report. We summarize the results here.

### The DARPA-Contract Work Statement Tasks (Now Completed)

Previous work in our laboratory using a very flexible manipulator (Ref. 9) has shown that it is possible to achieve good control of the tip position of a very flexible manipulator beam using direct sensing of the endpoint position. Closed-loop bandwidths approaching the natural frequency of the first bending mode have been achieved.

*It has been the first and most extensive task under this DARPA contract to extend this earlier work to the realm of force control, to show (in Task 4.1.1) that precise control of contact forces is possible using feedback from a tip-mounted sensor on the robot arm, and to provide underlying theoretical structure for achieving such control. It has been a second, supporting objective to develop appropriate precision end-point sensors for demonstration purposes (Task 4.1.2).*

*A third objective that is central involves switching between Position Control and Force Control (Task 4.1.4). For any force control system to be truly useful, it must be capable of switching from position mode to force mode as initial contact is made, and vice versa when departing from an object. There are two reasons why switching is so important — and so difficult. The first is that during touchdown, the dynamics of the structure are changing abruptly. As the transition is made from position to touch, the bending modes of the beam change frequencies, and the rigid body mode disappears completely. The control system must be able to cope with this change in dynamics as it touches down gently on the target. The second reason relates to switching between sensor sets. This occurs during touchdown, but also can occur at other times, such as when a sensor is occluded or out of range. The study of these switching issues, with special attention to the initial touchdown transition, is also included in this research.*

Some of the major results and conclusions of this research are:

#### Task 4.1.1

- It has been demonstrated experimentally that it is possible to achieve good, fast closed-loop control of a flexible manipulator using end-point feedback of either position or force, and generic methodology for doing so has been developed.
- It has been established and demonstrated that the limit to performance of force control of a single robot-link beam is caused by the time delay required for a wave to propagate the length of the beam.
- Fast, smooth slew-and-touch have been demonstrated to both a stationary and a moving target.

- It has been established and demonstrated that, for a given manipulator and target, the initial force overshoot is a function only of the approach velocity.

#### **Task 4.1.3**

- Four different sensors have been developed and demonstrated in fast slew-and-touch maneuvers. Two are force sensors (one a cantilever "finger", the other a load cell). One is a contact sensor (using fiber optics). The fourth is an optical end-point position sensing system with which multiple points can be sensed precisely and reported continuously to the control computer.

#### **Task 4.1.4**

- Techniques have been developed and demonstrated to switch control parameters to accommodate smoothly to rapid changes from one plant condition to another, e.g., from position to touch. In particular, it is found that, given a fast estimator of the plant states, the switching algorithm can be especially simple.
- The possibility has been discovered and demonstrated of a sustained or unstable bouncing condition even when proper control algorithms are applied and are appropriately switched. Techniques to avoid and recover from bouncing are developed and demonstrated.

## TASK 4.1.1: CONTROL OF TIP FORCE AND TIP POSITION OF A FLEXIBLE MANIPULATOR; AND SLEW-AND-TOUCH MANEUVERS

### Experimental Design

*Rationale.* To study the interaction of structural flexibility and servo performance in a fundamental way, it was decided to build an experimental apparatus that would highlight the specific issues we wished to address, while avoiding as much as possible any complicating side issues. Two areas in particular were felt to be inappropriate for these experiments: having a manipulator with time-varying geometry, and accounting for gravitational effects on a flexible manipulator link. Accordingly, it was decided to use a single link manipulator, and to work with flexibility only in the horizontal plane. Once the issues of flexibility and servo performance are understood in this setting, they can be extended to other, more complicated cases.

Having made this decision, it was then decided to exaggerate the problem on which we wished to focus: flexibility of the link member itself. The manipulator beam constructed for these experiments is extremely flexible in the horizontal plane, with its lowest frequencies in the 1 Hz range. By having this exaggerated, time-scaled version of an industrial manipulator, we required that the problem of controlling a non-colocated system be solved in a much more fundamental way than ever before. \*

A second advantage of having the resonant frequencies in this range is that it allows motions to proceed slowly enough so that they are visible to the unaided eye, greatly increasing the ability to develop an intuitive feel for the action of the control algorithms. As a further benefit, the lower frequencies also allow for slower sampling rates. This means that control algorithms can be written in a higher level computer language (e.g., FORTRAN), making it easier to modify these routines as knowledge of the problem is gained.

It is interesting to compare the fundamental frequencies of the manipulator used here with those of some commercially available robot arms. Values of 40, 20 or even 10 Hz are found in common, supposedly "stiff" industrial manipulators (Ref. 8). In the case of the space shuttle's remote manipulator, the resonant frequencies are quite comparable with those of the present experiments. It should be kept in mind, then, that although the theory developed here was experimentally verified on a low frequency manipulator, the results scale easily to the frequencies found in other manipulators. The same phenomena occur, but the time scale is 10 or 20 times faster.

To get a concrete feel for the setting of the experiments, results, and conclusions presented in this dissertation, the rest of this chapter is devoted to familiarizing the reader with the flexible beam apparatus itself, along with the supporting actuator, sensors, and electronics.

*Experimental Equipment.* The basic layout of the experimental apparatus used in this research is shown in Figure II-2. The flexible beam itself is approximately 48 inches long

---

\* The original design concept for the flexible beam was developed by Moshe Tekacz and Eric Schmitz in connection with other research in our laboratory (Ref. 9).

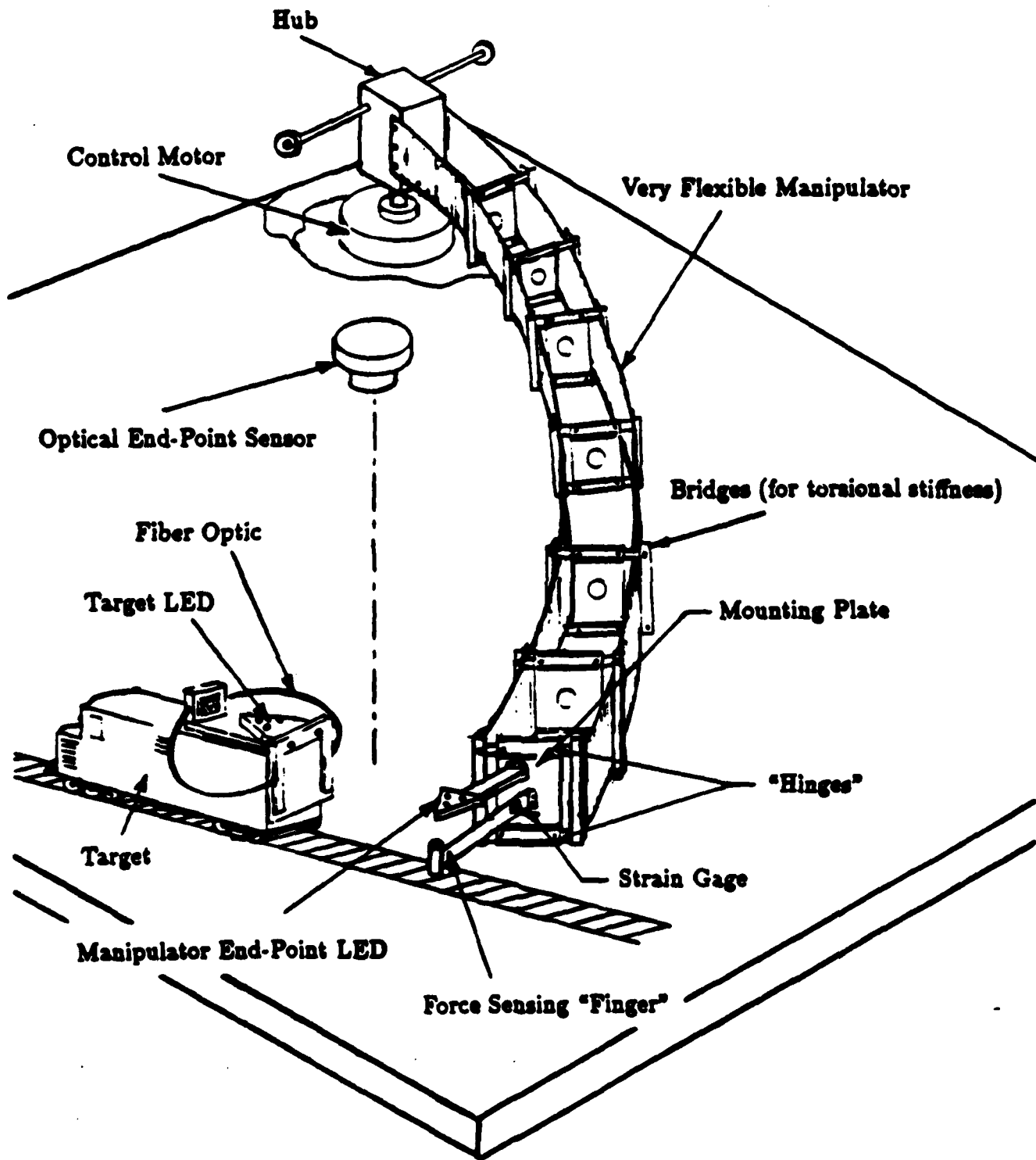


**Figure II-2. Apparatus for Force Control of Very Flexible Manipulator.**

and is constructed of two side plates of 0.040 inch thick aluminum. These side plates are held together by eight "bridges" which are connected to the side plates through beryllium copper flexures. This arrangement of side plates and bridges allows the beam to flex easily in the horizontal plane, while maintaining stiffness in torsion and in the vertical plane. The lowest frequency of vibration for this apparatus occurs with the hub clamped and the beam vibrating in its lowest cantilever mode. This vibration has a period of approximately 2 seconds or a natural frequency of 0.5 Hz. With the hub free to rotate, the first pinned-free resonant mode occurs at 1.8 Hz.

Associated with the beam is a target which is used for tracking and for touching with the force sensor. To keep things simple, it was decided to use a model HO railroad train as the tracking target. Although its performance is very limited, it does serve the purpose, while also providing a bit of levity to the setup. Not immediately apparent from the diagram is the fact that the target is constrained to move only in a circular arc. This makes tracking a one dimensional problem, to match the single degree of freedom of the beam.

There are a single actuator and multiple sensors attached to the manipulator beam. At the hub of the beam is a limited-angle, brushless DC torquer. Also on the hub shaft is a plastic film potentiometer. The signal from the hub potentiometer is passed through an analog differentiator to get a derived rate signal which is read into the control computer (along with the other sensor signals) via a 12 bit A/D converter. Both the torquer and the potentiometer were chosen for their very low friction characteristics. Since there is no brush friction or motor cogging, the beam swings quite freely, with the primary disturbance coming from the wires attaching to the beam at the hub. (If the table is not kept very close to level, the arm swings freely enough so that it will move to a preferred position.)

Along the length of the beam, approximately equally spaced, are a series of eight strain gage pairs to measure the bending of the beam. All eight strain gages are used for open loop testing to characterize the beam; however, under closed loop control, only one set is used. The output from this gage pair is also sent through an analog differentiator to get a rate signal.

At the tip of the beam are two pieces of instrumentation. The first is a strain gage equipped "finger" which can measure the contact force developed when the beam touches down on the target. Contact forces are in the range of 5-30 grams. The second piece of apparatus is a set of LED's (light emitting diodes) whose light output is detected by an optical sensor placed overhead. This sensor can determine the position of the tip of the beam with a repeatability of 1 mm, although the absolute accuracy is much worse. Not shown in the diagram is a hood over the optical sensor which prevents stray light from contaminating the signal.

The target train carries a duplicate set of LED's. By using a time multiplexing technique, the single optical sensor can track the position of both the train and the beam. This is done by illuminating the LED's on the beam for a brief instant and then turning on those on the target. This successive illumination is repeated over and over again at a very rapid rate (1000 Hz) so that information from each set of LED's appears to be instantaneous.

Also mounted on the target is a fiber optic touch sensor. This device uses fiber optics

to shine a beam of light horizontally across the face of the touchdown pad. When the finger from the beam makes contact with the target, the beam of light is broken, creating a signal which can be detected by the control computer. Knowing the exact instant of touchdown proved vital to obtaining a smooth transition from position to force control.

Closing the loop on this apparatus is an LSI 11/23 minicomputer. It is equipped with floating point hardware, a 12 bit multiplexed A/D converter, and a 12 bit D/A converter. All servo algorithms are interrupt driven at a 30 ms (33 Hz) rate.

### **Control Strategy**

There are three regimes for controlling the slew-and-touch maneuver: Position Control (before contact), Force Control (after contact), and Switching Control (exactly at contact). These will each be summarized.

### **Tip-Position Control System Design and Performance**

For position control the primary sensor consists of the overhead optics (Fig. II-2) sensing the location of the floating LED at the manipulator tip. This signal, together with certain others, is used by the estimator section of the control computer to compute all the instantaneous states of the system — i.e., the amount of each bending mode that is instantaneously present in its configuration. These reported states (some measured directly, the rest inferred by the estimator) are then used by the controller section to exert just the right torque at the manipulator's *hub* to cause the manipulator's *tip* to have followed commanded motions, vs. time, promptly, and to reject disturbances to the tip.

Such fast, stable control of the end point of a flexible manipulator member was achieved for the first time (in our laboratory) by Eric Schmits (Ref. 8); and the position control part of the present system is based on Schmits' design approach.

*Natural Frequencies:* Tip-free configuration. The first step is to establish, by experiment, a good mathematical model of the flexible-beam portion of the manipulator arm, which can then be used for the control computer. The specific manipulator arm of Fig. II-1a and Fig. II-2 was found, by measurement, to have the following first three natural frequencies when the tip is free:

$$\omega_1 = 1.78 Hz$$

$$\omega_2 = 3.28 Hz$$

$$\omega_3 = 7.21 Hz$$

and these were used (with their measured damping) by the estimator part of the control computer to model the manipulator, along with appropriate zeros (also measured). For example, the important transfer function from hub torque to manipulator tip is given by:

$$G(s)_{tip} = A_0 \frac{(s + 12.7)(s - 12.9)(s + 32.9 \pm j13.9)(s - 32.6 \pm j15.3)}{s(s + 0.2)(s + 0.2 \pm j11.2)(s + 0.4 \pm j20.6)(s + 0.9 \pm j45.3)} \quad (1)$$

Note the nonminimum phase zeros, which are associated with the wave propagation delay.

**Wave Propagation Speed.** Another open loop parameter that will prove to be of interest is the time it takes for a wave to propagate down the length of the beam. As has been previously shown (Ref. 8) this speed places a limit on the closed loop response of the beam. This response is measured in Figure II-3, where it is seen to be approximately 140 ms.

For reasons to be explained subsequently, a 2 Hz single pole filter has been placed in the signal line leading from the computer to the power amplifier for the hub motor. This filter adds delay to the response from computer output, (i.e., "CONTROL EFFORT" \*), to hub torque. Adding this to the wave propagation delay, the total delay — corresponding to the final experimental setup — is measured as 170 ms, an increase of 30 ms.

**Controller Design.** The position controller developed here for the flexible beam was designed using a discretized LQG optimal control algorithm. The computer program used for the design (called "DISC" (Ref. 6)) takes as input a continuous model of the plant along with a continuous quadratic loss function  $J$ .

$$J = \frac{1}{2} \int_0^{\infty} (\mathbf{x}^T \mathbf{A} \mathbf{x} + u^T \mathbf{B} u) dt \quad (2)$$

After discretizing both the plant model and the loss function, control design code DISC computes the full state feedback gains that minimize this performance index.

The resulting control gains are:

$$\mathbf{K} = (-43.6 \quad -17.9 \quad -106 \quad -5.71 \quad -168 \quad -1.69 \quad -7.90 \quad -3.78) \quad (3)$$

---

\* In all of the graphs presented here, the trace labeled "CONTROL EFFORT" is the output of the digital to analog converter. In all graphs of the closed-loop system, this signal was processed by the 2 Hz filter before being sent to the hub motor's power amplifier.

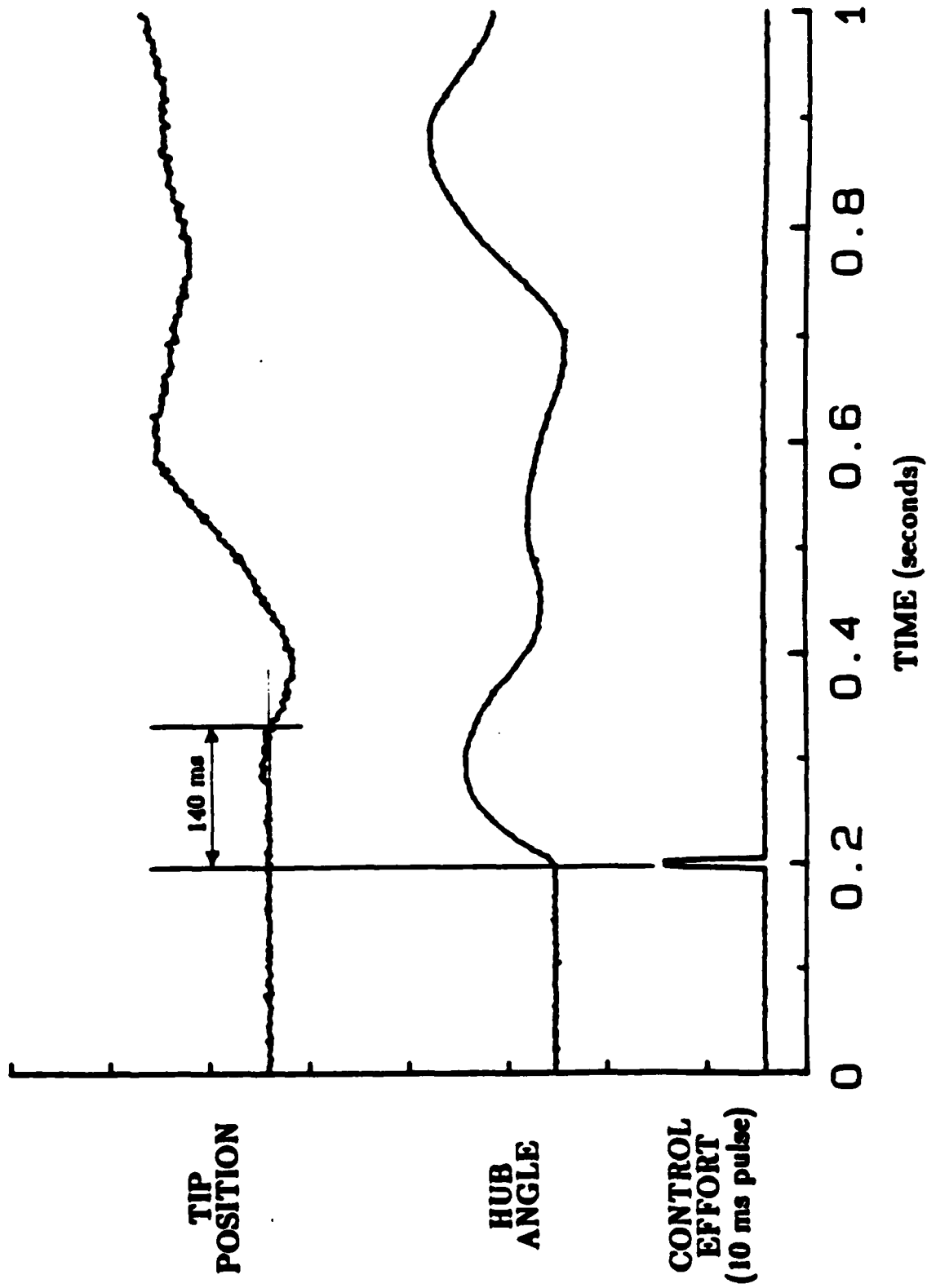


Figure II-3. Wave propagation time - position mode.

Using these control gains results in movement of the closed loop poles to:

$\omega_n$ (Hz)	$\zeta$
0.6	—
8.4	—
1.8	0.42
3.3	0.31
7.2	0.14

### Performance of Tip-Position Control System

*Response to Commands.* The closed loop step response of the final system is shown in Figure II-4. The command is a 4 inch positive step followed 5 seconds later by a negative 4 inch step returning to the original location. This response is shown with a faster time scale in Figure II-5.

To get an intuitive feel for the action of the beam during the step command, Figure II-6 shows a "stop-action" diagram of the beam in motion. It can be seen that while the hub goes quickly in the correct direction, the tip does nothing for a time while the wave propagates the length of the beam (A). Following this, the tip moves in the wrong direction due to the non-minimum phase characteristic of the beam (B). Eventually, the tip starts moving in the correct direction (C). However, as the tip whips over to the final position, the hub reverses itself to put on the brakes (D). Finally, as the tip reaches the newly commanded setpoint, the hub gradually relaxes to its final position, at the same time pumping down the energy stored in the bending modes of the beam.

*Disturbance Rejection.* The disturbance rejection of this controller is shown in Figure II-7. A disturbance has been introduced by an external force holding the beam tip at a fixed offset from the commanded position. As can be seen, once the beam is released, the tip position quickly returns to nominal. This can be contrasted with the response to disturbance seen in Figure II-8 which occurs when the tip sensor is occluded. This response is much slower due to the limitation on the speed of the hub based estimator.

### Tip-Force Control System Design and Performance

*Natural Frequencies: Touch Configuration.* Plant identification for the beam in contact with the target follows the same general lines as the identification process for position

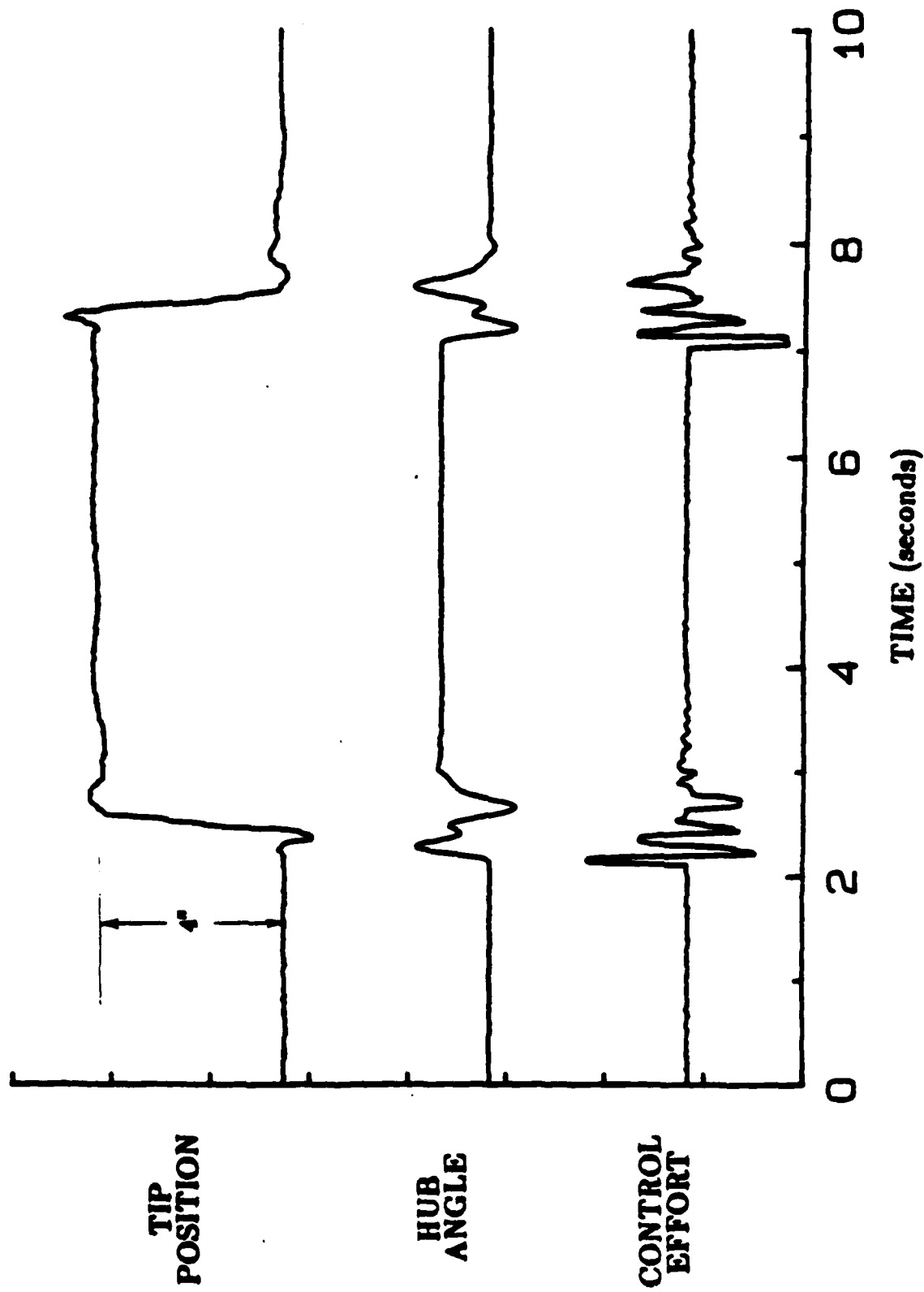


Figure II-4. Step response - position mode.

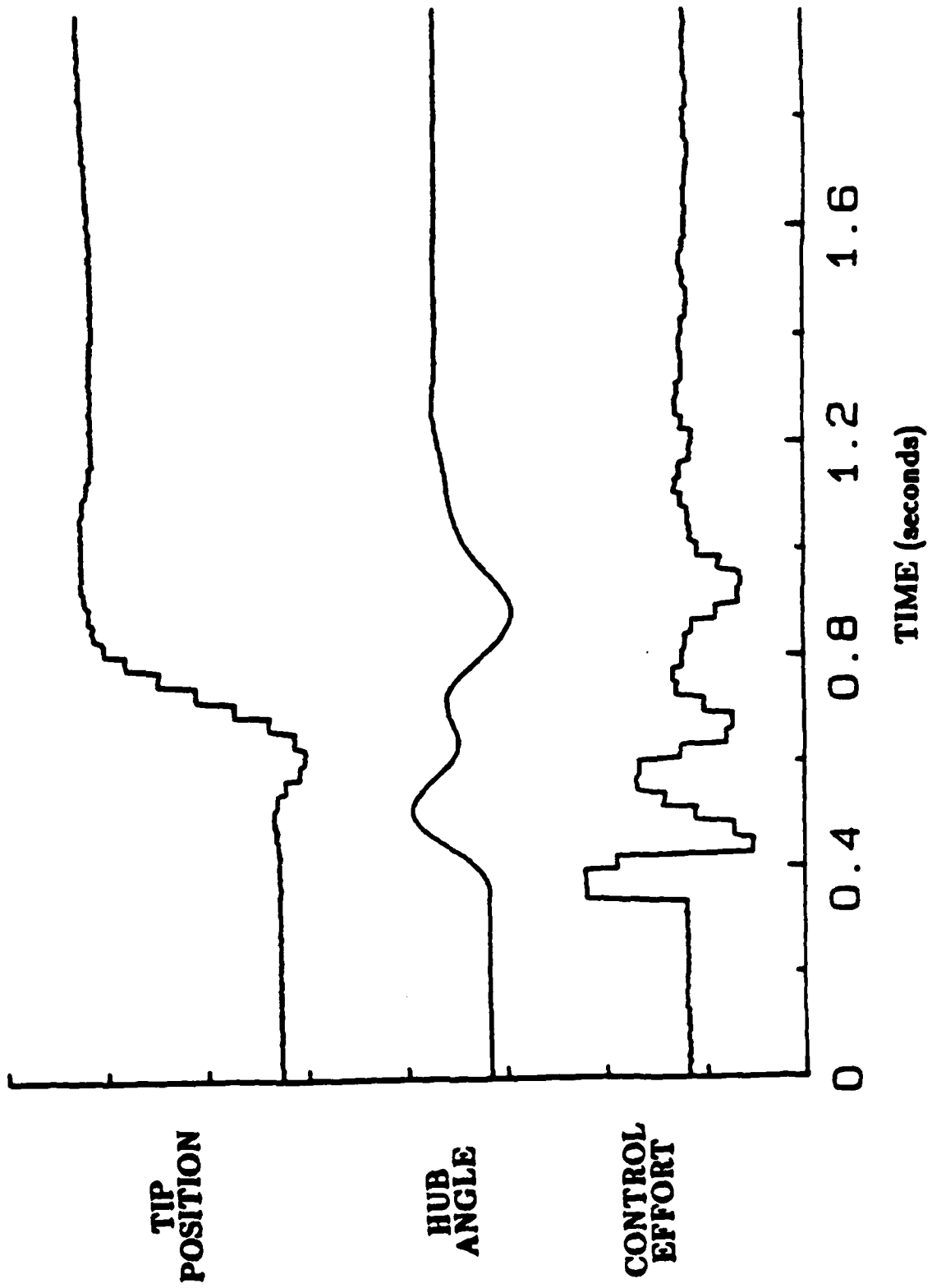
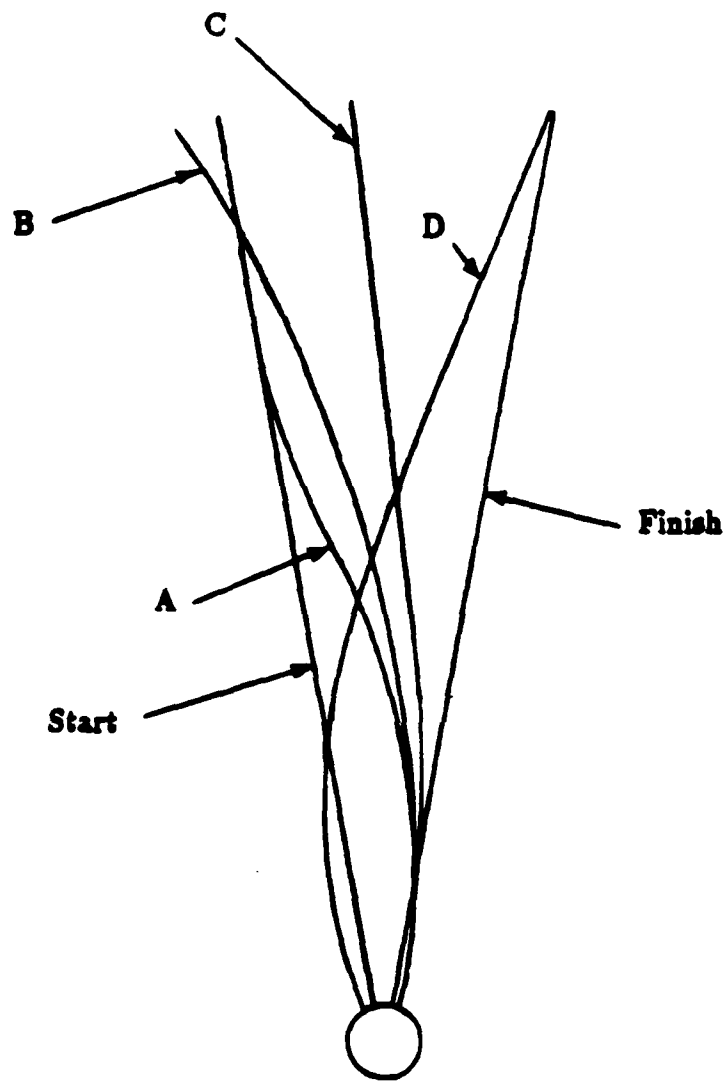


Figure II-5. Step response, expanded scale - position mode.



**Figure II-6. Beam shape during step command.**

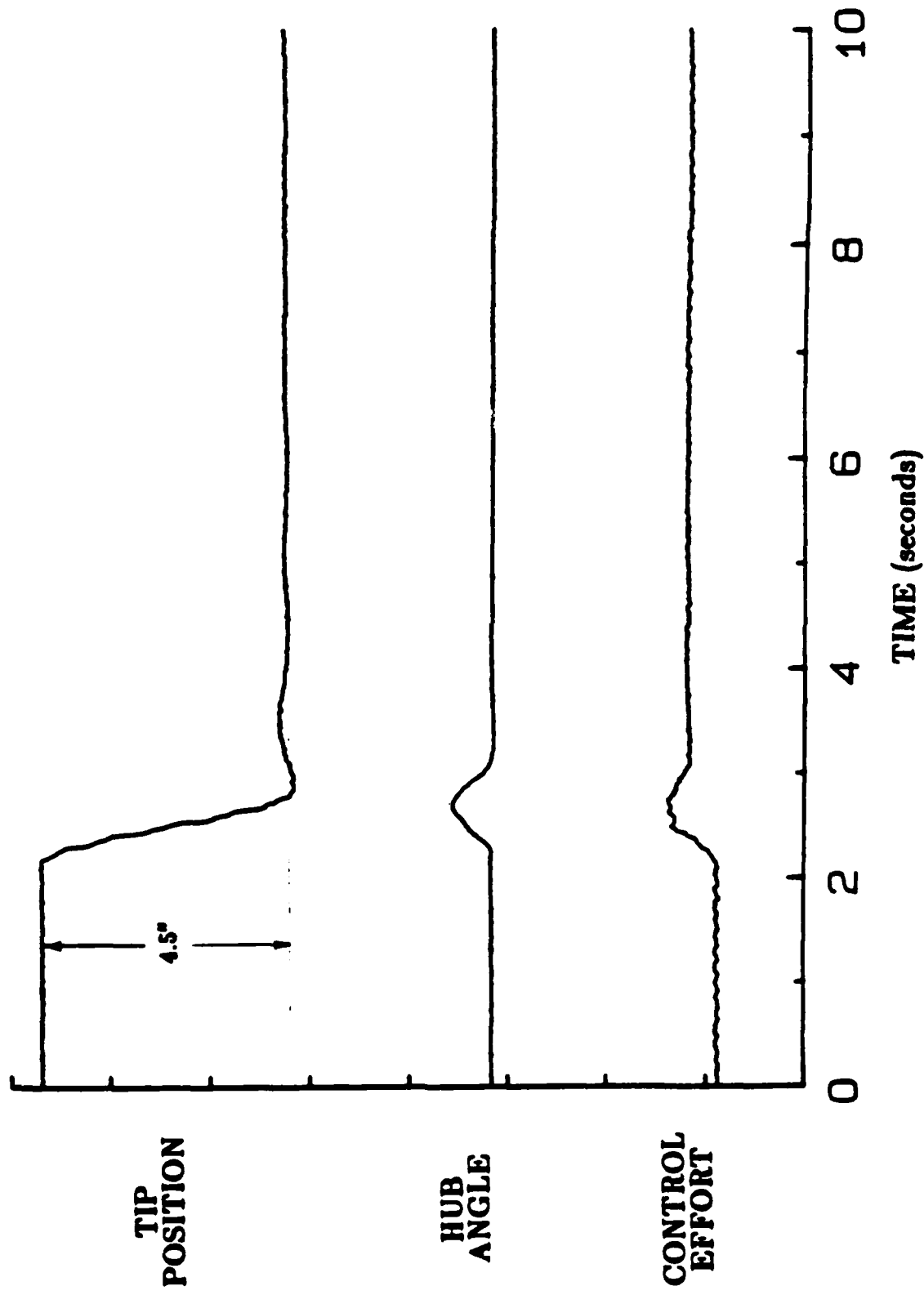


Figure II-7. Disturbance rejection using tip sensor.

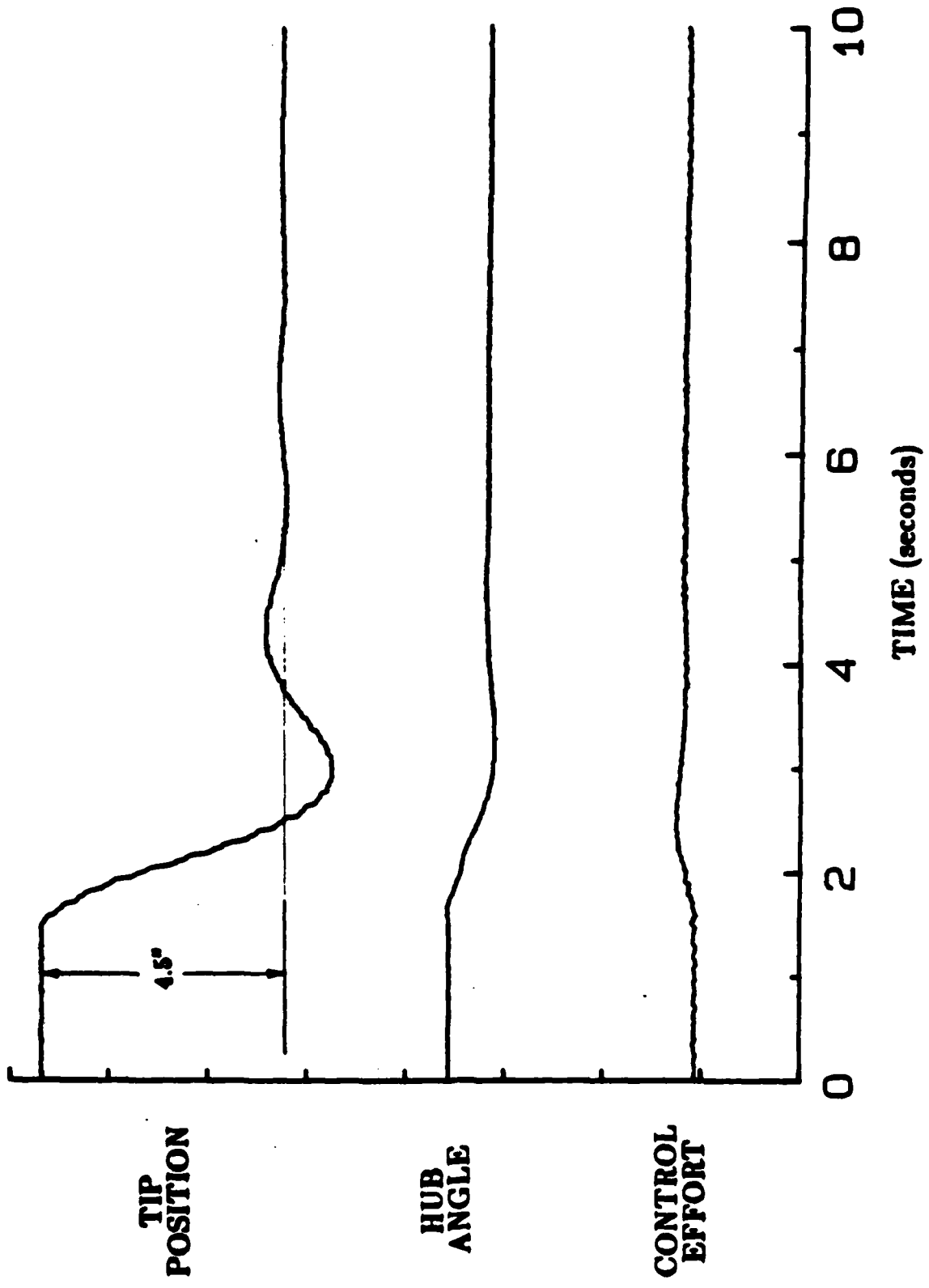


Figure II-8. Disturbance rejection without tip sensor.

mode. In the case of force control, there is no rigid body motion, and so  $\omega_0$  becomes the first flexible mode. For comparison purposes, the measured resonant frequencies of position mode and touch mode are listed side by side in Table 1, along with the zeros in the transfer function from hub torque to hub angle.

<u>POSITION</u>		<u>TOUCH</u>	
<u>rigid body</u>	———— pole ————	<u>0.99 Hz</u>	
<u>0.49 Hz</u>	———— zero ————	<u>1.39 Hz</u>	
<u>1.78 Hz</u>	———— pole ————	<u>2.35 Hz</u>	
<u>2.60 Hz</u>	———— zero ————	<u>3.24 Hz</u>	
<u>3.28 Hz</u>	———— pole ————	<u>3.64 Hz</u>	
<u>7.01 Hz</u>	———— zero ————	<u>7.22 Hz</u>	
<u>7.21 Hz</u>	———— pole ————	<u>7.52 Hz</u>	

Table 1 Resonant Frequency Comparison

The change in dynamics that occurs when the beam touches down (on a target) can be seen immediately. This change occurs abruptly and instantaneously, which is one of the reasons it is challenging to account for it in the control. The rigid body mode disappears completely; or looked at another way, it moves from zero frequency up to 0.99 Hz. The higher frequencies also shift up, the shift getting progressively less as we move up in frequency.

There are an infinite number of modes for the beam, whereas only the first four are shown. For the apparatus used here, the response of the beam falls off quite rapidly after the third bending mode. As shown in the tables, the separation of the pole-zero pair at the fourth bending mode (7 Hz) is down to only 4%. This near cancellation is also evidenced by the small residue for this pole in the partial fraction expansion of the transfer function. During the identification process it was difficult to separate these two frequencies. As we progress to frequencies above this, the pole-zero spacing becomes very close, the residues become smaller, and in a practical sense, it is very hard to separate the pole-zero pairs for identification purposes.

*Controller Design.* As with position control, the force-control loop is closed on the beam by using a full state estimator and full-state feedback gains. The control gains are designed using the LQG optimal control design program DISC (Ref. 6). There are a few twists to this design which need explanation. One is the inclusion of integral control.

Initial attempts were made to use straightforward full state feedback, (corresponding to proportional plus derivative feedback). However, this author was never able to arrive at a controller that gave satisfactory command following performance using this technique. Conversely, as soon as integral control was added, the general performance, and command following response in particular, were very good. This author attributes this to the difference of the transfer functions of the beam in free mode versus touch mode. A quick inspection of these functions shows that they are actually quite similar except for the

double pole at the origin in free mode. This double integrator means that the total loop gain in position mode will always be very high at low frequencies. On the other hand, in touch mode, the open loop response is flat at DC. Because of this, the integrator is needed to give high loop gain at DC and to roll it off before reaching the resonances. In related work on force control of 6 degree of freedom industrial manipulators, this author has found that integral, or at least lag, and sometimes even double lag compensation can be used effectively (Ref. 8).

The method to apply an integrator in a digital control loop has been previously documented (Ref. 5). Only the results of the derivation are given here.

If we have a discrete-time system:\*

$$\mathbf{x}(k+1) = \Phi \mathbf{x}(k) + \Gamma u(k) \quad (3)$$

$$y(k) = \mathbf{H} \mathbf{x}(k) \quad (4)$$

then to add integral control, we form a new system:

$$\mathbf{w}(k+1) = \begin{pmatrix} \Phi & 0 \\ \mathbf{H} & 1 \end{pmatrix} \mathbf{w}(k) + \begin{pmatrix} \Gamma \\ 0 \end{pmatrix} u(k) \quad (5)$$

which contains the additional integrator state. Any suitable design method may be used to find a set of control gains for the new system. The resulting  $n+1$  control gains may be divided into a gain  $K_I = K_{n+1}$  which is the integrator gain, and the gains  $\mathbf{K}_0 = K_1 \dots K_n$ , which are the normal full state feedback gains. These are then applied as illustrated in Figure II-9.

The controller gains presented here were developed with the help of the Stanford program DISC, using an augmented loss matrix  $\mathbf{A}$  to which an extra row and column have been added to specify the loss for the integral error term. One special consideration for using this technique is that since the system matrices must be discretized before adding the integrator state, the inputs to DISC must all refer to discrete time values. This includes the loss matrices, which in position mode were input as continuous loss matrices that were converted to discrete time equivalents. Using discrete time loss matrices directly proved to present no particular difficulty for this problem.

The resulting control gains are:

$$\mathbf{K} = (-134 \quad -44.0 \quad -203 \quad 11.2 \quad -231 \quad -2.52 \quad -96.8 \quad -10.2 \quad -0.123) \quad (6)$$

---

\* Note that for a single actuator,  $y$  must be a scalar. It is the output variable to which we wish to apply integral control. This technique can be expanded to a non-scalar  $y$  for the case of multiple actuators.

and the closed loop pole locations are:

$\omega_n$ (Hz)	$\zeta$
1.2	—
1.8	0.91
3.3	0.55
4.5	0.24
7.1	0.62

### Performance of Tip-Force Control System

**Response to Commands.** The closed loop step response of the touch control system is shown in Figure II-10. As before, this response is also plotted with a faster time scale, Figure II-11. It is possible to get an open loop step response in touch mode, simply by commanding a step in torque to the hub motor. This could be considered a "before" picture, and is given for reference in Figure II-12.

An aspect of the closed loop step response that merits further explanation is the small amplitude limit cycle at approximately 8 Hz. It is very apparent in Figure II-10 in the steady state response just prior to the step, and again after the step has settled. This is indeed a limit cycle and not a growing instability, since it will continue indefinitely at a small amplitude.

After tracking this problem for some time, it was determined that this effect is due to a nonlinearity in the structure of the beam itself. It was experimentally verified that the frequency of the fourth bending mode is amplitude dependent at very small amplitudes, varying from 8.8 Hz at very low amplitudes to 7.7 Hz at moderate excitation levels. The exact cause of this nonlinearity has never been determined; a nonlinear spring effect is the chief suspect. In any event, the result is that making the system stable in the large makes it unstable at very low amplitudes. This instability will grow until the resonant frequency has shifted enough that it can be stabilized by the closed loop system.

**Disturbance Rejection.** Disturbance rejection is more difficult to illustrate in touch mode than in position mode due to the action of the integral controller. Response to a constant disturbance is excellent, with the integrator giving zero error within the limitations of the beam and torquer system. Dynamic response is a tougher problem. To give some illustration of the general character of response, an uncalibrated disturbance force was introduced at the tip of the beam and then released abruptly. The resulting curves are given in Figure II-13. The action of the hub in trying to counteract the disturbance as the integrator charges is clear. The integrator has a limiter on it, however, for this test, the beam was released before the integrator saturated. It is clear that the beam rebounds after the disturbance is released and takes some time to discharge the integrator. During this time the controller is also pumping down the bending modes which have been excited by the disturbance. Control then continues smoothly at the given setpoint.

To give some basis for comparison, the "disturbance rejection" of the open loop system

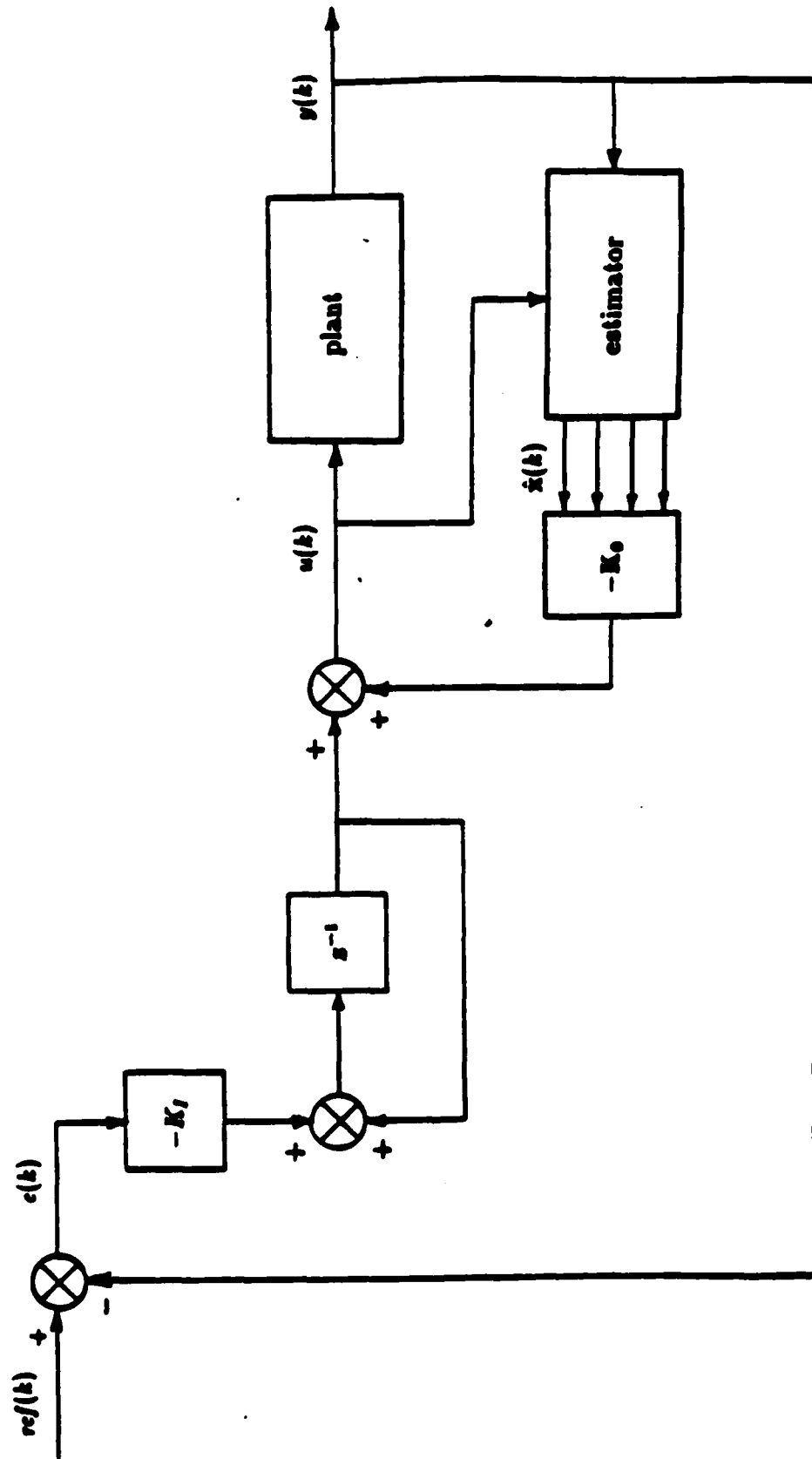


Figure II-9. Applying integral controller gains.

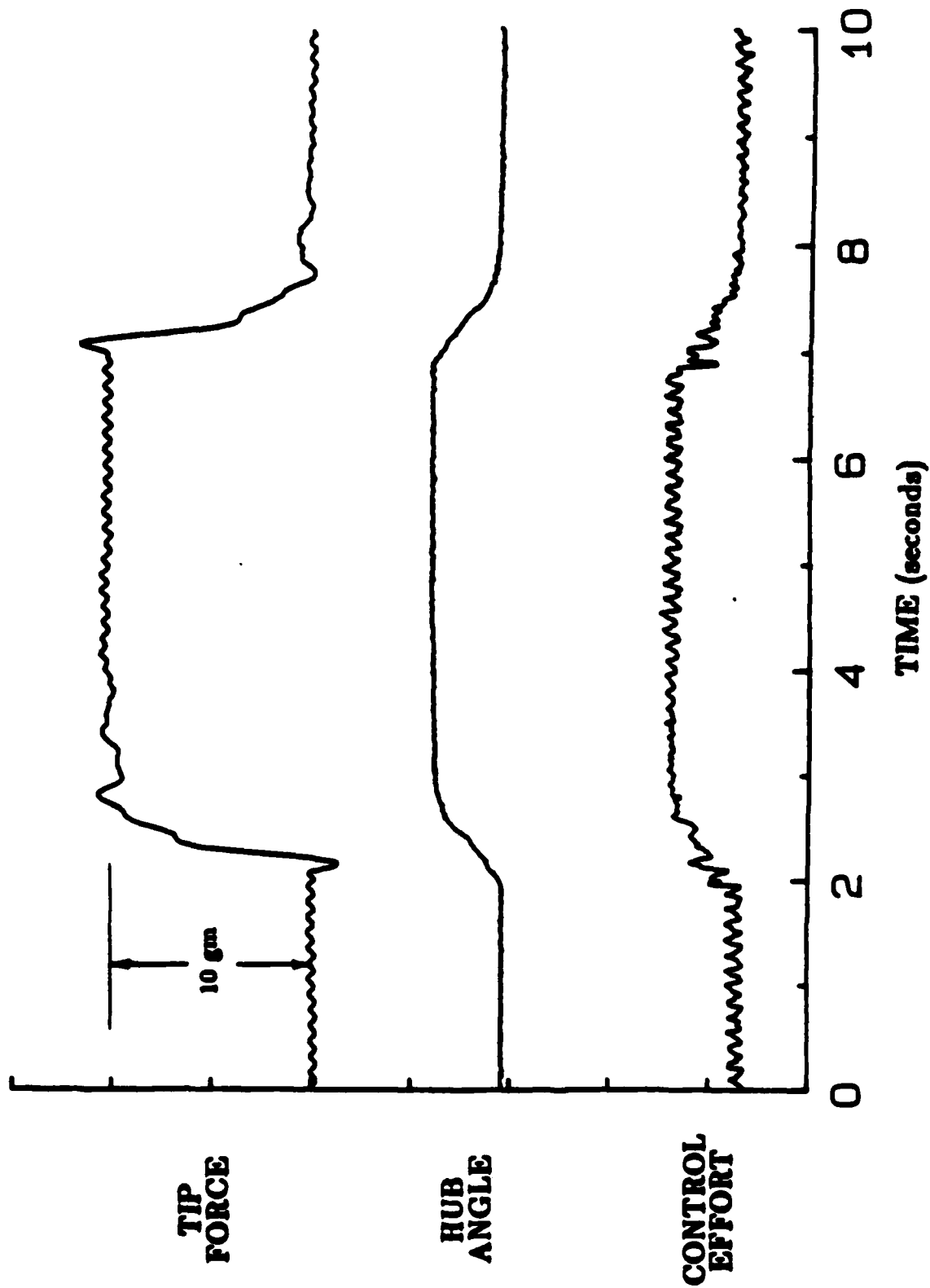


Figure II-10. Step response - touch mode.

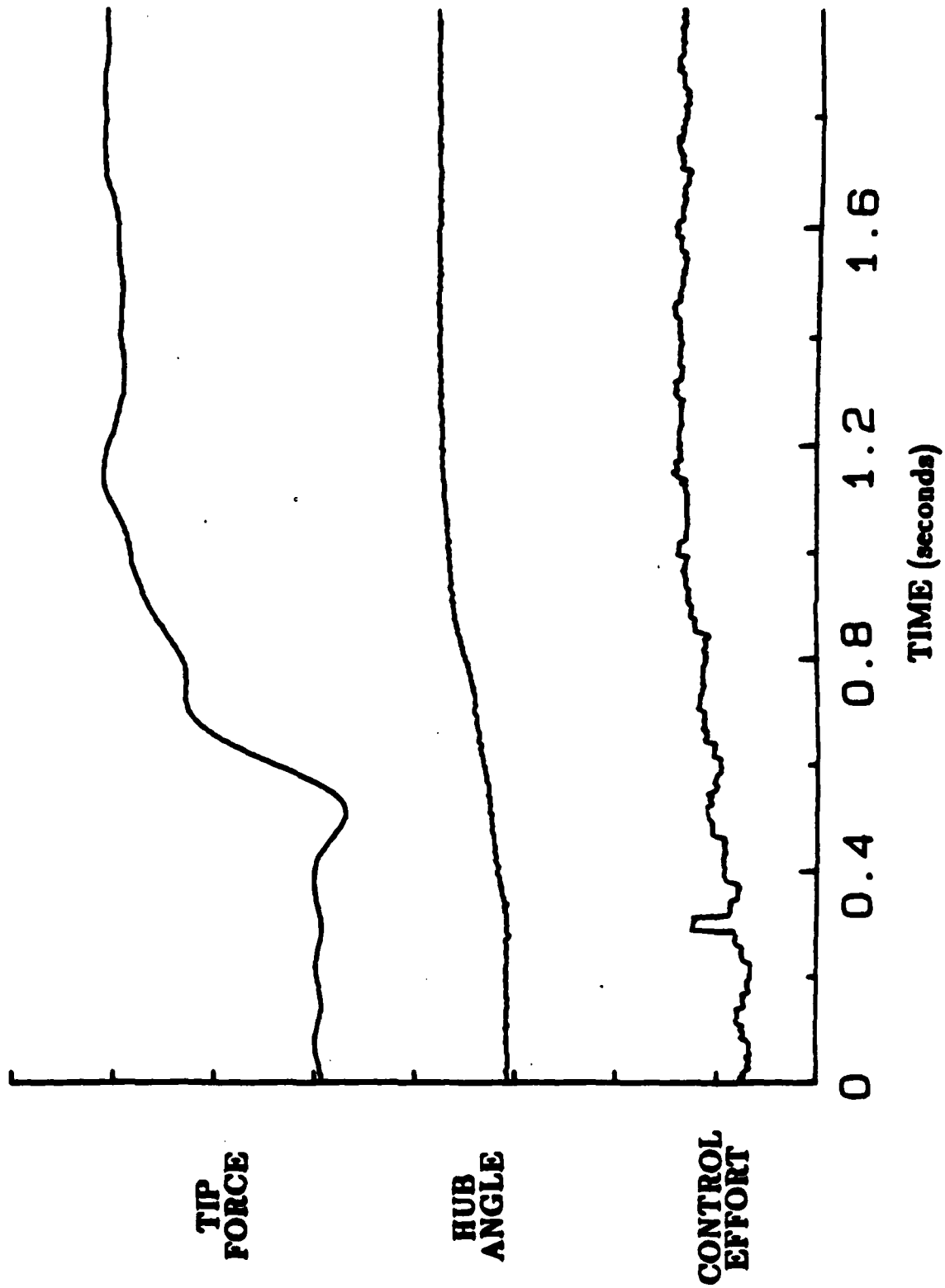


Figure II-11. Step response, expanded scale - touch mode.

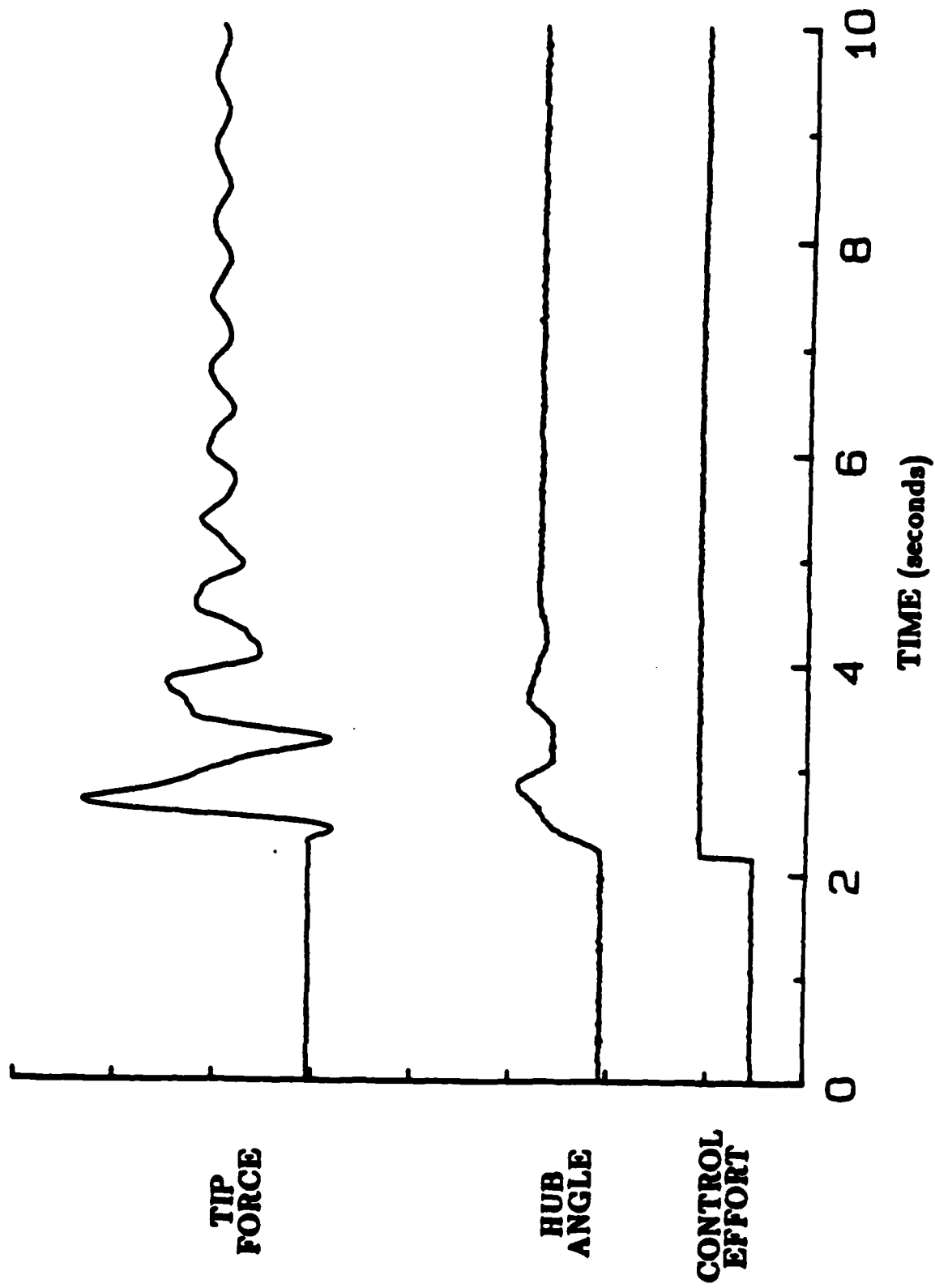


Figure II-12. Open loop step response - touch mode.

is also plotted. That is, a constant bias torque is applied to the beam and then the same test as before is made. The results are plotted in Figure II-14. As seen here, the beam can be held at a constant offset since there is no integrator fighting the action. Upon release of the beam, the touch signal oscillates for a bit and then settles back to its previous value.

From these plots, it is seen that the integrator is both a boon and a hinderance. While it gives excellent response to command and DC disturbance rejection, it can cause overshoot when subject to large disturbances. It is likely that the disturbance rejection of the integral controller could be improved by additional work, especially by experimenting with different ways to limit the charging of the integrator.

### **Switching From Tip-Position Control to Tip-Force Control**

In order to carry out useful tasks that involve, generically, moving rapidly to a target and touching it precisely with a specified force, the difficult problem of switching from tip-position control to tip-force control must be solved. Switching must be smooth, avoiding bouncing and minimizing other transient behavior. The problem is made especially difficult by the fact that the set of control gains that are needed for tip-force control will render the system very unstable if the tip bounces free from the target.

That is, at the instant of touchdown, the entire control problem changes abruptly: the plant dynamics change from that of a pinned-free beam to a pinned-pinned beam, the quantity being controlled changes from tip position to tip contact force, and the sensors being used change to reflect this. The abrupt, non-linear switch between control regions is what makes this problem so challenging.

We assume that suitable control algorithms for both plant conditions have already been obtained, so that we now need only to switch between them. Referring to Figure II-15, we recall that the control gain section of the compensator has no memory, and therefore needs no initialization. On the other hand, the estimator contains the estimated plant states, and it is the initialization of these states that poses the problem.

Since the equations of motion of the plant change at the instant of touchdown, the definition of the plant states changes also; we can no longer simply copy the old states to initialize the new estimator. If we had enough sensors, we could perform a linear transformation on the sensor outputs and arrive at the plant states immediately. (In fact, if we had all these sensors, there would be no need for an estimator at all and switching would be instantaneous, since the compensator would have no memory and therefore nothing to initialize.) For an eighth order model such as used here, however, this would require eight sensors — not a likely situation, due to the high cost of sensors.

What we *do* have is a time history of the sensors. The information in these time histories has been processed and is available as the latest estimate of the current plant state.

At the exact instant of touchdown, when the touching force is still zero, there are two equally valid descriptions of the beam — according to the mode shapes of position (free-end arm, or according to the mode shapes of touch (pinned-end arm). Depending

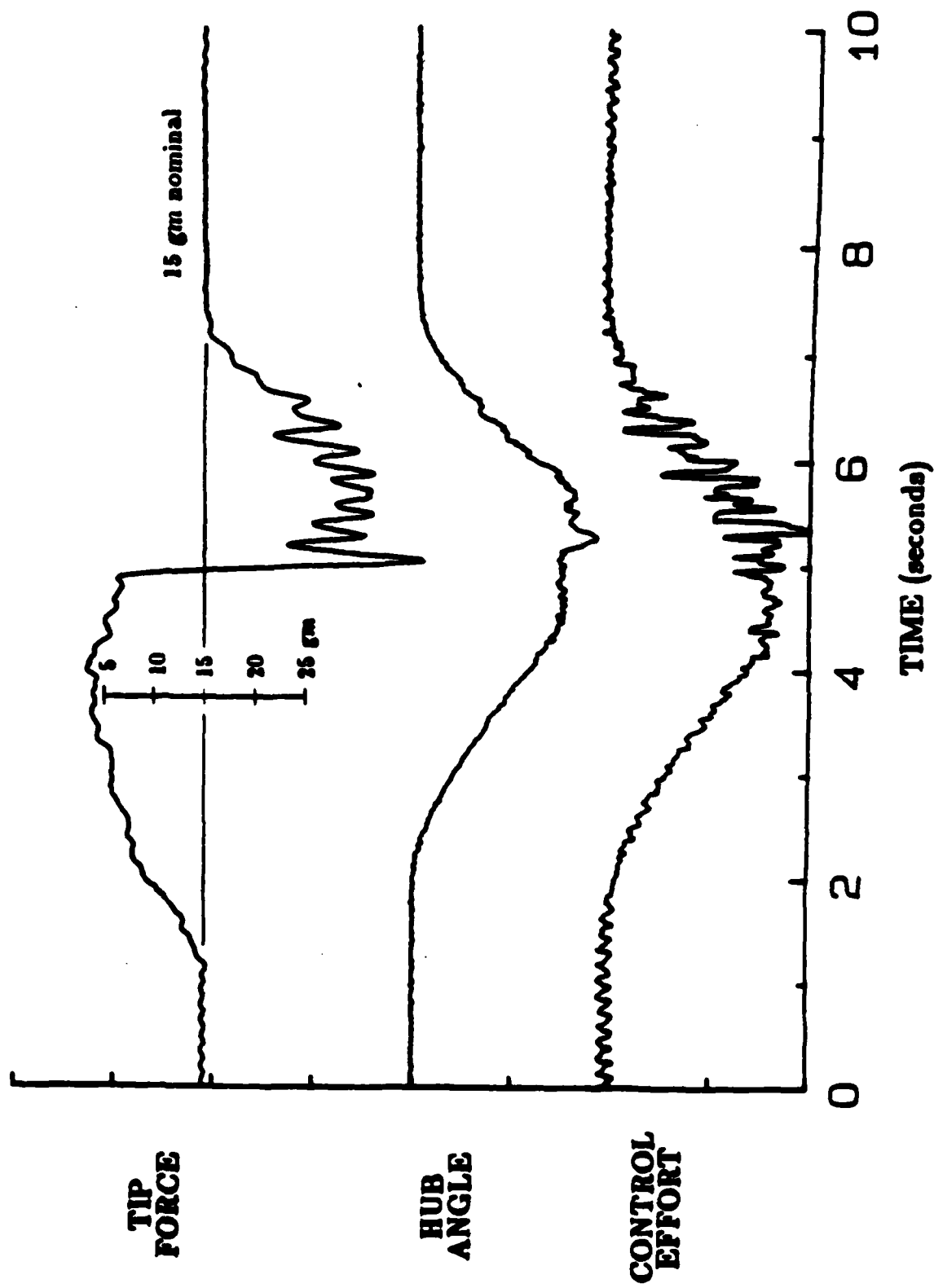


Figure II-13. Disturbance rejection - touch mode.

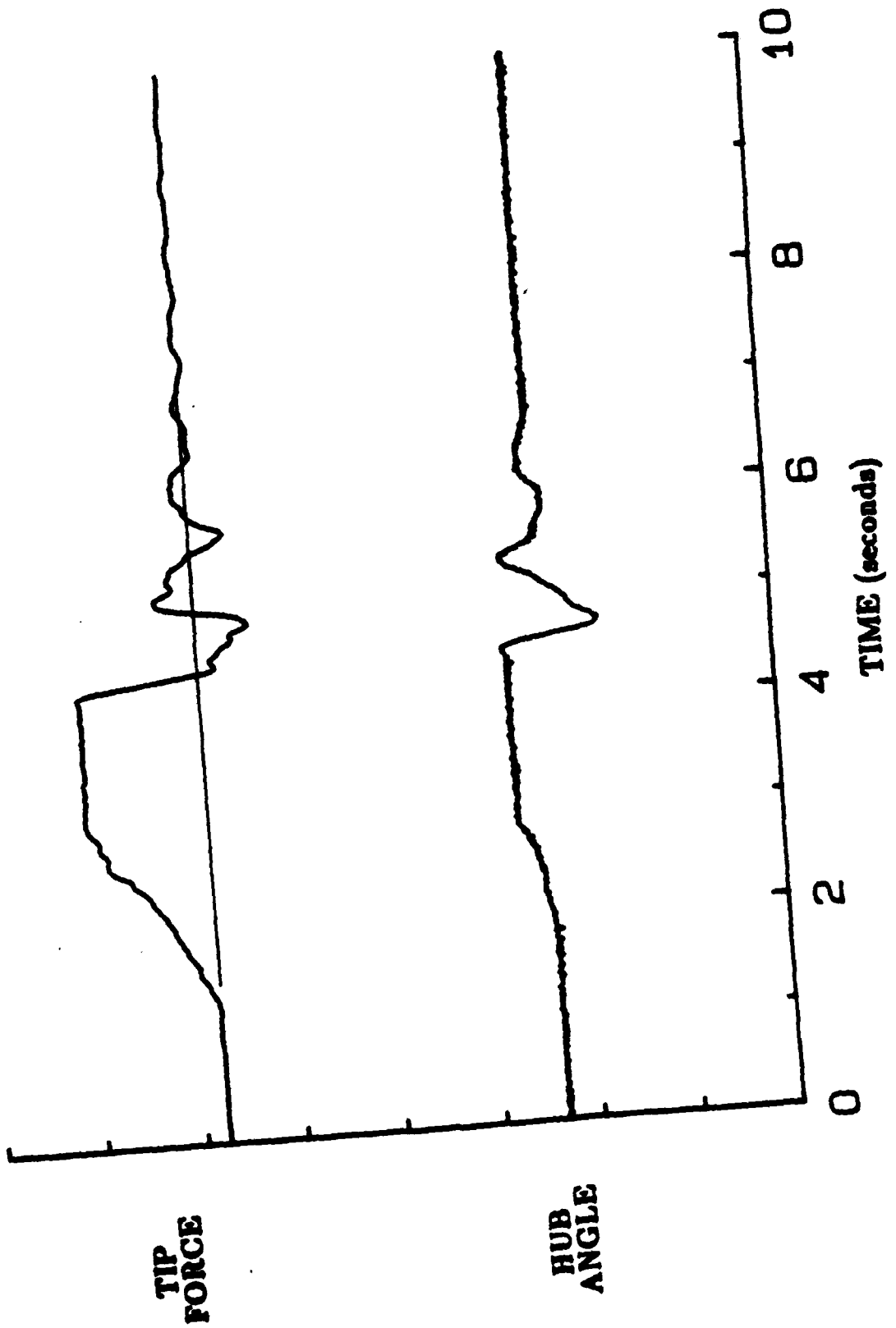


Figure II-14. Open loop disturbance rejection - touch mode.

upon whether the beam is coming into or leaving contact, one of the two descriptions will be valid for previous time, and one will be useful for future time. At the instant of contact both descriptions are valid.

We can make use of this fact to derive the necessary transformation matrix (which we shall call a "switching matrix"). In general, the vector of sensor readings,  $y$ , can be expressed as a linear combination of the plant states:  $y = Hx$ . This is possible for both plant conditions, touch mode or position mode:

$$y = H_t x_t \quad (7)$$

or

$$y = H_p x_p \quad (8)$$

At the instant of contact, both of these descriptions are valid:

$$H_t x_t = y = H_p x_p \quad (9)$$

That is, the sensor readings have only one value at the instant of contact, but they can be described according to two different plant models. Further, if the  $H$  matrices are invertible, we can form the switching matrix directly:

$$H_t x_t = H_p x_p \quad (10)$$

$$x_t = H_t^{-1} H_p x_p \quad (11)$$

Therefore,

$$S_{\text{position} \rightarrow \text{touch}} = H_t^{-1} H_p \quad (12)$$

is the required switching matrix which transforms the position states  $x_p$  to the touch states  $x_t$ . The inverse transformation is, of course:

$$S_{\text{touch} \rightarrow \text{position}} = H_p^{-1} H_t \quad (13)$$

which could alternatively be derived as

$$S_{\text{touch} \rightarrow \text{position}} = S_{\text{position} \rightarrow \text{touch}}^{-1} \quad (14)$$

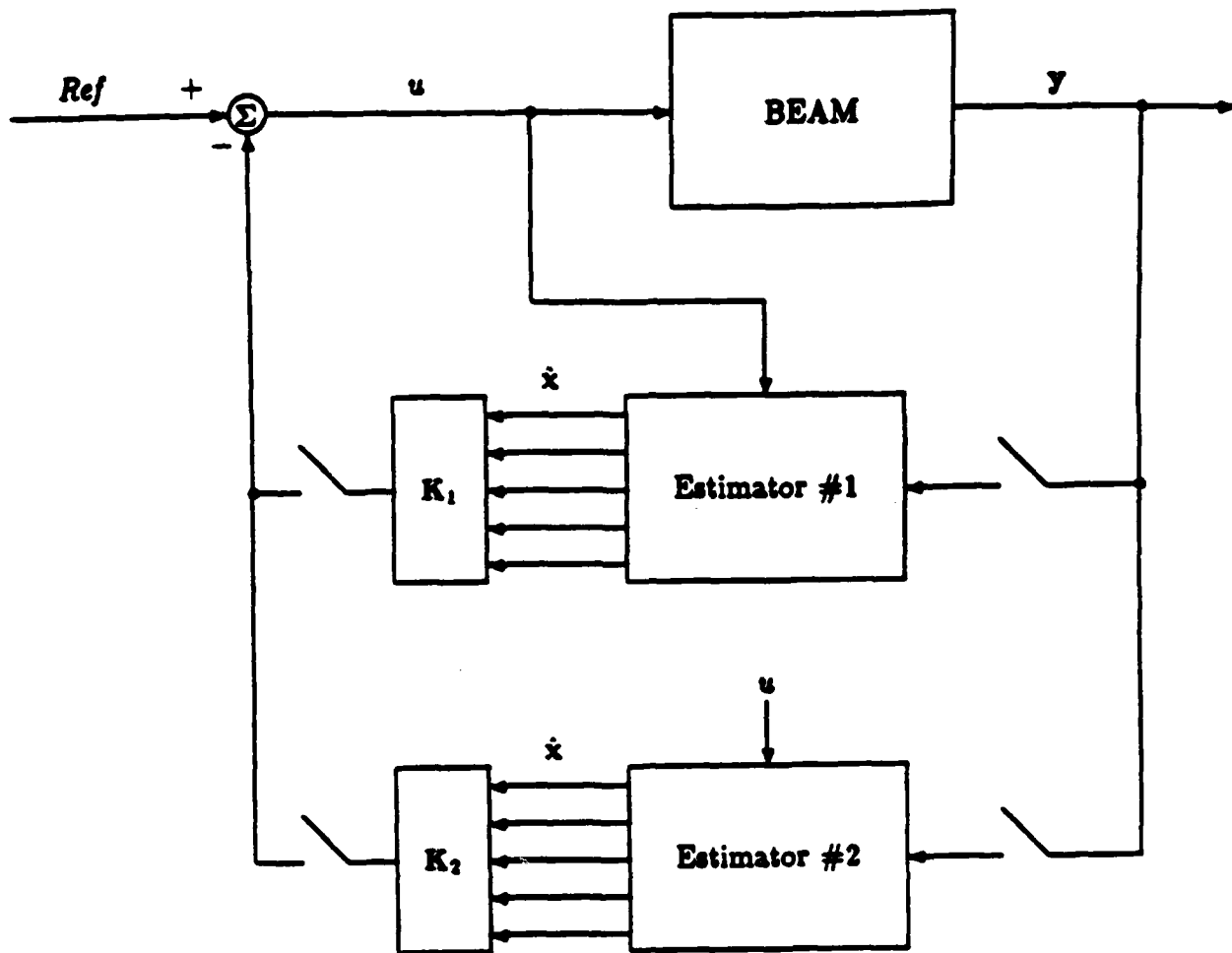
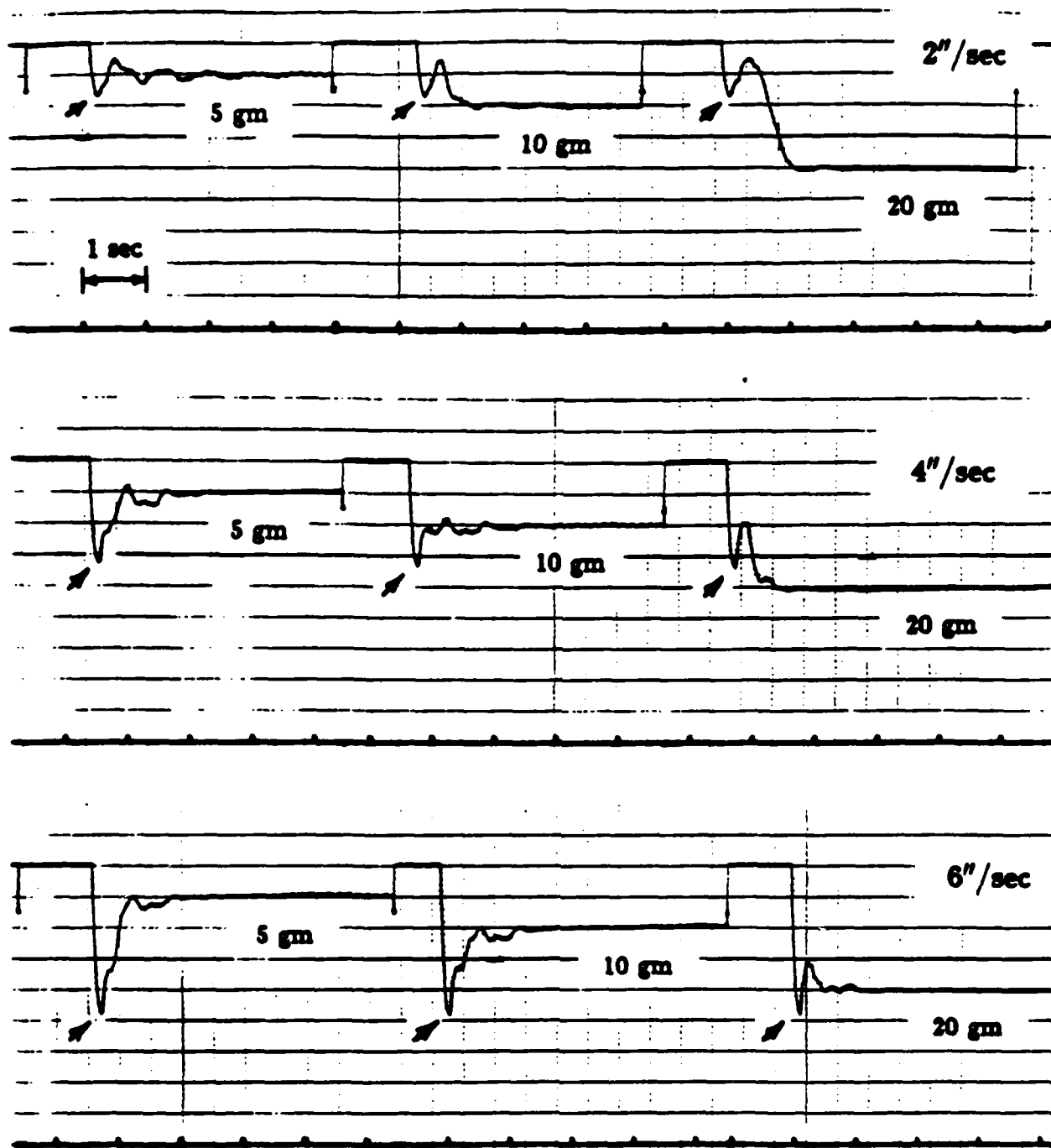


Figure II-15. Switching compensators.



Initial force overshoot indicated by arrows →

Figure II-16. Force overshoot as a function of contact velocity.

**Experimental Results.** Many times, when one attempts to verify a hypothesis experimentally, it is discovered that what was thought to be important is overshadowed by matters not previously considered. This proved to be the case when investigating the beam touching down on the target. While initially embarking on experiments to verify the switching theory described above, many side issues were encountered which grew to become dominant concerns. First and foremost among these was the realization that the amount of force overshoot occurring at touchdown is a function of the initial contact velocity and nothing else.

**Force Overshoot.** When designing a force control system, minimizing force overshoot is obviously an important factor. In the current experiment, the overshoot is determined solely by the velocity of the beam at the time of contact. This is illustrated in Figure II-16. Each trace in this figure shows a set of three touchdown trials; the variable recorded is contact force. (Again, note that all traces of force in this document have force increasing downward.) The flat portions at the top of each trace represent times when the beam is out of contact with the target, with the strip chart being halted during these intervals. Time proceeds from left to right with tick marks occurring at 1 second intervals. All of these trials were conducted by commanding the beam to approach the target with a fixed velocity, switching to force control as soon as contact is made. In the uppermost trace, the approach velocity is 2 inches per second, for the middle trace, it is 4 inches per second, and for the bottom trace it is 6 inches per second. From left to right, the trials differ in their commanded setpoint. The trials at the left settle to a final value corresponding to 5 grams, middle to 10 grams, and right to 20 grams. The response consists of an initial overshoot and rebound, followed by a period of activity while the controller pumps down the energy of the beam, ending in a stable trace at the final setpoint. As shown in the diagram, the force magnitude reached during the initial overshoot depends only on the approach velocity and not on the setpoint.

That this should be so is obvious when one considers the fact that the wave propagation speed of the beam is 124 ms. and the overshoot peaks at 150 ms.: There is simply not enough time for the controller to have any effect on the beam tip before the overshoot occurs. If one desires to lessen the overshoot, then the only recourse is to slow the beam as it approaches the target. This requires the use of some sort of proximity sensor, since it is not desirable to use slow speeds for all approach maneuvers. (Unfortunately, for this experiment, the optical tip sensor was not useable as a proximity sensor due to gain variations over its active range.) In a stiffer system, a possible solution would be to add a contact sensing "whisker" to tell the manipulator to slow down. Alternately, some sort of passive compliance could be added to the point of contact, allowing the manipulator some time to slow down before the compliance bottoms out and large contact forces are developed.

**Bouncing.** A second major issue that became apparent was the possibility of a sustained bouncing condition, Figure II-17. In this figure, we see the beam bouncing off of the target at approximately a 2 Hz rate. The tip excursion represents a peak to peak travel of 1/4 inch, while the maximum force developed is about 10 grams. This bounce condition occurs even though the proper controllers are switched in during the appropriate time intervals.

Because of this, the controller must have some method of detecting a bounce and extinguishing it. For the experiment at hand, a preliminary method to do this recovery has been developed.

Because of the problems associated with bouncing, it is worth making efforts to avoid it. One way to do this is through manipulation of the command input. In particular, the force setpoint at touchdown can have a great influence on the settling response and the likelihood of a bounce.

Fortunately, a simple solution exists for this case, and that is to put a profile on the command input to smooth it or "fair" it in gradually. The time duration of this profile can be relatively fast and still have the desired effect. For this experiment, a duration of 0.7 seconds gives reasonable response. Figure II-18 shows a touchdown using this procedure. As before, approach velocity is 0.05 inches per second and the final setpoint is 25 grams. It can be seen that the actual contact force increases smoothly to the final setpoint, lagging the command input by slightly more than the propagation delay. Because the initially commanded contact force was not large, the beam did not jump out of contact, and the controller did not switch back to position mode.

*Performance of Switching Matrices.* Having finished with the more mundane, but important matters of characterizing force overshoot and avoiding bouncing, we can turn to the experimental results of using the switching matrices described in the first part of this chapter. The first step in deriving numerical values for these matrices is to obtain the **H** matrices for all sensors in both modes. For these calculations a total of 10 sensors were used:

$$y = \begin{pmatrix} \text{hub potentiometer} \\ \text{strain gage \#1} \\ \text{strain gage \#2} \\ \text{strain gage \#3} \\ \text{strain gage \#4} \\ \text{strain gage \#5} \\ \text{strain gage \#6} \\ \text{strain gage \#7} \\ \text{strain gage \#8} \\ \text{tip position} \end{pmatrix} \quad (15)$$

All of these sensors depend only on the position states and not on any rate information. As mentioned before, the switching matrices are derived independently for the four position states.

Figure II-19 shows a touchdown transition using the full switching matrix technique on both position and velocity states, while Figure II-20 shows a similar event, this time simply initializing the touch mode estimator states to zero. These recordings were made at 25 mm/sec, with the event marks at 1 second intervals. The top trace shows the estimated value of the first mode in bending. Below this, extra auxilliary sensors (not part of the control system) are used to compute the instantaneous value of the same plant state, while the error between the top two traces (the estimator error signal) is shown as the third

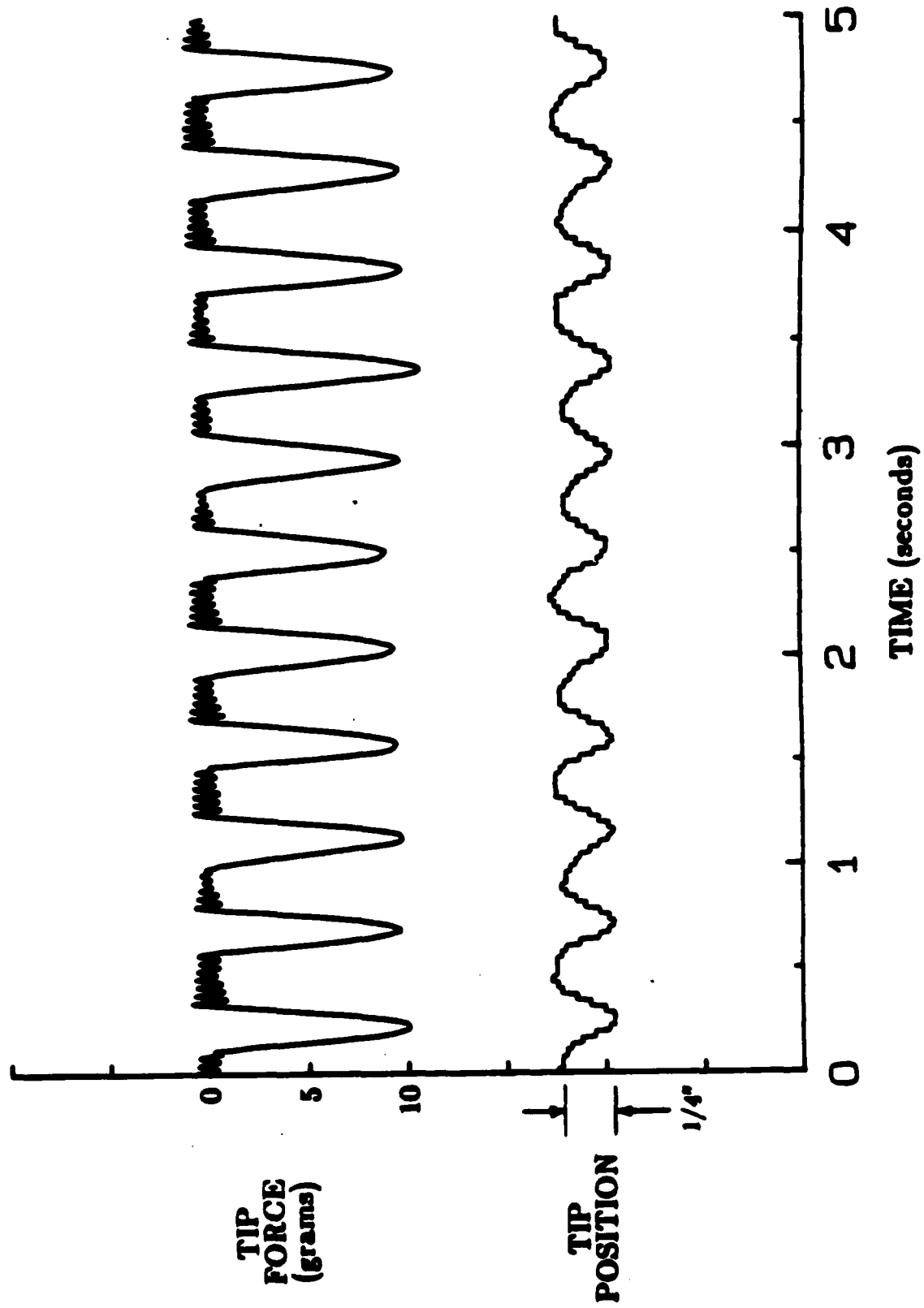


Figure II-17. Sustained bounce condition.

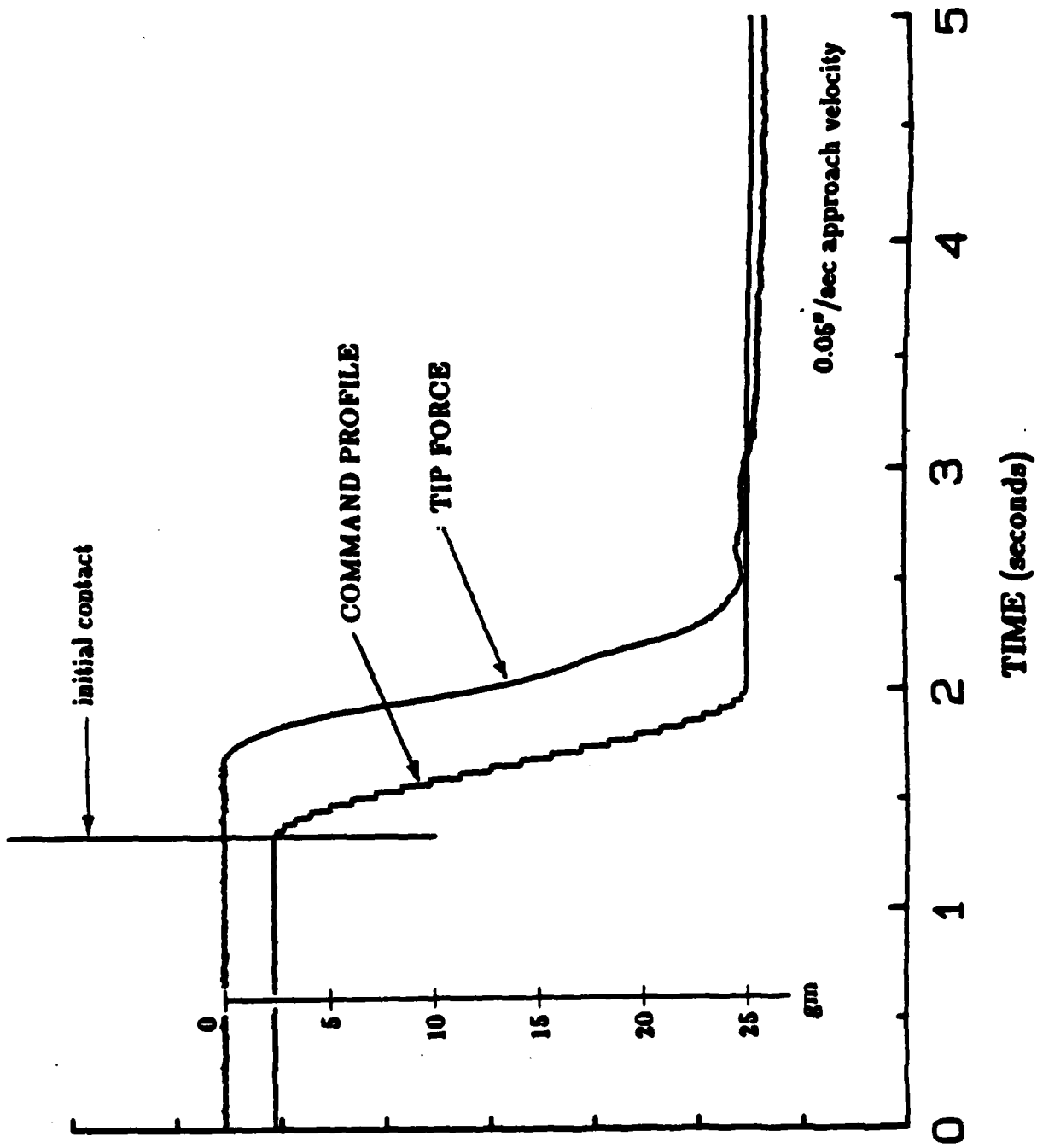


Figure II-18. Low velocity touchdown - with fairing.

trace. All three of these traces are to the same scale. Finally, at the bottom is shown the output from the force sensor as the beam touches down on the target.

A number of things are apparent from these traces. First, and most obvious, is that there isn't a great deal of difference between the two figures. We need to examine things more closely to see why this is so. The key trace is the estimator error. Once the system has settled, we note that this signal consists mostly of noise. As would be expected, the estimated value of the plant state has less noise than the instantaneous values obtained by direct measurement. The sensor noise in the direct measurement trace feeds directly through to the error signal causing it to appear noisy also. More importantly, if we look at the error signal just after touchdown, we see that the error decays to zero with a time constant on the order of 200 ms. This is the reason that these figures appear so similar. The estimator for touch mode is sufficiently fast that even if the estimator states are incorrectly initialized, they are corrected by the system so quickly, that very little difference can be observed at the force sensing output.

Comparing the two figures, we see that correct state initialization reduced the size of the second force overshoot. Although the effect does not appear to be a major one, it is supported by repeated trials. We can also verify that the switching matrix is actually working by comparing the estimated plant state with the actual plant state just after touchdown. In Figure II-19, we see that the state was correctly initialized to a small positive value, while in Figure II-20, we see that it was simply set to zero. This is further supported by the fact that the initial estimator error is smaller in Figure II-19 than in II-20.

So while it appears that the switching techniques outlined in this chapter can work quite well, my conclusion is that, given a fast estimator, the need for them is marginal. For many applications, quite adequate results can be obtained simply by initializing the estimator states to zero. This is reinforced by the fact that in most cases the control system will have had a chance to pump down any energy in the flexible modes before contact is made with the target. (In fact, to obtain the traces for Figures II-19 and II-20, it was necessary to introduce a disturbance to the beam just before it touched down so that the bending modes would have some non-zero value at touchdown.)

### **Tracking and Contacting a Moving Target**

*Maintaining a fixed distance from a moving target.* Once a position controller has been fabricated for the flexible beam, maintaining a fixed position from a moving target (station keeping) is a matter of giving the position controller the proper command input. Since the optical sensor reports the position of the target as well as that of the beam tip, the most logical choice is to add a fixed separation distance to the target position and use this as the command input. In the work reported here, no feedforward was used other than this straightforward introduction of the target position. However, one would expect that feeding forward additional parameters such as target velocity would give improved tracking performance.

The sensors used in position mode were selected to help achieve good performance in

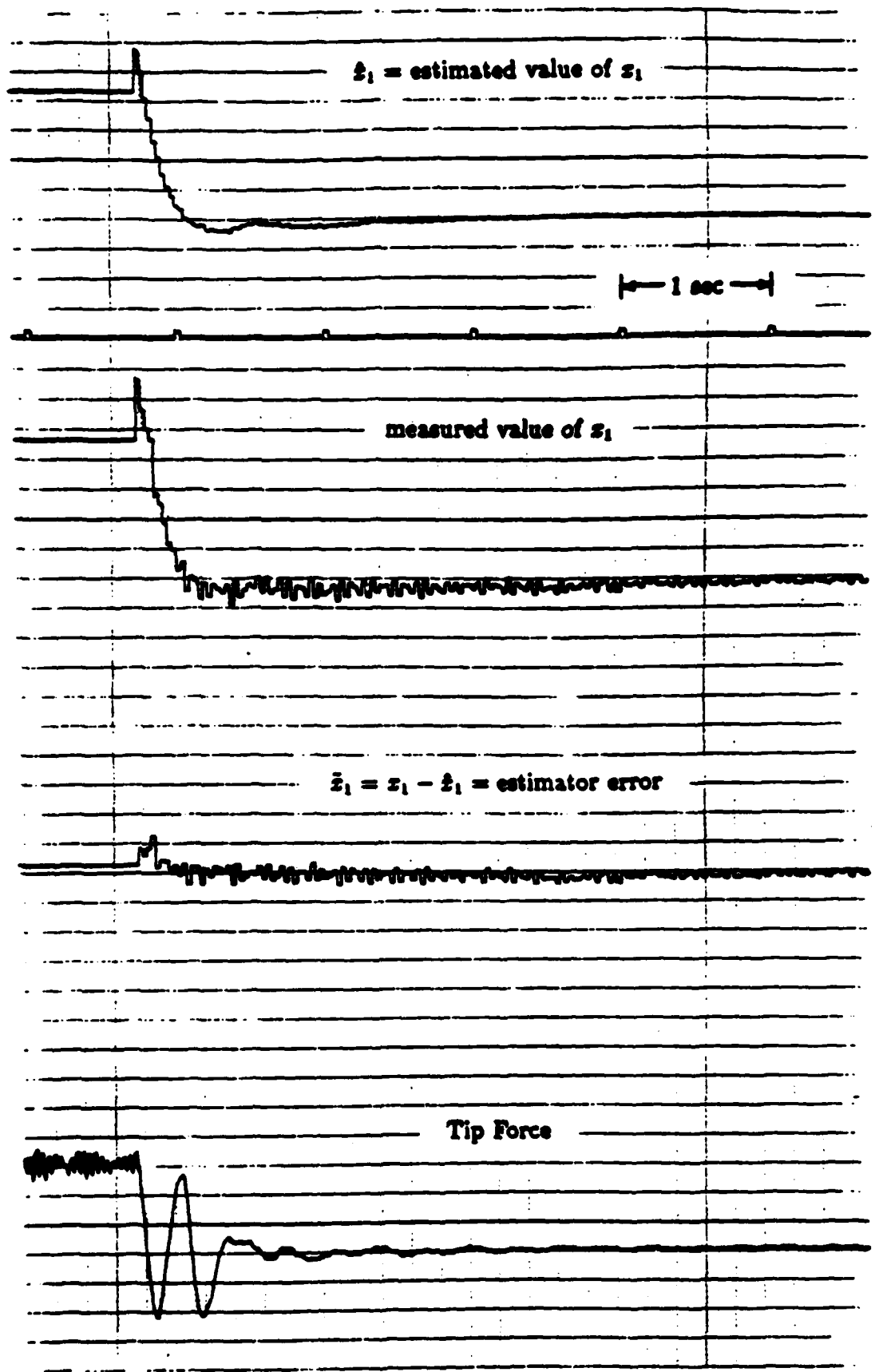


Figure II-19. Touchdown using switching matrices.

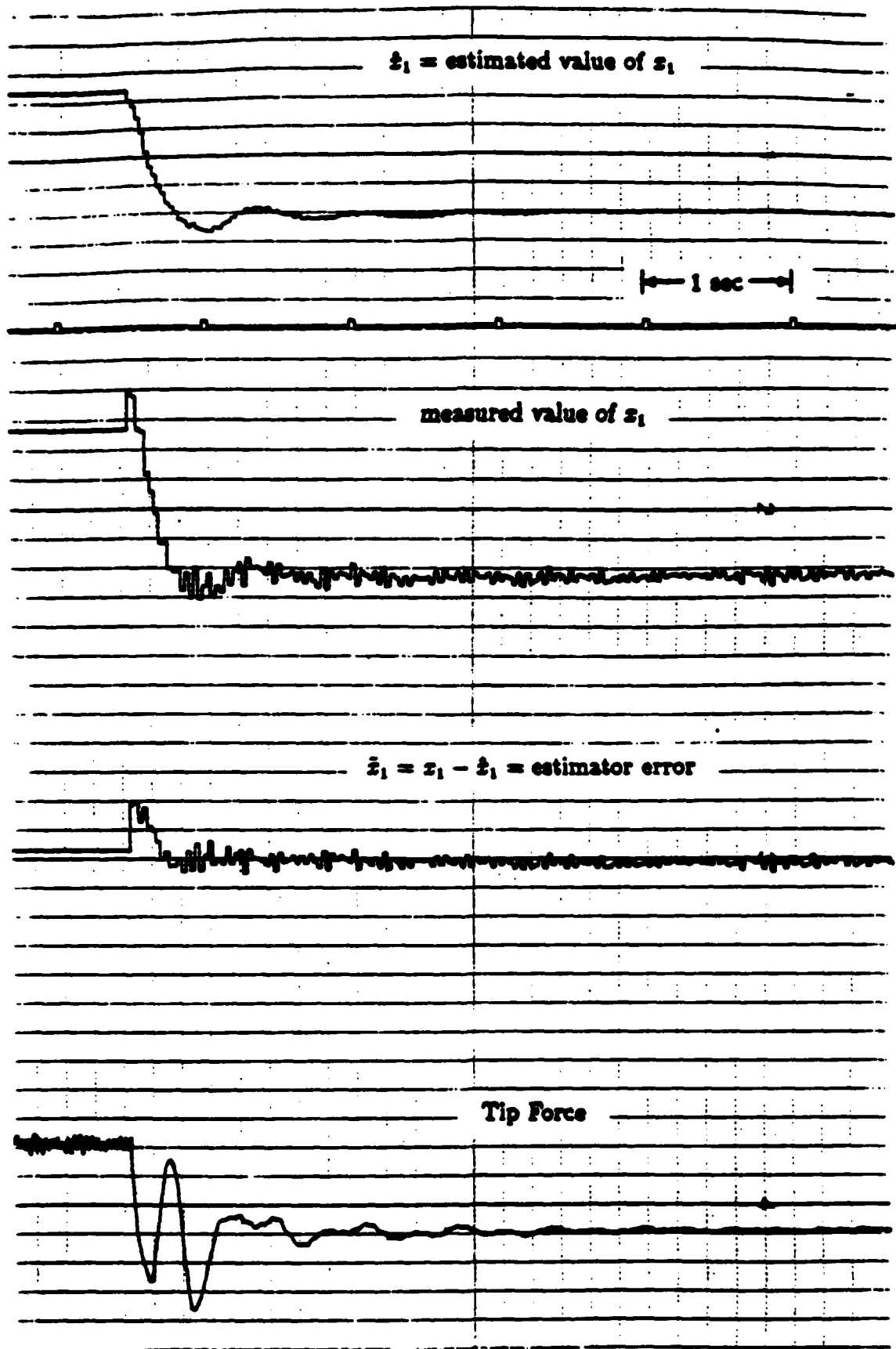


Figure II-20. Touchdown initialising states to zero.

the tracking task. In this mode, the only sensor with DC content is the optical tip sensor — the same sensor that is used to track the moving target. Thus any sensor biases are automatically cancelled. The same is not true for gain variations since the LED's cannot physically coincide in space. There is a finite difference (approximately 2 inches) in the sensed positions of beam and target when they are in contact, and this difference is affected by gain variations.

An accurate measure of tracking accuracy is a plot of position error as a fraction of command input, Figure II-21. Note that if the beam sat absolutely still, position error could get no worse than 1.0 (In that case, the position error would simply be equal to the command). The controller is actually making things worse at frequencies around 1 Hz (because, at this frequency, it moves in the wrong direction due to phase reversal). To compensate for this, one could consider adding a prefilter to the command input to roll off the gain characteristic before the phase reversal, however this must be traded off against the added delay which such a filter would add.

As one might suspect, much of this behavior is due to the wave propagation delay of the beam. *The salient point is that this time delay establishes an upper limit to the tracking ability of the beam.*

*Maintaining a specified contact force with a moving target.* As in the previous section, maintaining a fixed contact force with a moving target requires proper sensor selection and appropriate control design. In touch mode, the only sensor with DC signal content is the contact force sensor, and therefore offset and bias from other sensors do not compete with the primary measurement. This also means that no information about the beam's rigid body position enters the control loop and so the system will track a moving target with no modification and with no additions to the command input. This is the method used in the results reported here. Note, however, that any accelerations of the rigid body position must be supported by errors in the force signal. Additionally, the hub rate sensor detects rigid body velocity as well as flexible mode velocities. For these reasons, one would expect that feeding forward target position and velocity would improve the response of the system to rigid body motions.

One major difference between tracking at a fixed distance and tracking while actually touching the target is the role disturbance rejection plays. Because the target actually touches the beam, it is a major source of disturbance forces. These disturbances can only be controlled within the bandwidth of the control system, and this is limited by the wave propagation of the beam. Inevitably, with a moving target, there will be high frequency disturbances superimposed on the contact force output signal.

Figure II-22 shows the beam attempting to maintain a constant 20 gram contact force while the target accelerates from a stop to a constant velocity and then decelerates back to a stop. Target speed during this trace was in the range of 5 inches per second; however, since the target is a model HO railroad train, its speed cannot be accurately controlled, nor is its motion especially smooth. The direction of the target was to move away from the beam.

Referring to the figure, we see that at the beginning of the motion, a large force error is generated as the target accelerates. This is the error referred to above, which is required to support the acceleration of the mass of the beam. Following this, the system regulates

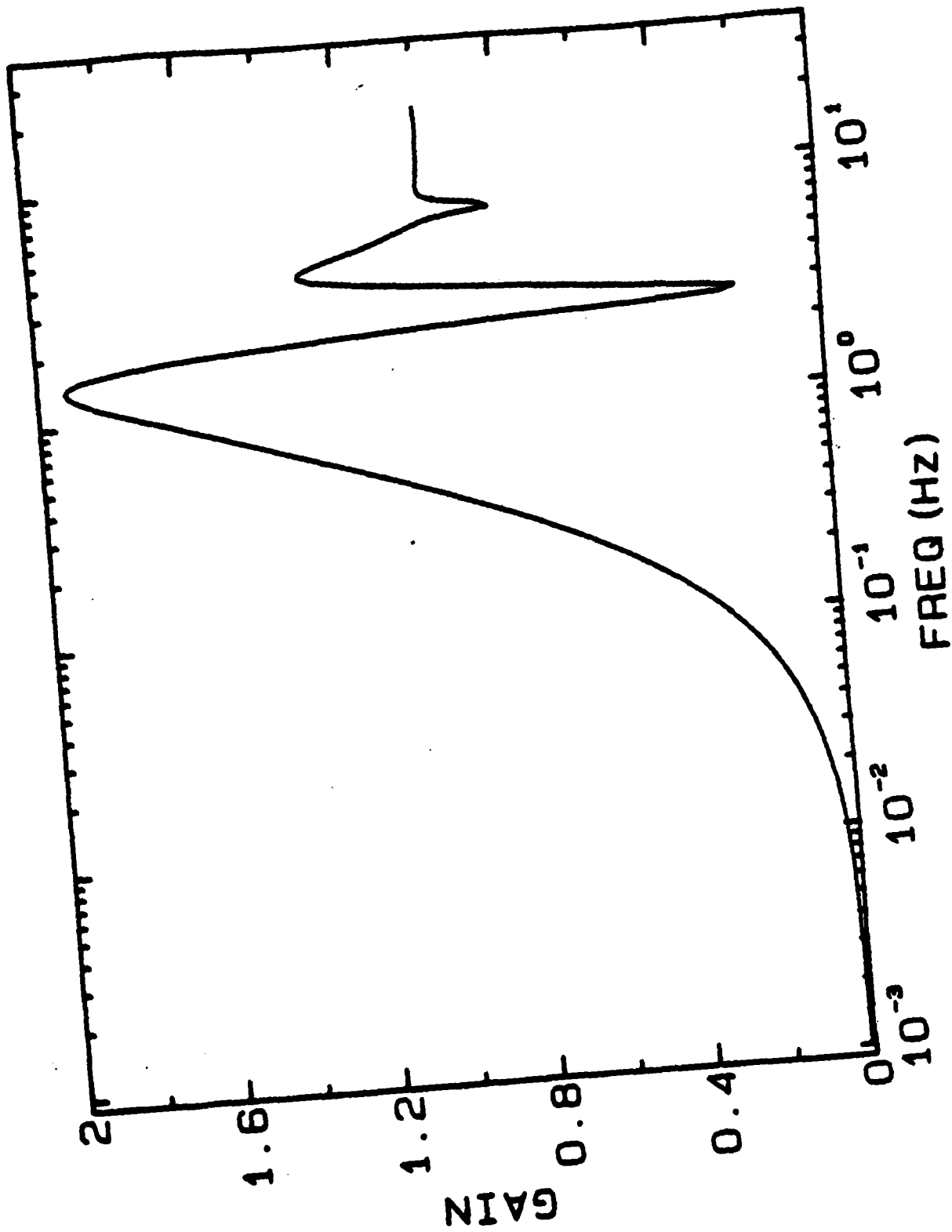


Figure II-21. Position error versus frequency.

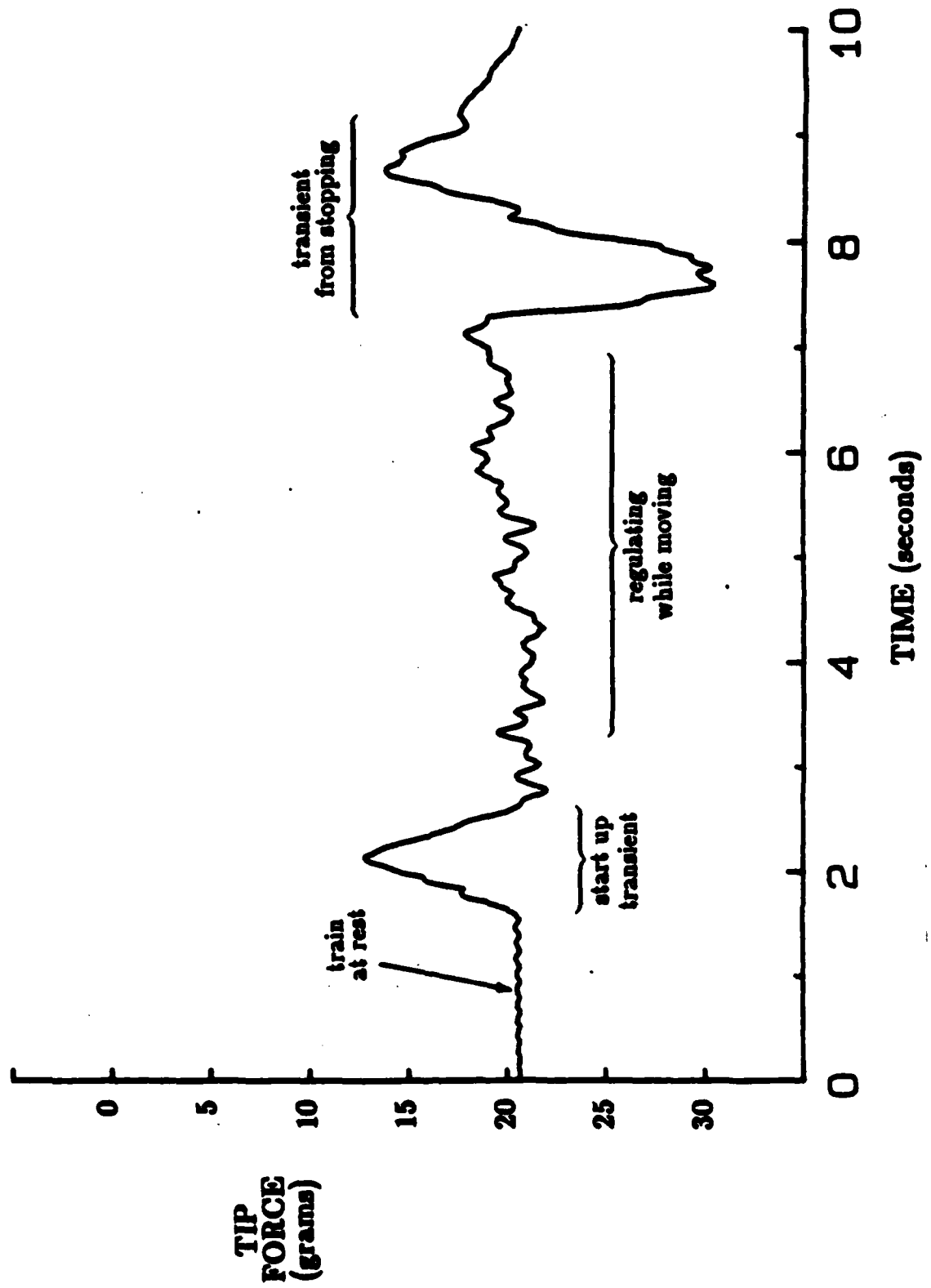


Figure II-22. Maintaining constant force on moving target.

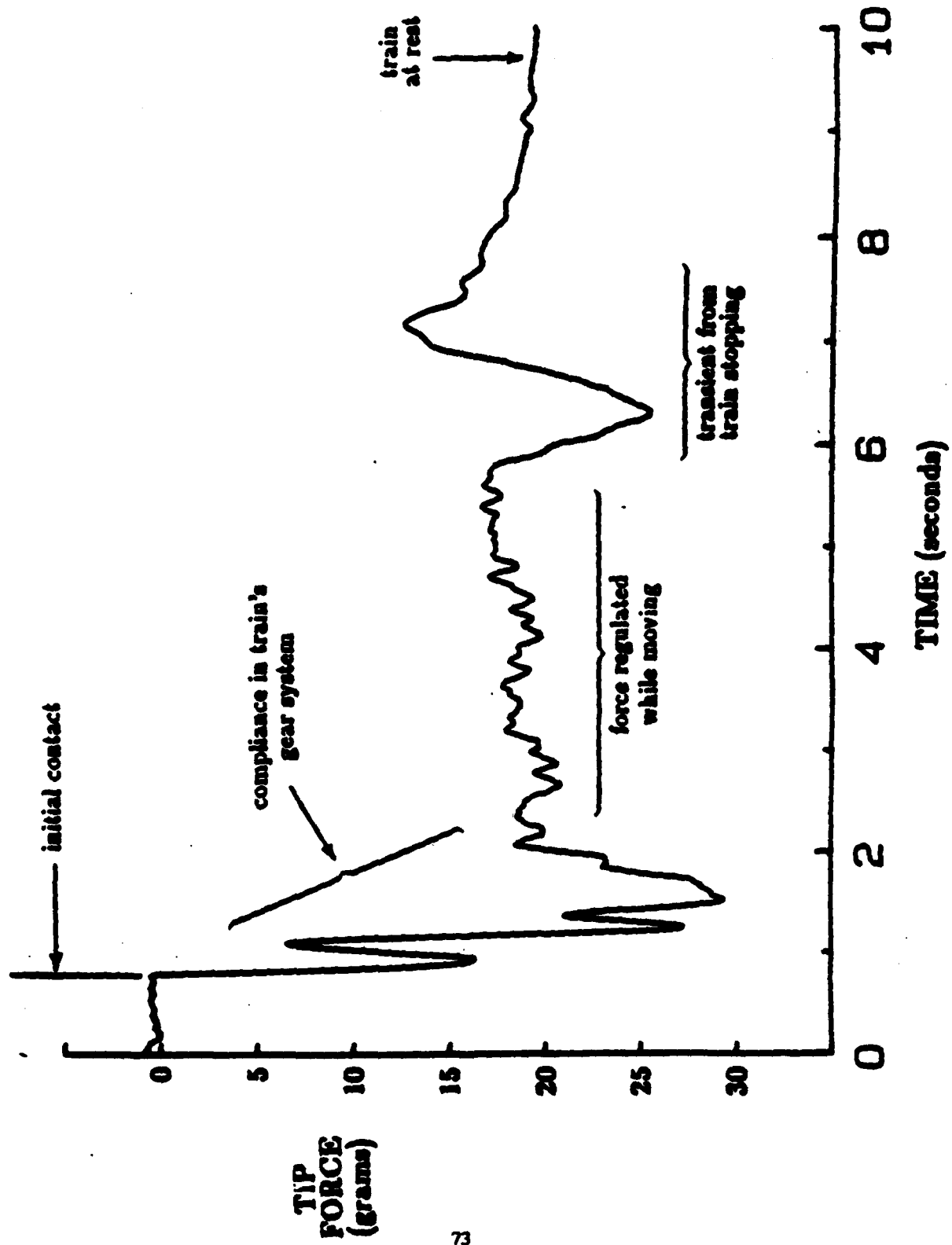


Figure II-23. Touching down on a moving target.

at the 20 gram level with high frequency disturbance forces being superimposed on the signal. Finally, the target decelerates and comes to a rest, again causing force errors as it does so.

*Pursuit and contact of a moving target.* Putting everything together and touching down on a moving target requires a combination of the previous algorithms. Starting in position mode, the command input is the target position plus a separation distance. While the target is moving, the separation distance is ramped through zero, and as contact is detected a switch is made to force control. Since the disturbance level will be inevitably high for this maneuver, the best way to avoid bouncing is to approach the target with a medium to high closing velocity, and maintain contact at a reasonably high force level.

A recording of the force sensor output during such a maneuver is shown in Figure II-23. The target train was moving at a constant speed of approximately 5 inches per second during this recording, decelerating to a stop at the end. The commanded closing velocity of the beam is 6 inches per second and the commanded contact force is 20 grams. At the beginning of the trace the force sensor records zero as the beam sweeps in to the target. Then, immediately after contact is made, there is some force overshoot and oscillation as the controller switches to force control and pumps down the resonant modes of the beam. The large oscillations are actually caused by compliance in the drive train of the model HO railroad engine used as the target. Once the initial transient has died, the controller maintains a constant 20 gram force with, as before, high frequency disturbances superimposed. At the end of the maneuver, the train slows to a stop, generating a force error as the mass of the beam is decelerated.

## SUMMARY

The successful development and demonstration of a control system capable of rapid, precise slew-and-touch maneuvers of a very flexible manipulator (Fig. II-2) which involves both end-point position control and end-point force control, and switching smoothly and promptly between the two -- along with development of new end-point sensors and the investigation of four new robotic arm designs, (Figs II-2, II-24, II-27 and II-28) and development and demonstration of control algorithm for three of them, constitutes successful completion of essentially all of Tasks 4.1.1 through 4.1.8 of this DARPA Contract.

This research is the absolutely essential starting point for the new research now at the advanced planning stage (see Section II-4) -- that we will be doing on two cooperating robot arms under a new DARPA Contract.

## SECTION II-2: FLEXIBLE ARM WITH QUICK WRIST FOR PRECISION FORCE CONTROL

A load cell force sensor in conjunction with a quick wrist (see Fig. II-24a, b, and c) was used to investigate end point force control of a very flexible manipulator. This configuration was expected to have many advantages over a system without a quick wrist and using a leaf spring as a force sensor.

A load cell is a force measuring device which has very low mass and compliance: thus the sensor has no dynamics of its own. The particular load cell used in this experiment was capable of measuring forces up to 500 grams to within 1 gram. The load cell was equipped with a safety spring to provide load limiting. Tests showed the load cell to exhibit no hysteresis, unlike a leaf spring force sensor which may undergo non-elastic deformation.

The experiment consisted of having the flexible arm slew over to a target, and then regulating the end point force to a desired level (15 grams force). The flexibility in the arm was not modeled in this initial experiment; thus the arm controller had to be relatively slow so as not to excite any modes of oscillation in the arm. However, the force control response achieved in this way should be a good indication of the type of response that may be achieved with a higher order controller, since the rigid quick wrist provides almost all of the action.

A proportional controller based on arm hub error was used to provide the bias torque necessary to maintain a contact force. With such a controller, the arm tip could manually be pulled a certain distance away from the target, and the resulting impact velocity would then be a function of the controller gain and the distance the tip was pulled away. In this way, an impact velocity of 4 in/sec was repeatably achieved.

One problem that arises is that the torque exerted on the hub does not necessarily match the torque exerted by the hub torquer. Also, even if they are matched, a slight perturbation in wrist angle produces a situation which is unstable. To overcome these problems, a lead compensator was used to correct the hub torque based on errors in the wrist angle. One will note that this arrangement results in a steady state error in wrist angle: but this is not critical so long as it is not too large.

Since the sensor and the quick wrist have no dynamics in force control, pure integral control was used. This was implemented digitally at a sample frequency of 200 Hz.

In short, the following control was used:

### Hub Control

$$T_{\text{hub}} = K_1 \Theta_{\text{hub error}} + K_2 [(z - 0.95)/z - 0.1] \Theta_{\text{wrist error}}$$

### Wrist Control

$$T_{\text{wrist}} = K_3 \int F_{\text{error}} dt$$

Using the above control logic, the following performance characteristics were achieved:

	<u>Load Cell &amp; Quick Wrist</u>	<u>Leaf Spring w/o Quick Wrist</u>
Touchdown Velocity	4 in/sec	4 in/sec
Rise Time	0.01 sec	0.10 sec
Settling Time	0.06 sec	0.78 sec
Damping	20%	55%
Overshoot	60%	15%
Damped Frequency	70 Hz	3 Hz

These results are illustrated in Figures II-25 and II-26.

In summary, the use of a quick wrist in conjunction with a load cell force sensor provided much better force control response than was attained previously without a quick wrist and with a leaf spring force sensor. Part of the increased bandwidth is due to the fact that the lack of compliance in the wrist and the force sensor means that a change in force level requires no noticeable motion. With a leaf spring sensor and without a quick wrist, a great deal of time-consuming arm motion is necessary to change force levels. Finally, the use of a quick wrist in conjunction with a load cell force sensor greatly simplifies the control law necessary for force control. In this experiment, two simple first order controllers were used instead of an 8th order controller as was done in the past.

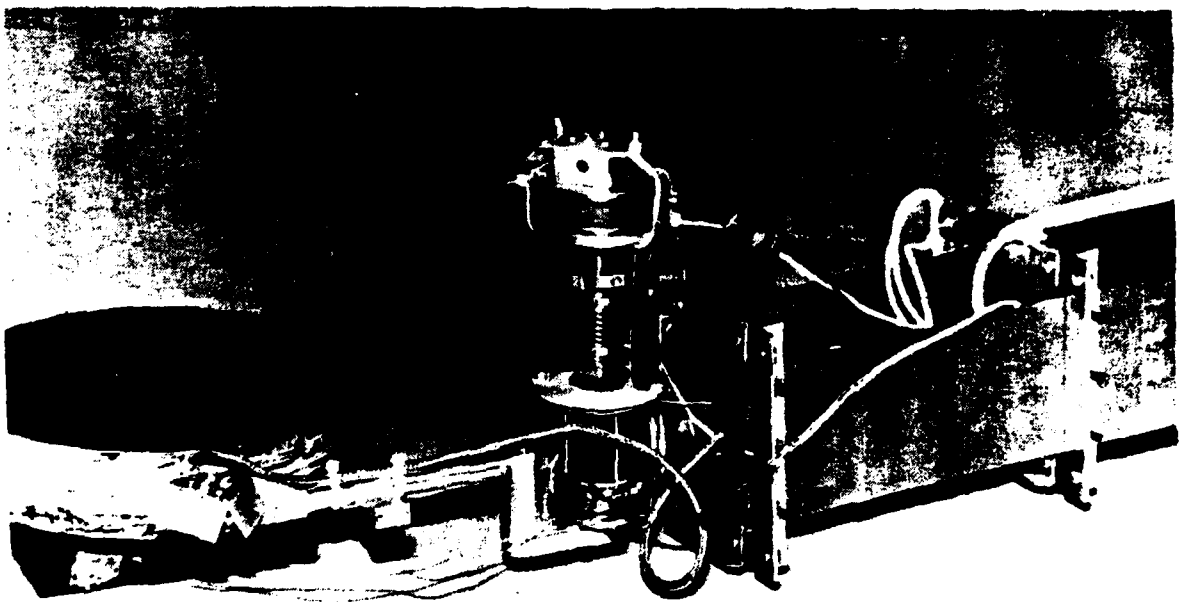
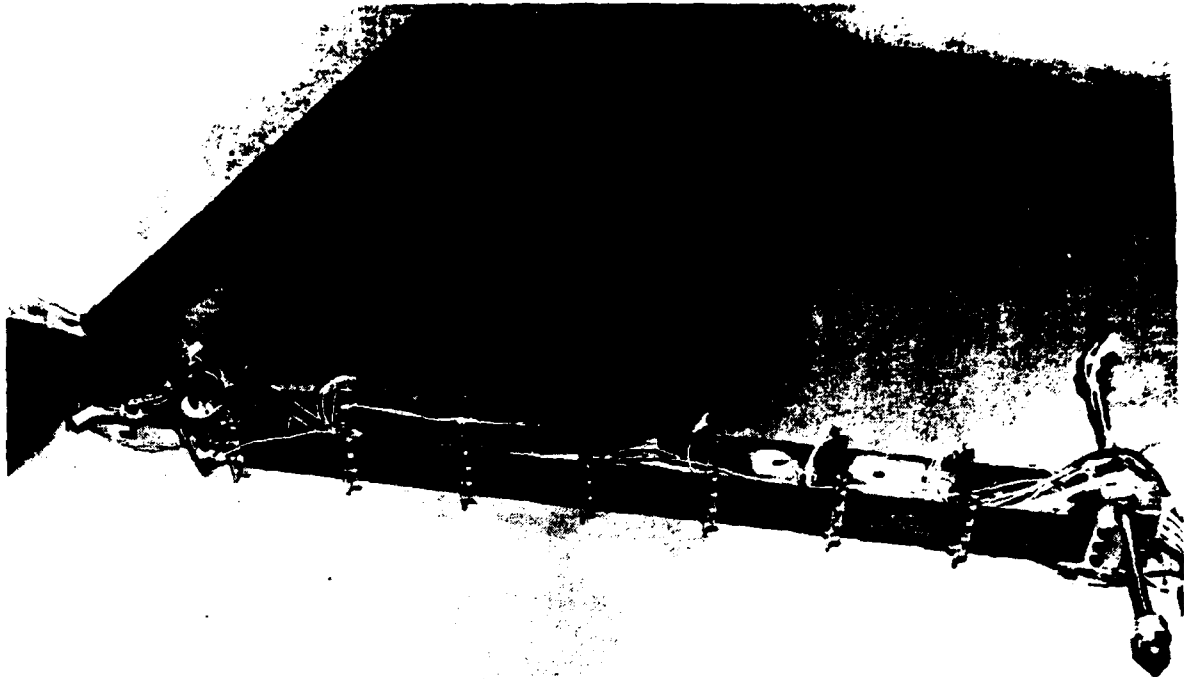


**Figure II-24a and b. Photographs of flexible arm with quick wrist in contact with stationary target.**

**Top: System overview, Bottom: Detail of wrist and sensors.**

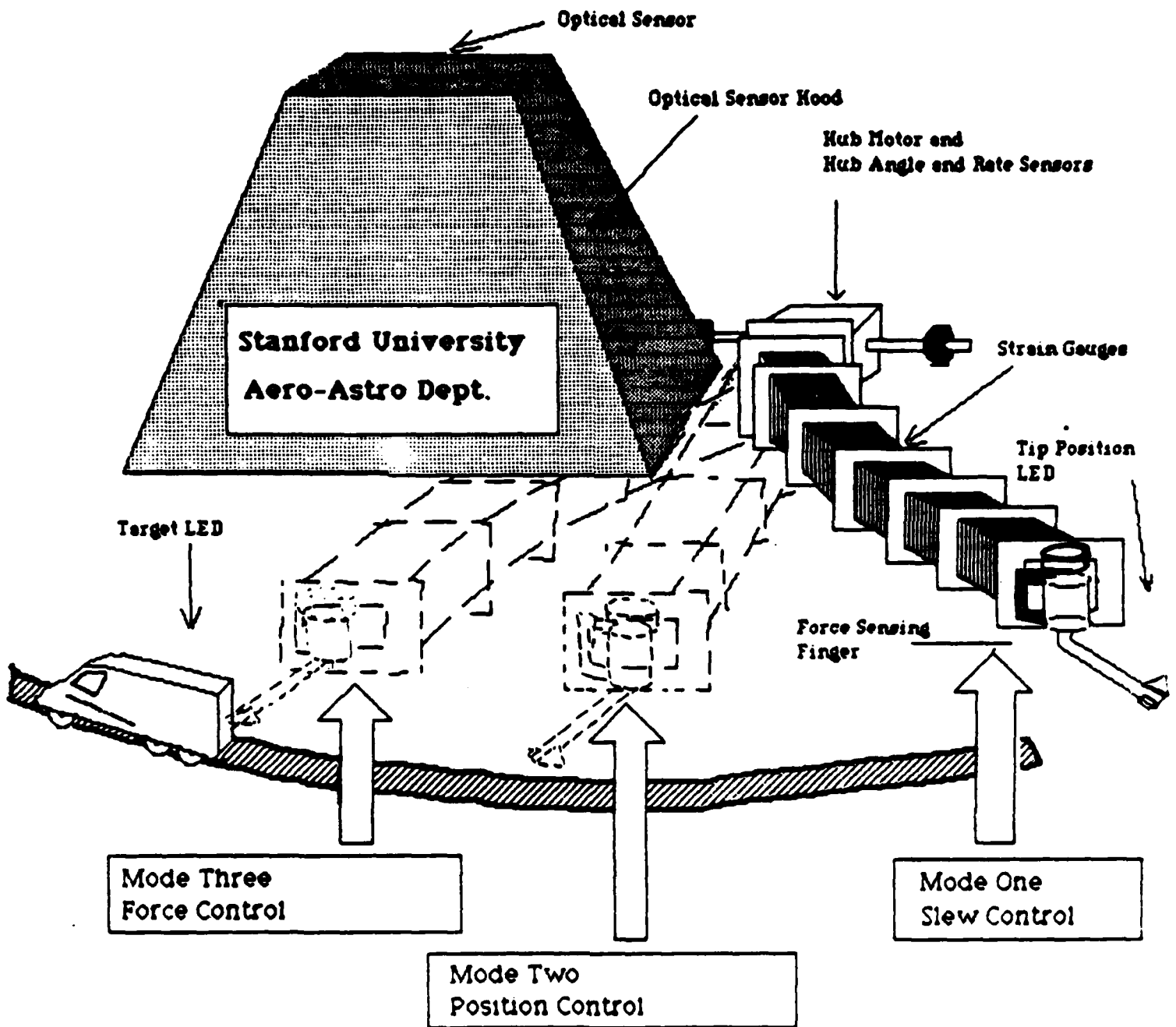


Figure II-24c. Flexible arm with rigid, quick wrist in slew and touch maneuver.

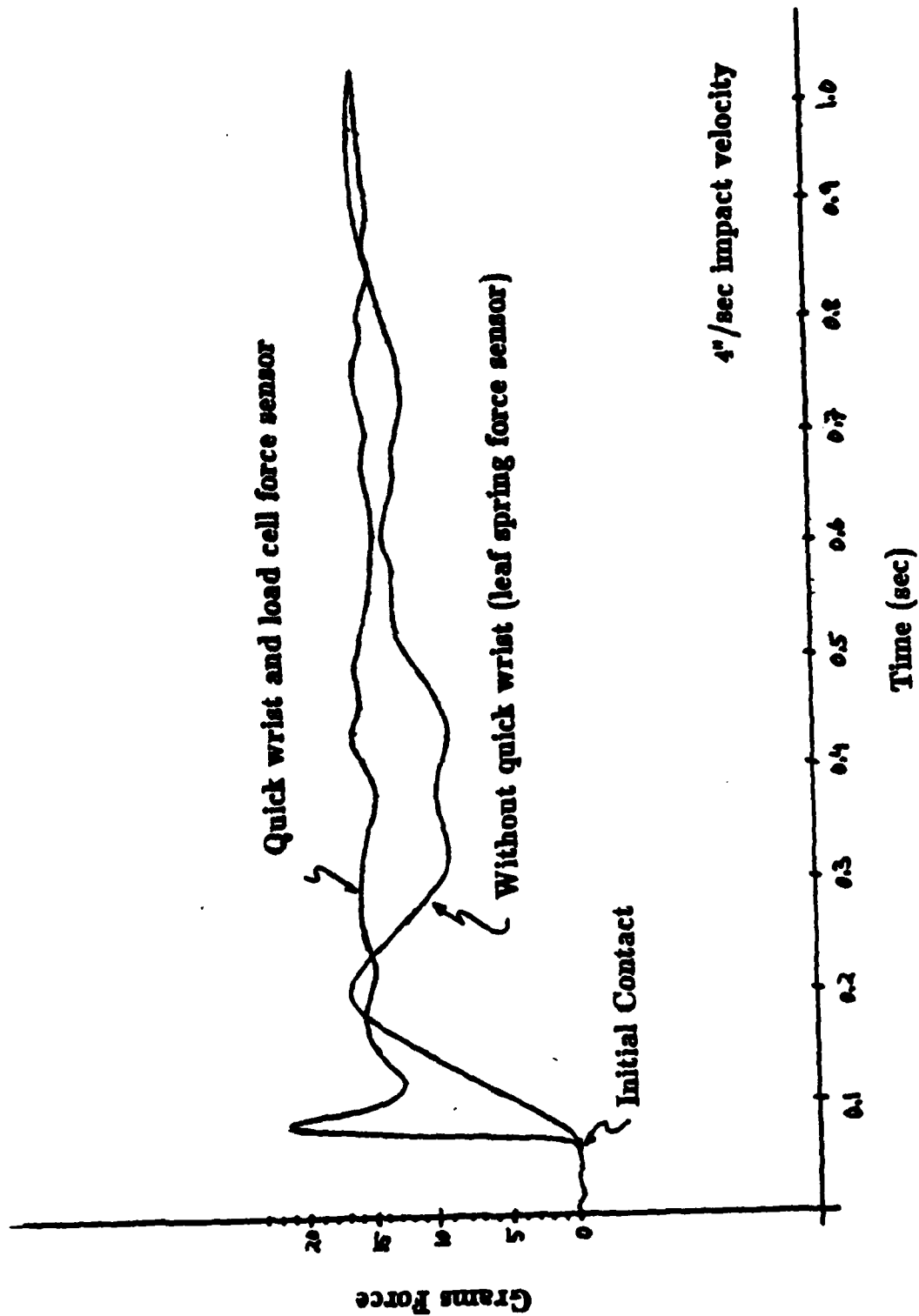


Figure II-25. Force history for a very flexible arm with and without a quick wrist going from out of contact to a commanded 15 gram force level.

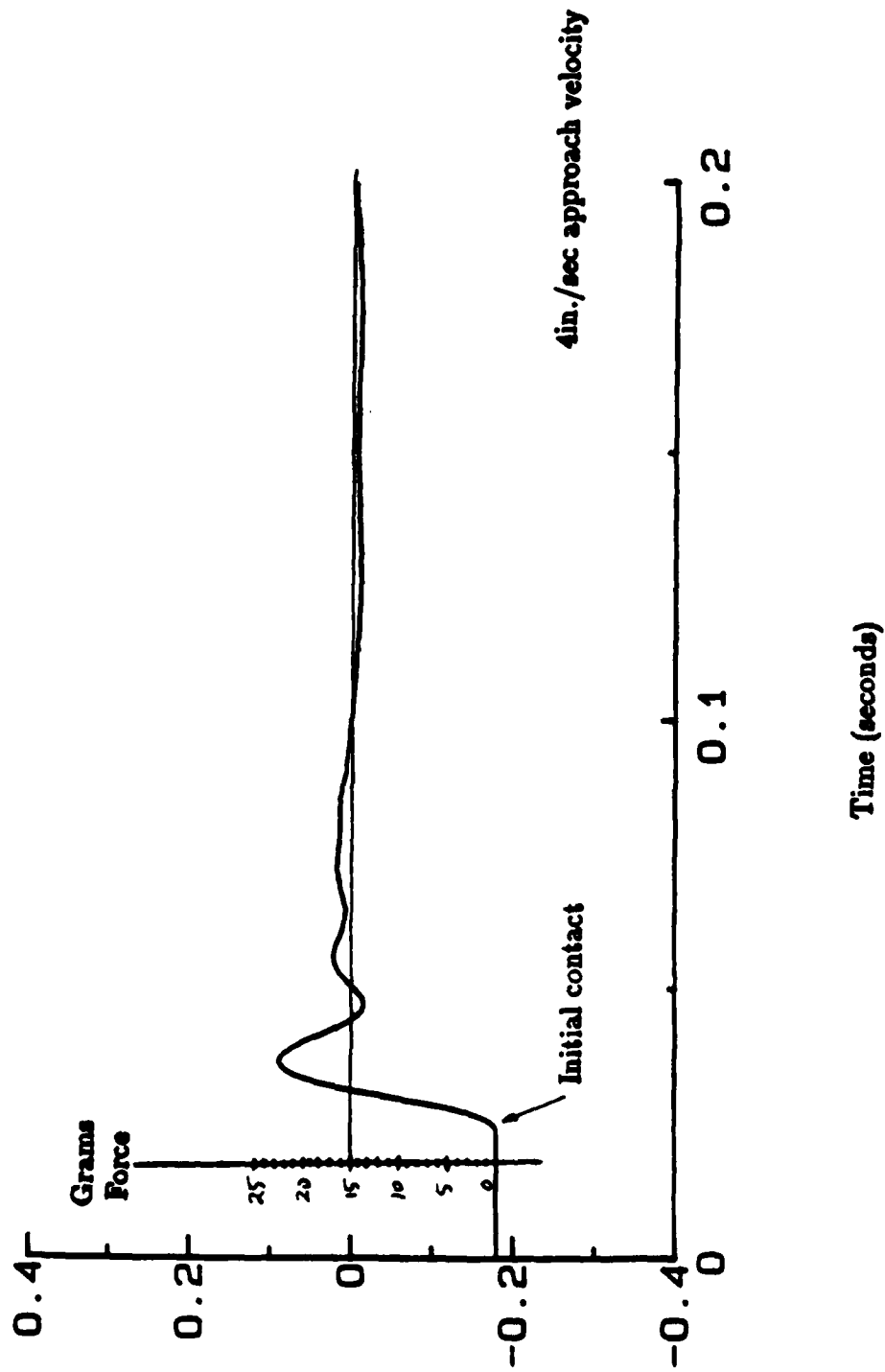


Figure II-26. Force history for a very flexible arm with a quick wrist and a load cell force sensor going from out of contact to a commanded 15 gram force level.

## SECTION II-3: TWO-LINK-ARM CONTROL

As noted in the Introduction to Part II, our DARPA-supported manipulator research focuses on developing and demonstrating high-performance end-point force control of very flexible manipulators. In parallel, we are pursuing research in fast, precise control of manipulator end-point *position* under AFOSR sponsorship. The two programs have been found to enhance one another's progress in many ways.

In particular, at an early point it was determined in joint discussion with our two sponsors that there was much to gain by designing our first experimental two-link arm so that it could be used alternately for tests in both programs. It was to serve first as a test bed for our initial basic AFOSR research in two-link-arm end-point *position* control and later as a prototype tool for designing the two-cooperating two-link-arm robot (which will be *force-control* based).

Both programs have proceeded according to plan: the experimental two-link arm was built jointly during the first year (as reported in our First Annual Report, Ref. 1), and was then used first for basic research in the AFOSR program (which is summarized in this section for convenience), and subsequently as the baseline for designing the DARPA Two-Cooperating-Arm System described in Section II-4 (as called for in Task 4.1: "Investigate many flexible-manipulator configurations").

In a new DARPA-sponsored program it is planned to take the Two-Cooperating Two-Link-Arm System to the experimental stage. To this end, numerous preliminary experiments will first be done on end-point *force* control of the single two-link arm described below:

### Introduction

The successful achievement of accurate, high bandwidth end-point control of the Stanford one-link flexible manipulator provided the groundwork for extending the technology to the general multi-link flexible manipulator case. Toward this goal, we constructed a two-link manipulator in the horizontal plane (so-called SCARA configuration) with a vertical drive at the working end.

The end-point control of a two-link arm represents a significant increase in complexity over the one-link flexible arm research pioneered in our lab. The complexities are introduced in three main areas. First, the two-link arm dynamics and kinematics are highly non-linear. Second, the two-link arm system is inherently multi-input, multi-output (MIMO) since the dynamics are highly coupled and in general cannot be decoupled into smaller single-input, multi-output (SIMO) systems. Third, the design and construction of an end-point sensor system that gives a high signal-to-noise ratio and high repeatability over a planar sensing area was required.

There is one area where the two-link arm has been intentionally made simpler than the one-link arm: the system flexibility has been discretely lumped in the form of springs in the

drive train instead of continuously distributed in the structure. Thus, the problem has been initially simplified in one respect so that we can more easily handle the new complexities of two links. Later versions of the two-link arm will include continuously flexible structural elements. In fact, the rigid wrist attached to the one-link flexible manipulator represents initial studies of the case of a flexible upper link and a rigid forearm link.

### *Non-Linear Dynamics and Kinematics*

The two-link arm dynamics are non-linear in three different ways. First, the inertia of the complete arm about the shoulder joint is a cosine function of the elbow joint angle. Thus, pulling the arm in will decrease the overall arm inertia, and the system's vibration frequencies will change. Second, there are centripetal accelerations present which are functions of the square of the link angular velocities. For the high speeds at which our system operates, these non-linear acceleration terms are roughly the same order of magnitude as the linear acceleration terms and cannot be ignored. The third major non-linearity is the large variation in inertia due to large changes in payload mass. Other practical non-linearities that have to be compensated or eliminated through careful design include motor and joint stiction, friction, hysteresis, backlash, and gravity effects.

These non-linear dynamics and kinematics have always been present on robotic systems built in the past, but could be accommodated with little adverse impact on performance by operating the system at very low bandwidths. The unique features of our manipulator, which require meticulous consideration of these non-linearities, are the high operating speeds, the presence of variable flexible modes, the large payload-to-arm-inertia ratio about the shoulder joint (about 1:1 for our arm compared to 1:10 for most arms), and especially the use of end-point sensing.

### *Multi-Input-Multi-Output (MIMO) Character*

The MIMO aspect of the two-link arm (along with the quick-wrist system, Section 1.1) represents a major step for our robotics lab. Most of our previous experiments with the one-link manipulator position and touch control have been SIMO systems which can be treated with classical control analysis and design techniques (such as Root Locus, Bode and Nyquist). The two-link arm is inherently a MIMO system and is difficult to treat with these techniques. State-space methodologies such as Linear Quadratic Loss and Sandy Gradient Search techniques have been successfully used in our research.

### **Experimental Apparatus**

The experimental apparatus consists of four major components: (1) the manipulator structure and drive system; (2) the sensors and associated electronics; (3) the control computer and associated interface electronics; and (4) the software for control design, analysis, and real-time control implementation.

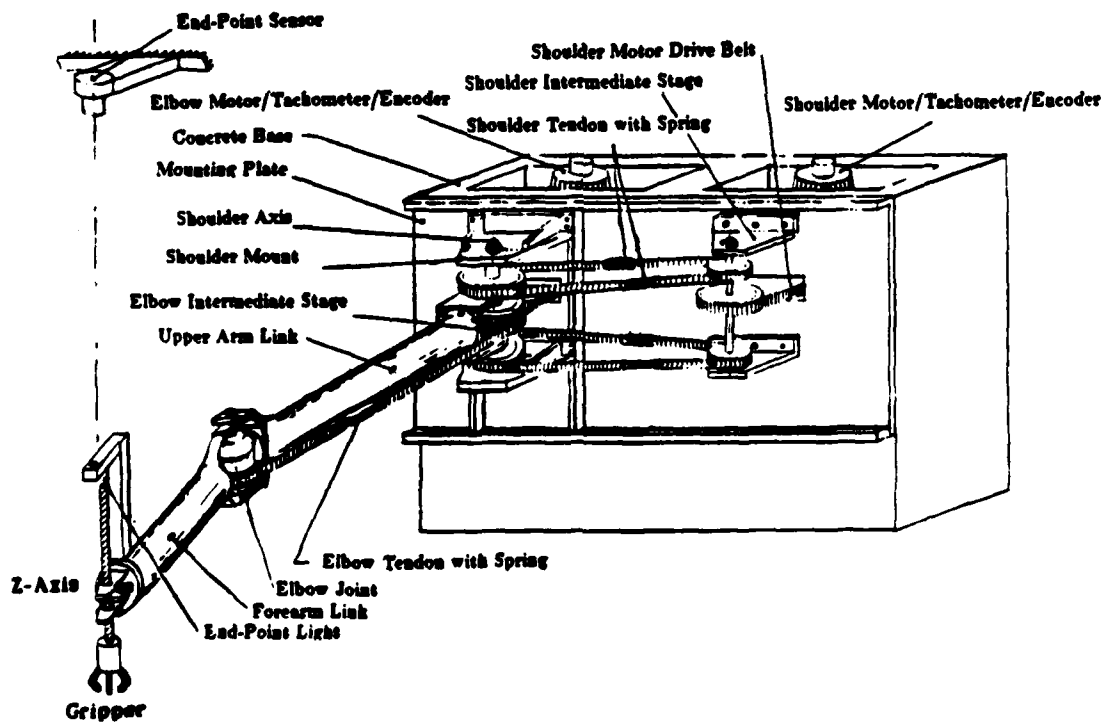
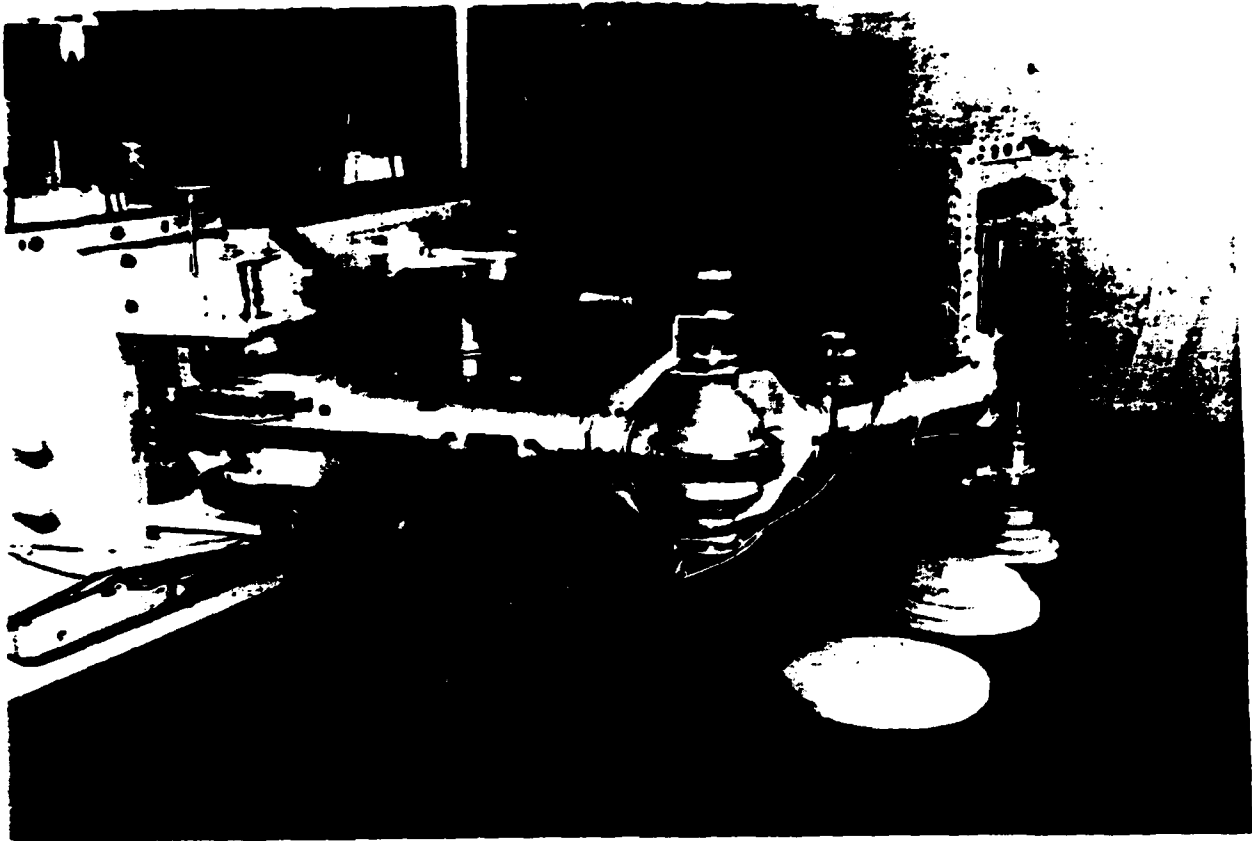
## *Manipulator Structure and Drive System*

Figure II-27 is a photograph of the two-link rigid arm with flexible tendon drives. The basic structure consists of a support base and two rigid links lying in a plane perpendicular to gravity and connected by revolute joints. The drive motors are attached to the base and transmit torque to the links via a lightly geared tendon drive train. The tendons have springs connected in-line as the source of exaggerated flexibility. At the end of the arm is a decoupled vertical axis and simple gripper that gives the arm complete three dimensional positioning capability.

The support base was constructed with about 1000 kg of reinforced concrete and a 3/4 in. thick aluminum mounting plate for the motors, drive train, and first joint. The concept behind such a massive base was to provide an essentially immovable and rigid support structure which does not interact dynamically with the flexible manipulator and adversely affect the results. The aluminum mounting plate also has provisions for balancing the manipulator or tilting it up to 15 degrees to allow up to a 25% component of gravity to affect the system.

As shown in the schematic of the manipulator in Figure II-27, the motor in the right cavity of the base drives the shoulder joint and upper arm link through four springs, while the motor in the left cavity of the base drives the elbow joint and fore arm link via an idler pulley centered about the shoulder joint and then through two springs. Each spring has a nominal spring constant of 40 lb/in (7000 N/m). The arm was designed to have minimum weight and inertia about the joints and yet be very stiff structurally by using aluminum tube and shell construction. The maximum vertical sag when fully loaded was designed to be less than 1 mm, and any structural vibration frequencies are well beyond those created with the springs in the tendon drives. Each link is about one-half meter long. The shoulder joint has a range of  $\pm 90$  degrees and the elbow joint has a range of  $\pm 120$  degrees. This gives the manipulator a 180 degree arc-shaped operational envelope with a minimum reach of 0.5 meter and a maximum reach of 1.0 meter from the shoulder joint. The vertical axis gives about 15 cm of vertical operational space. The arm was designed to have a payload-to-arm-inertia ratio about the shoulder of about one. The large payload capability, combined with the ability to change the springs in the tendon drives and the inertia at the motor shaft, gives the system a very wide range of plant dynamics for study.

The drive motors are so-called "printed circuit" electric DC motors that have no ferrous material in the armature. Thus the motors have no cogging torque and the ripple torque is minimized. The dominant non-linearity in the motors is brush friction and stiction, and these have been reduced to acceptable levels by feedforward and dither. The motors can provide up to 1580 os-in. (11.2 N-m) of torque, while the motor torque non-linearities can be held to less than 5 os-in. (0.04 N-m). The motors and gearing were sized such that the unloaded arm can theoretically move between any two points in its operational envelope within one second. For the one meter arm this gives accelerations on the order of one gravity ( $10 \text{ m/sec}^2$ ) at the tip. The shoulder drive train has a 6.06 to 1 gear reduction, and the elbow drive train has a 2.91 to 1 gear reduction. The gearing was sized to provide almost direct drive capability to minimize gearing problems such as backlash and large friction, rather than to provide the optimum impedance match for power transmission.



**Figure II-27. The Stanford Two-Link Manipulator with Flexible Tendons.**  
 a) Photograph b) Schematic

The vertical-axis drive system was designed to move up to a 1 kg payload through the full 15 cm range of motion in about two seconds. The vertical axis is driven with its own decoupled actuation system consisting of a small DC torque motor with optical encoder position sensor which drives a lead screw which in turn moves the gripper vertically. A pneumatic gripper at the tip of the vertical axis provides grip actuation on the order of 50 msec and is designed to pick-up one type of payload, a disk (of mass  $\leq 1$  kg) with a cylindrical grip hole machined in the center.

The two-link arm hardware has undergone several upgrades and "tuning" to improve performance. The elbow joint had to be stiffened, the other joints realigned and all the bearings replaced with higher grade bearings or self-aligning bearings to reduce stiction in the system. The final major change will be to replace the plastic/steel tendons with all steel tendons to further improve drive train linearity.

### *Sensors and Associated Electronics*

Initially, the primary sensor for the two-link arm is the optical end-point sensor. The basic construction of the sensor is a single large silicon wafer photodetector with associated optics. The center of brightness observed by the photodetector is output as a ratio of voltages across two perpendicular axes on the wafer. The new version has a 40 dB improvement in signal-to-noise ratio over the original one-link manipulator end-point sensor. The sensor is tuned to observe rapidly flashing infrared LED's mounted on the tip of the arm without the need of a light isolation hood. The bandwidth of the sensor for tracking one point is about 500 Hz and provides a resolution of 1 part in 1000 over the range of the sensor (i.e., 1 mm for a 1 meter range).

The system is also well instrumented with secondary sensors. Each motor has a tachometer and an 1800 line optical encoder. The shoulder joint has a 4096 line optical encoder, and the elbow joint has a 2540 line encoder. End-point position can be inferred to an accuracy of about 1 mm using these encoders (assuming rigid links and current calibration data), and rate information can be derived from the optical encoders using a special electronics board developed in our lab.

An electronics rack has been built to house the sensor electronics, motor power supplies and amplifiers, and computer input/output connections. The sensor electronics housed includes the end-point sensor electronics, five optical encoder position and rate boards (two for the motors, two for the joints and one for the vertical axis), and motor tachometer outputs. The motor controller includes three separate analog inputs to each motor, current limiters, and motor disabling electronics for safe and quick shut down of the system in case of computer failure, intermittent power failure, or imminent harm to equipment or people. The computer I/O connections include twelve 12-bit digital to analog converters, 32 differential 12-bit analog to digital converters, and a digital I/O cable for the encoder electronics.

## *Control Computer*

The control computer is a DEC PDP 11/24 mini-computer with a hardwired floating point board. In addition to the I/O electronics listed above, the computer system has a real-time clock, IEEE 488 bus, two RL02 removeable hard disks and asynchronous communication ports for connections to printers and direct lines to a VAX 11/780 mainframe computer cluster. The VAX computers are used for control design, analysis and simulation, while the PDP 11/24 is used to implement the controllers in real-time. The PDP 11/24 is running under RT11 version 5.2 operating system, and the control programs are written in FORTRAN and PDP assembly language.

## *Software*

Most of the control analysis, design, and simulation software used on this project was either commercially available or previously written here at Stanford. These include the Stanford developed OPTSYS, DISC, and SANDY, which are state-space linear quadratic gaussian design tools for MIMO systems. OPTSYS designs estimators and regulators for continuous analog control. DISC designs estimators and regulators using discrete, sampled data controllers such as digital computers. SANDY designs low order, robust controllers for continuous analog control. Analysis and simulation tools including the commercially available MatrixX and Control-C have proven very useful in our research. A graphical simulation tool has also been developed here (Section II-4) during the course of our research.

Most of the real-time control and peripheral software was developed in our lab using FORTRAN and PDP assembly language. The software developed for the one-link flexible arm was modified and enhanced for use on the two-link arm. The software includes assembly language drivers for the clock, analog-to-digital converters, digital-to-analog converters, end-point sensor, and optical encoders. Assembly routines were also written to speed up matrix and other floating point calculations used in the control loop. FORTRAN programs include, of course, the control programs, testing and calibration programs for all of the hardware, and a library of useful subroutines that perform the kinematic arm solution, inverse dynamics solution, data storage and retrieval, data transmission to and from the VAX, system identification software, and I/O handlers for the control programs.

## **SECTION II-4: DESIGN FOR A TWO-COOPERATING-ARM SYSTEM**

The work here is in fulfillment of Task 3 (Work Statement Section 4.1.3): Investigate New Robotic Arm Designs.

Several different aspects of our research concerned new robotic designs, the subject of Task 3 in the statement of work. The three main areas were the design and testing of a fast wrist for force control, design of an improved flexible drive system for the two link manipulator, and the analysis and design of a pair of full six degree of freedom manipulators for research on endpoint force control and cooperative manipulation. These designs have the common characteristics of decreased mass and rapid tip motion, as specified in Task 4.1.3.1. All three have at least two revolute joints, the cooperative arm design has five revolute joints in each of the manipulators (for a total of ten).

Impulsive force transients on targets were minimized by a variety of techniques (SOW 4.1.3.1.2.) These included the use of compliant structure and sensors (Ref. 8), the use of a low mass minimanipulator in both position and force control, the use of compliant drive systems, and the use of joint torque control to improve transient response.

### **(4.1.3.1.4)**

A study of the mass distribution of minimanipulators was performed, to provide understanding of the effect of mass distribution on dynamic performance. This led to an understanding of both manipulator design criteria and sensor placement for optimum response.

### **(4.2.4.2.5)**

We have performed both an analysis of requirements to extend endpoint control techniques to cooperating robots, and developed candidate designs of critical components. Areas of emphasis have been kinematic requirements, actuation and power transmission, endpoint sensing, control strategies, and computer architecture for realtime control.

The cooperating manipulators are a matched pair of six-degree-of-freedom robot arms, each with five revolute and one translational joints. The geometry is similar in its first three degrees of freedom to both our two-link flexible manipulator, from which it is directly derived, and more generally to commercial SCARA robots commonly used for assembly. These manipulators have two rotational joints with vertical axes so that the first two links operate in a horizontal plane, thus avoiding steady gravity torques. The next joint is a vertical translational joint. The benefit of this arrangement is that it suits many assembly tasks which typically involve vertical part mating and horizontal "pick-and-place" part acquisition. An additional benefit for research is that the vertical axis motion is orthogonal to, and decoupled from, the nonlinear dynamics of the first two joints.

The departures from conventional SCARA design are twofold: First, we introduce lumped flexibility into the drivetrains of the two main revolute joints, in a manner similar to the existing two link arm. Second, we add a wrist, with three intersecting revolute degrees of freedom. The addition of the wrist yields a six degree of freedom manipulator

which can both locate and orient within its work volume.

#### Sensing:

Sensing for force control and manipulator cooperation requires high-performance endpoint sensing for both position and force/torque. Robot cooperation places new demands on the bandwidth, accuracy and versatility of endpoint sensors. To this end, we have designed new sensing techniques for use in the new robot systems. The position sensing system is an extension of the endpoint sensing system developed by Maples already described (Section II-1). The force sensing systems are of two types: the loadcell-based sensor used on the fast wrist, and the joint torque sensor. Additional work has been done in evaluating six axis force/torque sensor performance.

#### Position:

The endpoint position sensor for position/force control studies and cooperation research must be capable of the following goals to be of practical value to experimentation:

- Measurements in two dimensions (ideally expandable to three)
- Tracking of multiple points, minimum of two.
- Wide area coverage, 0.25 M. minimum radius.
- Resolution of 1:1000, minimum.

The system we have developed is a time division multiplexing scheme for tracking multiple infrared light-emitting diodes. The illumination is sensed by a planar photodiode which yields analog signals proportional to the position and intensity of the centroid of illumination. A variety of techniques, both digital and analog, are used to remove noise from ambient illumination, sensor Schott noise, and drift.

The sensor includes the planar photodiode, an infrared filter, and an aspheric lens with an extremely low  $f$  number,  $f=0.65$ . The low  $f$  number is crucial for improving the signal-to-noise ratio of the system. The signal power  $S$  varies in an inverse square relationship to  $f$  number:

$$S = \frac{k}{f^2}$$

where

$S$  = Signal power

$K$  = Constant determined by emitter power/solid angle

$f$  = Lens diameter/ focal length

The nonlinearity of the lens is a function of radius, and can be corrected by curve fitting algorithms in software. Multiple targets are measured by pulsing the emitters in

sequence, with measurements of the ambient illumination made between them. The output of the sensor is passed through low noise field effect transistor preamplifiers, and is then integrated for the duration of the pulse (or the noise measurement period.) This analog integration suppresses high frequency Schott noise from the sensor, preamp, and emitters. The integrated response is then sampled, and converted to digital form.

In the controlling microprocessor, The average ambient signal is subtracted from the measurements, and an adjustable moving average is applied. These operations cancel low-frequency noise and diminish the effect of analog-to-digital quantization. Finally, normalization for emitter brightness and the radial correction are performed.

This system is already operational with two targets, and the minimum specifications have already been met or exceeded. Work is continuing to increase the number of targets that can be tracked simultaneously, and to increase the field of view.

### Force-Sensing Wrists

Our work with force sensing wrists has had two thrusts, the first is characterizing and using a currently available force wrist, and the second is exploring design modifications and completely new designs to improve performance. The force wrist we have is a six-axis device (both forces and torques about three axes). This wrist is based on the Maltese Cross or Scheinman configuration, named respectively for its appearance or inventor. This wrist was both designed and fabricated earlier at Stanford; the availability of detailed design information, supporting analysis, and the people responsible make possible insight and modifications not possible with commercially available sensors.

The Maltese Cross is so named after the shape of its inner structure of four sensing beams and supports. The key components of this sensor are four rectangular cross section beams. The four beams lie in a single plane, in the shape of a +. The four beams are cantilever-supported at their intersection and supported by thin T joints at their outer ends, providing compliance to small axial motions. Eight pairs of Constantan foil strain gages are affixed to opposite faces of the four beams. Each pair of gages is arranged as a voltage divider driven by a constant reference voltage. Eight signals from the middle of the voltage dividers are proportional to the bending strains in the beams (four beams x two directions of bending/beam). The geometry of the beams and the axially compliant support at their outer ends insure that the beams support forces and torques primarily by bending, rather than extension. The eight strain signals are amplified, converted to digital form, and resolved into forces and moments (in the desired frame) by matrix multiplication with a predefined matrix of gains.

One problem with such devices is that the analog signals from the strain gages are very small compared to the reference voltage used:

$$\frac{\Delta V}{V_{\text{ref}}} = G \cdot \epsilon$$

Where:

$\Delta V$  is the change in sensor signal due to applied forces

$V_{\text{ref}}$  is a constant reference voltage

$G$  is the gage factor, related to the bulk modulus material, typically around 2

$\epsilon$  is the strain

The strain,  $\epsilon$ , is typically  $10^{-6}$  to  $10^{-3}$ , and cannot go much higher without inducing yield in the material of the beam, leading to permanent offsets and eventual failure. These small signals suffer from noise contamination, and from bias/drift effects in the high gain electronics they require. A new analog interface circuit has been designed to reduce noise and drift below previous levels. The design employs FET input operational amplifiers, and a buffered bias reference to produce clean, steady signals.

Additional progress has been made to simplify the overload protection hardware. The overload hardware is a system of mechanical stops that carry excess or impulsive loads, protecting the beams and gages from overstress and failure. The current design is difficult to fabricate, and suffers from accumulation of machining tolerances. The new approach is based on cylindrical pins, which are press fit into the frame and rest in slightly oversize holes or slots in the central body. Excess loads deform the beams until at least one pin is in contact with the edge of its oversize hole. Any additional loading is supported by the pin and frame. This design avoids the tolerance accumulation in the previous assembly of several pieces. Close tolerances can be held by making the final overboring the last machining operation prior to assembly and gaging. Additional research on alternative geometries, materials, and gages is ongoing.

#### Actuation:

We have designed the new manipulators with all-electric actuation. Although electric motors have generally lower specific power levels than hydraulic or pneumatic actuators (at typical working pressures and flow rates), electric drives are more suited to our research because they do not introduce problems that might overshadow our main effort: researching the dynamics and control of robots. (Among the effects avoided by this choice are leakage for hydraulics, nonlinear compressibility for pneumatics, and nonrepeatable forces due to supply lines for both.)

For our manipulator design the two primary joint actuators ("shoulder" and "elbow") have radically different characteristics from the secondary joints (vertical stage and the three wrist axes). The shoulder and elbow motors are not carried by the robot: they transmit their power to the joints by means of a cable/pulley transmission that has flexibility deliberately added. The shoulder and elbow motors are not subject to gravity loading except under unusual interactions with payloads. In contrast, the motors for the secondary joints are all carried by the robot, and are often subjected to significant gravity loads even with the robot unladen. As a result of this dichotomy, the motors and transmissions used are quite different.

AD-A172 287

END-POINT CONTROL OF FLEXIBLE MANIPULATORS(U) STANFORD

2/2

UNIV CA DEPT OF AERONAUTICS AND ASTRONAUTICS

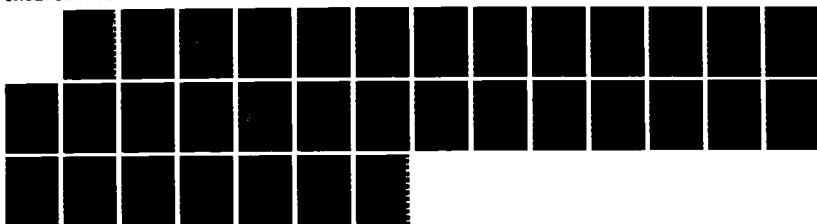
R H CANNON ET AL. SEP 86 AFMAL-TR-86-4051

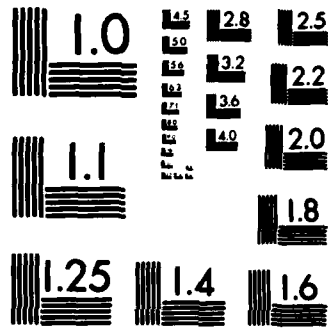
UNCLASSIFIED

F33615-82-K-5108

F/G 5/8

NL





1055

Since the primary motors do not move, their specific power (Mechanical power/Mass) and torque/mass ratios are not critical, because this motor mass is never accelerated. Similarly, the number of wires each motor requires is inconsequential. Since gravity loads are rare, large reduction ratios are not needed to avoid thermal overload due to resisting gravity loads. Thus, large motors (specifically, large radius) offer greater efficiency ( $K_m = \text{Torque}/\text{square-root}(\text{electrical power})$ ) in the comparatively low speed, high torque regime indicated by our desire to study flexibility as a phenomenon separate from cogging/backlash effects of gearing. Brushless motors offer lower friction and superior operation at low speeds, at the expense (which is an acceptable one to us) of more complicated drive circuitry and wiring.

The secondary motors (vertical stage and wrist) all move with the robot. Thus, it is important to use small, low mass motors that require the minimum of cabling. It is also necessary to gear them so that they are efficiently coupled to their loads, so that they can provide adequate acceleration, static forces at the end effector, and resistance to steady gravity loads without overheating. For these reasons, we designed the secondary joints with small rare-earth permanent magnet motors, with conventional brush commutation. The high field strength of the Samarium-Cobalt magnets, the two-wire drive, and the gearing all work to provide high torque/inertia for the secondary joints. The effects of the gearing are an acceptable cost in these stages because of the smaller sizes of the secondary links, and the proximity of the six-axis force wrist.

To drive these motors, we again depart from current commercial practice. We plan to avoid pulse-width modulation amplifiers wherever possible, and use isolation (electrical and physical) to suppress noise from those PMW devices we cannot replace. Although PMW amplifiers are less expensive, they produce large amounts of electrical noise due to rapid switching ( pulse modulating) of large currents. Noise of this type degrades analog sensor signals unless extensive grounding and shielding are maintained.

Although we intend to use linear (Class AB) amplifiers for all of the secondary joints, the power levels required by the primary motors, along with the commutation requirements of brushless motors, may make linear amplifiers impracticable. To avoid noise, should PMW amplifiers be required, we have planned for physically separate cabinets for the power electronics and the sensor electronics. Isolation amplifiers, to maintain separate grounds, have been incorporated into the design. Avoiding noise and shielding problems by original planning is especially crucial given the rapidly evolving nature of the robots, as we experiment with new control methods, new sensors, and new actuators.

#### (SOW 4.1.3.1.3)

The mechanical transmissions in the new manipulators have been designed to facilitate the study of robot control, coordination and cooperation. The transmission from the primary drive motors to the shoulder and elbow joints of each manipulator are a system of stranded steel cables pinned to aluminum drive disks. This arrangement makes it easy to add, vary, or remove flexibility, at the same time it avoids the friction, cogging torques, and backlash of gear based transmissions. The vertical stage is driven via a ballnut and leadscrew to provide a rotary-to-linear conversion with low friction.

The wrist (see Fig. II-28) uses a bevel gear system to achieve three axes with a common

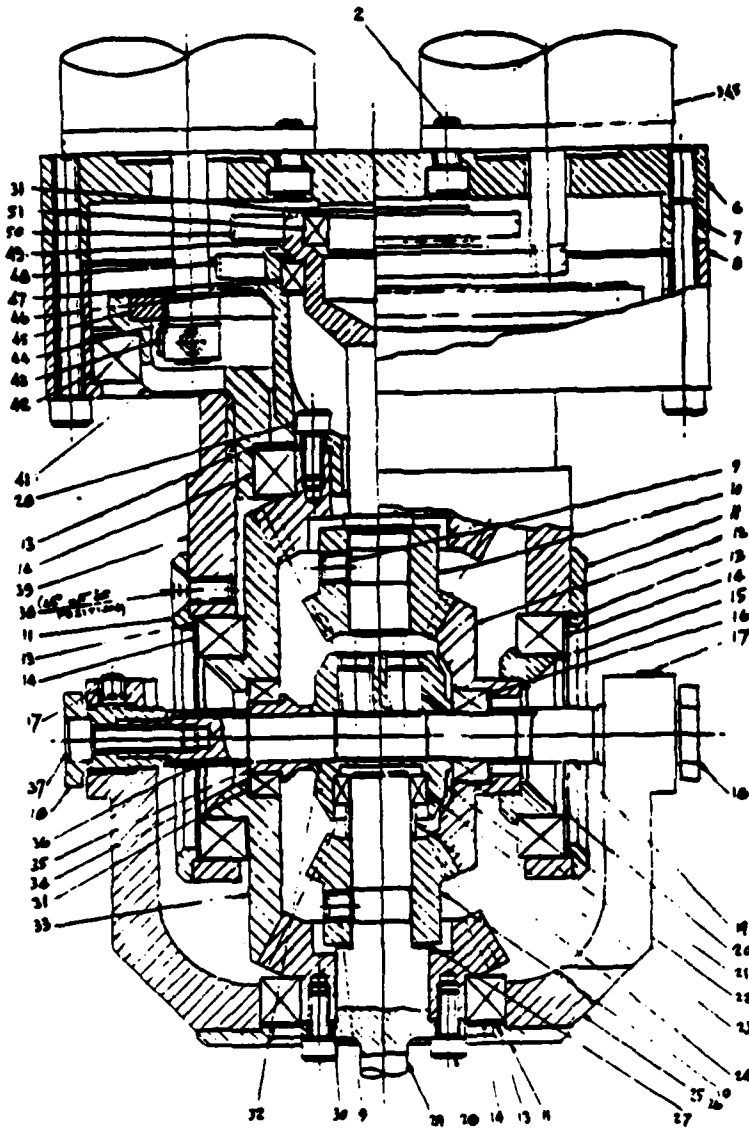


**Figure II-28. Initial design of a robotic wrist with three intersecting, revolute axes, shown roughly full scale.**

intersection point. Intersecting axes permit decoupling the inverse kinematics of the arm from a single sixth order problem into two third order problems: locating the wrist point (intersection) and orienting the end tool/gripper about the wrist point. This decoupling ensures closed-form solutions for the inverse kinematics which may be computed in a known amount of time, which is necessary for fixed sample rate digital control techniques. The wrist is driven by three rare-earth magnet servomotors, and is designed to work with payloads of up to two kilograms. A six-axis force wrist will be installed between the wrist and the D.C. motor driven parallel jaw gripper.

#### **Control:**

The main purpose of the new manipulator designs is to provide both springboards for new robotic concepts and, most importantly, testbed environments for new control algorithms. In light of these goals, the following characteristics have been incorporated into the design:

- A rich set of sensors for position, velocity, force, and torque located at the actuators, intermediate joints, the endpoint of the manipulators.
- Actuators that have linear characteristics, large amounts of control effort, and high bandwidth.
- Mechanical transmissions that allow the flexibility to be easily varied, as required by the experiments.
- A computer architecture that provides high speed implementation of control algorithms by virtue of well defined interfaces, hierarchical control, and multiple processor design.

With these qualities incorporated into the manipulators, we can plan to develop a series of control systems for the arms. The intended series proceeds from simple, conventional control techniques to new control systems that demonstrate the greater speed, precision, utility, and cooperation possible using end-point sensing. The planned sequence of control strategies is detailed below, with a brief explanation of the purpose of each step within the sequence:

#### **PID-Actuator control:**

The first control system attempted will be a simple, low order control system based on colocated measurements only. Such a system is the easiest to stabilize, and will aid in debugging the various subsystems and integrating them into a working whole. A simple, low order controller will also aid in an initial phase of model identification.

#### **Full state colocated control:**

This system can be used to refine the system model and to establish performance limits in speed and accuracy for the best conventional control of the manipulators. These limits are useful for comparison to performance using endpoint control algorithms.

#### **Simple endpoint position control:**

**Test and integrate the endpoint position sensor into the simplest control system that will stabilize the manipulator. Use this system to determine models of the non-colocated dynamics of the manipulator.**

#### **State feedback using endpoint position sensing:**

**Find performance limits in speed and accuracy for comparison to colocated control; refine system model; experiment with performance/robustness tradeoffs.**

#### **Multirate control:**

**Investigate the performance benefits from multirate control systems. Continue with these as part of later designs if theoretical benefits are substantially realized. Plan to use the intermediate joint torque and joint position sensors as the primary inputs to the fast control loop.**

#### **Endpoint force control:**

**Integrate and test the force sensing wrist starting with a simple, low performance controller to help identify the new system model. Continue with higher order control systems as model of dynamics in the force mode are refined. Study the effects of endpoint constraints on performance. Develop a robust force controller.**

#### **Hybrid endpoint force/position control:**

**Combine the relevant portions of the position and force control algorithms to produce a control system capable of programmable compliance. Experiment with performance and robustness. This is the basis of a multiple robot cooperation capability.**

#### **Generalized compliance:**

**Augment the hybrid controller to provide the ability to synthesize both mass and damping as well as stiffness. Demonstrate the increased utility of this system over the simple hybrid controller.**

#### **Add integral force terms:**

**Add the ability to provide force terms proportional to the integral of position error. Provide logic to prevent conflicting integral terms between the two robots. This is the basis of master/slave cooperation.**

#### **Smooth switching:**

**Develop algorithms to switch manipulators' control modes and/or gains in a manner that is smooth during the transient and yet acceptably rapid.**

### **Computer system architecture:**

The amount of computation required for this testbed is large, both for the complex control algorithms we intend to develop, and for the complexities inherent in the interface and task management of two cooperating robot manipulators. We require a computer architecture that provides sufficient processing power for the tasks, and the flexibility to increase the available computational power in an incremental manner, as tasks increase in complexity, or new tasks are envisioned. Further, we wish to design a system that lets us separate the computational burden in a manner that prevents changes in one subsystem from having unforeseen and/or dangerous effect on the others. Such a separation, in addition to being sound practice for a large software system, has the benefit that distinct tasks that are decoupled from one another may be handled by different processors simultaneously. Multiprocessing is, in general, not an easy technique to apply efficiently and reliably, and research in this field is still in its early stages. Robot control has several characteristics that make it an excellent candidate for multiprocessing:

The time sequence of the control algorithm is fixed, and known a priori.

The data flow is similarly fixed, and can be partitioned into simple relationships, many of which are single direction, facilitating decoupling.

The data structures employed are generally simple and small.

A multiprocessing system is consistent with our desire for high throughput, freedom to add power (processors) incrementally, and separation of distinct functions. In addition, such an architecture takes advantage of the special structure of the robot control problem to achieve these goals more economically than the use of a single very high speed processor would. This structure also makes it a very natural choice to separate the servo-control tasks of the robots from the task coordination/planning aspects. This separation into a hierarchy of planning, coordination, and control, with clean interfaces between levels will make this system easy to use and to improve. By designing a multiprocessor/hierarchical control system, experimenters will be able to add computer power incrementally (and economically) and benefit from the clean interface between a general, control structure, and a task scheduler/coordinator which is required to make the robot cooperation work to its fullest extent.

### **Benchmark study:**

It is essential in the design of the computer system described above to have measurements of the computational power of the available processors, in order to ensure that the system will provide the throughput required of it. Additionally, a communications structure must be chosen (or designed) to let the tasks and their processors communicate in a reliable fashion. For our planned research in control systems for robots, the great majority of time critical tasks perform large amounts of floating point computations. While commercial products often substitute integer math with scaling, the lack of generality and flexibility imposed is detrimental to research progress. There are many published studies of the speed of various computers, the best known is the Whetstone benchmark. However, none of the studies known to our group considered the type of calculations most representative of robot control tasks. (The Whetstone benchmarks were originally written for a

ministry of the British government, and were originally used - many years ago - to rank computers for business and economic data processing.) We have written our own series of benchmark programs to test various processors' abilities in the following areas:

- MATMULT** Tests speed of floating point matrix multiplication (this is a mix of indexing, and floating point add and multiply.)
- DIVIDE** Tests speed of floating point division.
- TRIG** Tests speed of Floating point trigonometric function evaluation. (specifically cosines)
- ARCTAN** Tests the speed of evaluation of the arctangent function. (Floating Point)
- DIOP** Tests the speed of solving systems of linear equations with floating point coefficients.

These routines were originally coded in the FORTRAN language. They have already been timed on our current control computers, a VAX Superminicomputer, and several microprocessors. The results are shown if in Fig. II-29. Further effort is being made to refine the programs, and to translate the into the C programming language, for additional testing. The data so far already illustrates the wide range of performance between candidate processors. More careful testing of the latest versions of microprocessors will be carried out before a final decision is made.

FUNCTION	PROGRAM	VAX 11-780 F.P. ACCEL MAX FORT/MS	11/23 F.P. BOARD FORT 77/RT11	11/24 F.P. BOARD FORT 77/RT11	NEC80 11/75 F.P. CHIP FORT 77/RT11	NEC80 11/83 F.P. CHIP FORT 77/RT11	IBM PC-XT 4.7MHz 8087 4.7MHz MS FORT 3.2/MS	IBM PC-AT 6MHz 80287 6MHz MS FORT 3.2/MS	IBM PC-AT 10MHz 80287 6.67 MHz MS FORT 3.2/MS	IBM PC-AT 10MHz 80287 10 MHz MS FORT 3.2/MS
MATRIX MULT.	MATRIX	11.00	100.00	105.00	58.00	24.00	249.00	155.00	93.00	78.00
DIOPHANTINE SOL.	DIOP	3.00	30.00	31.00	14.00	7.50	83.00	46.00	27.00	24.00
F.P. DIVISION 166 OPERATIONS	DIVIDE	0.36 0.10	63.00 15.75	66.00 16.50	36.00 9.50	24.00 6.00	7500.00 1825.00	425.00 106.25	255.00 63.75	194.00 48.50
COSINE 166 OPERATIONS	TRIG	1.50 1.39	18.00 16.67	19.00 17.59	18.50 9.72	7.00 6.48	900.00 833.33	917.00 849.07	550.00 509.26	420.00 388.89
ARCTAN2 166 OPERATIONS	ARCTAN	12.40 77.50	74.00 462.50	77.00 481.25	57.00 356.25	18.50 115.43	4000.00 25000.00	80.00 500.00	47.00 293.75	37.50 234.38

Figure II-29. Speed comparisons of nine computer systems using five mathematical benchmark routines developed in ARL. Shown here are results using single precision floating point calculations for families of DEC and IBM computers. Times are in seconds, and times for purely repetitive calculations have been normalized to one million operations for ease of comparison to other computers. Future plans include benchmarking other processor families.

## SECTION II-5: TIGHT CONTROL OF JOINT TORQUE

### Introduction:

In our work in the areas of force sensors (Task 2) and control algorithms (Task 4), we have had success due to collaboration between the Aerospace Robotics Laboratory (ARL), under Professor Cannon and the Robotics Laboratory of SAIL, under Professor Binford. The work described in this section is joint torque control.

Joint torque control is shown to provide dramatic increases in robot speed and accuracy by reducing the effects of nonlinearity, flexibility, and inertia in the actuator and transmission. These improvements were achieved using a sensor based on a mature and low-cost technology - strain gages.

Joint torque control is the technique of sensing torques at joints of a system (or alternatively forces, for translational rather than rotary joints) and using these measurements in feedback control algorithms to control the joint torques to desired levels. A joint torque sensor was developed by students working with SAIL, and control algorithms were developed and tested in ARL.

### Overview/purpose:

The underlying reasons for the importance of joint torque control can be seen by considering the ways in which joint torques effect both the motions of the arm and the forces exerted between the arm and its environment. In both the static and the dynamic cases, the joint torques have a direct effect on the behavior. In fact, they can be looked at as the driving cause of the arm's behavior. A common form of these relationships are the following, using the basic form and definitions of Craig (Ref. 2):

Static Case, neglecting gravity and friction:

$$\tau = J^T F$$

Dynamic Case:

$$\tau = M(\Theta)\ddot{\Theta} + V(\Theta, \dot{\Theta}) + G(\Theta) + E(\Theta, \dot{\Theta}) + J^T F$$

Where

$F$  is a 6x1 Cartesian Force / Moment vector acting at the end-effector.

$\delta X$  is a 6x1 infinitesimal Cartesian displacement of the end-effector.

$\tau$  is a 6x1 vector of torques at the joints.

$\delta\Theta$  is a 6x1 vector of infinitesimal joint displacements.

$M(\Theta)$  is the  $n \times n$  inertia matrix of the manipulator.

$V(\Theta, \dot{\Theta})$  is an  $n \times 1$  vector of centrifugal and Coriolis terms.

$G(\Theta)$  is an  $n \times 1$  vector of gravity terms.

$E(\Theta, \dot{\Theta})$  is an  $n \times 1$  vector of friction terms.

and the definition of the Jacobian is:

$$\delta X = J \delta \Theta$$

Each element of  $M(\Theta)$  and  $G(\Theta)$  is a complex function which depends on  $\Theta$ , the position of all the joints of the manipulator. Each element of  $V(\Theta, \dot{\Theta})$  and  $E(\Theta, \dot{\Theta})$  is a complex function of both  $\Theta$  and  $\dot{\Theta}$ .

The key to understanding the importance of joint torque control is understanding that in these equations, torque is defined as torque actually applied to the links of the manipulator, NOT the torques presupposed by models (that neglect inertia, flexibility, and nonlinearity). Thus, if we wish to control the motions and forces of the manipulator, we must be able to control the torques delivered TO THE JOINTS.

A close analogy can be drawn between joint torque control and endpoint control: Both techniques use a direct measurement of a quantity that is crucial for high performance, both techniques can contain dynamic behavior and/or nonlinearities between sensor and actuator. Finally, although both techniques require careful analysis to yield stable control, they can provide dramatic improvements in performance that make the analysis very worthwhile. Joint torque control can be looked at as a special case of endpoint force control, where each link is considered a single link manipulator with endpoint force (torque) control applied to each link, in turn. In this way, many of the ideas and techniques used for force control of a single flexible link can be applied to joint control of a more complex manipulator.

Control systems for robot dynamics are never perfect, and there are many different ways to classify the types of errors and the effects they have on control analysis and performance. One major class of errors are errors in the dynamic model that result in commanding incorrect joint torques for the motions and forces desired. Such errors can be thought of as errors in (or complete disregard for) terms in the equations shown previously. Common reasons for such errors are:

- Linearisation of the dynamics
- Errors in inertia properties.
- Neglecting external disturbances such as gravity and payload forces.

The other class of errors are those effects that cause differences between the torques commanded and the torques actually applied to the joints. Common reasons for these errors are:

- Actuator nonlinearities, biases or gain changes
- Friction in joints, drive train, or in actuators themselves
- Flexibility and/or nonlinear effects between actuator and the joints.
- Disturbances such as cabling drag

Joint torque control directly fights this latter class of errors in modeling. As a high performance inner control loop, it allows outer control loops to do a better job of correcting errors of the first type. In actual robots, there are many significant effects that fall into the class directly affected by joint torque control, some common examples are:

- Friction in motors, gears, joints and potentiometers
- Magnetic cogging and saturation effects
- Temperature dependent effects of mechanical and electronic components
- Nonlinearities in pneumatics and hydraulics
- Different actuator behaviors in different regimes of speed, frequency, or power

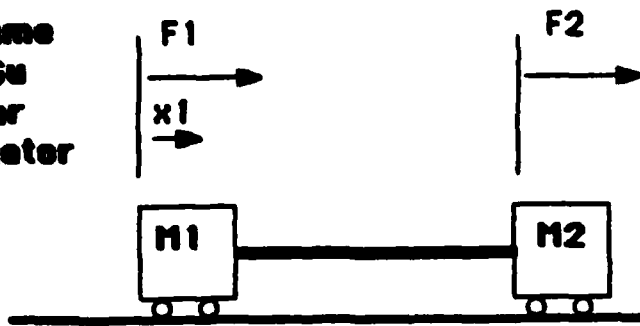
Many of these phenomena defy open loop compensation, because they depend on unmeasured quantities (e.g. local temperatures) or are not repeatable (e.g. wear induced changes in friction) or are difficult to model well in a realtime control system (e.g. hysteresis in pneuematics, magnetics, or friction.)

One can achieve tremendous reduction in variations, nonlinearities, and model errors/oversimplifications with an "intermediate" joint torque sensor. It is noncolocated, in that it is separated from the actuator by a link and any transmission, (and thus encloses the unmodeled phenonena), but is not at the tip of the arm.

Figures II-30 and II-31 show a series of methods to estimate the torque applied to a link. For ease of presentation, we illustrate linear forces and motions rather than their rotational analogs. The principal remains the same, but the schmatic representation is clearer. The first three cases, (Fig. II-30), show open loop methods to estimate force on a mass that represents a link. The increasing sophistication of the models includes inertial and friction effects, and could, in fact, include models of repeatable modelable nonlinearities. As stated previously, even with the increased computation, open loop models still cannot correct for dependence on unmeasured phenomena or nonrepeatability.

The next series of diagrams (Fig. II-31) shows sensing at the joint to correct for model deficiencies. The first uses position sensing on both sides of the modeled compliance to estimate the force. The compliance of the drive system is used in the same manner as a spring scale. This technique compensates for actuator nonlinearity, friction, and inertia, but errors from link friction remain. Practically, for stiff drive systems, sensitivity and nonlinearity due to the "spring" makes this a poor measurement. For deliberately flexible drives, such as our two link manipulator, this technique could yield good results, due to the linear characteristic of the compliance. The next diagram shows the first inclusion of direct joint torque measurement. The sensor is beyond the actuator, drive train, and all friction. The measurement is as good as the sensor is. The final diagram of the figure shows the combination of direct measurement and plant model using a Kalman filter. The Kalman filter combines knowledge of plant dynamics, plant and sensor noise with the

Assume  
 $F_1 = Gu$   
 linear  
 actuator

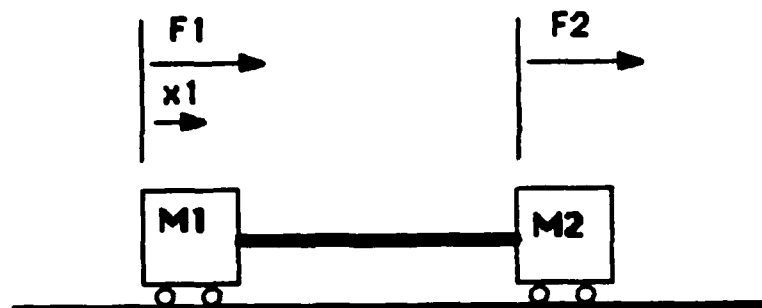


Estimate:

$$\hat{F}_2 = Gu$$

Neglects:

Friction  
 Actuator mass  
 Actuator nonlinearity  
 Flexibility in transmission

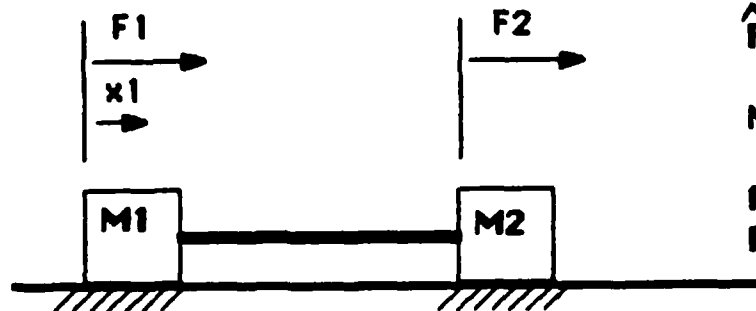


Estimate:

$$\hat{F}_2 = Gu - M_1 \ddot{x}$$

Neglects:

Friction  
 Actuator nonlinearity  
 Flexibility in transmission



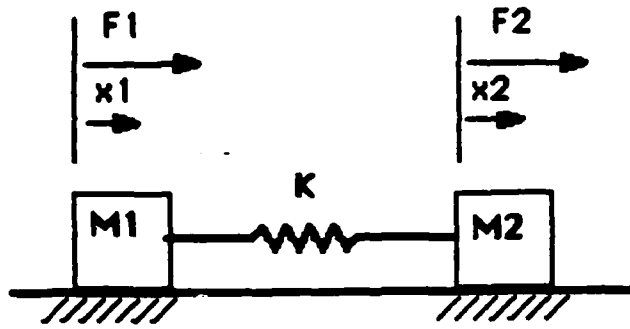
Estimate:

$$\hat{F}_2 = Gu - M_1 \ddot{x}_1 - \text{Friction}(x_1, \dot{x}_1)$$

Neglects:

Actuator nonlinearity  
 Flexibility in transmission

Figure II-30. Three methods of open loop force estimation.

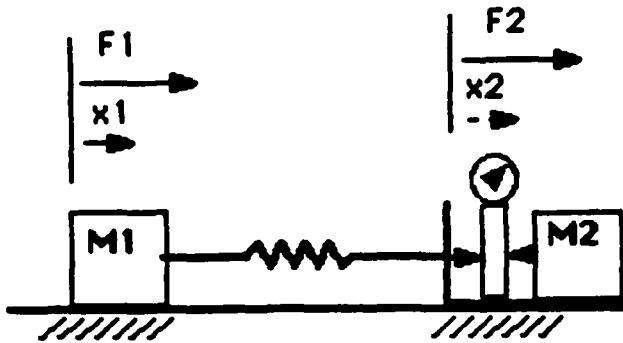


**Estimate:**

$$\hat{F}_2 = K(x_1 - x_2) - \text{Friction}(x_2, \dot{x}_2)$$

**Assumes:**

Linear spring  
Accurate, repeatable friction model

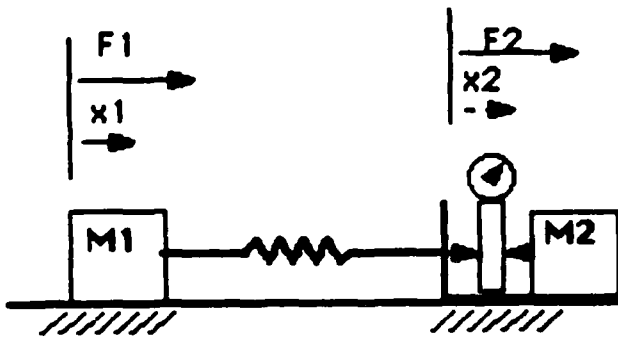


**Estimate:**

$$\hat{F}_2 = \text{Sensor measurement}$$

**Assumes:**

low sensor noise, bias, and nonlinearity



**Estimate:**

$$\hat{F}_2 = \text{Kalman}(\text{State}, \text{Sensor})$$

**Assumes:**

low sensor nonlinearity

**Figure II-31. Three methods to estimate force based on non-located measurements.**

measurements available to form the optimal estimate of force. If the sensor has low noise, the Kalman filter will track the sensor signal with little delay, providing an estimate which is both accurate and current.

The strength of this technique is that the model can be simple, yet the direct measurement of the torque (and position if available) makes the model very robust to both model errors and external disturbances. These robustness qualities are VERY important for manipulator control. As we have already commented on model complexity and errors, consider that the non-colocated techniques did NOT depend on modeling the dynamic interaction of subsequent links to achieve accuracy in joint torque estimation. These effects can be measured by the joint sensor because such forces are transmitted through the rigid link to the sensor, and are thus incorporated directly into the estimate. Such an estimation technique accounts for the dynamics of outboard links, payload, or collisions without having to model them explicitly. The technique is simple enough to use in a high bandwidth servo loop, yet it can yield tremendous benefits in performance.

The effect of the rigid link assumption is worth exploring, because we may wish to work with deliberately flexible links, or with bandwidths and payloads for which link flexibility becomes significant.

In the lumped flexibility case, the flexibility is restricted to the drive train, which acts as a pure compliance, without significant mass. The structural links are effectively rigid bodies, which transmit forces (essentially) instantly to the sensor. The force measurement incorporates the disturbances without pause, limited only by the speed of the Kalman filter (for a low noise sensor this will be fast compared to the rest of the system.) The flexibility between the link and its actuator is a lumped element. Control effort at high bandwidth is attenuated and phase shifted, but does not suffer the finite delay associated with wave propagation. Therefore, with sufficient control effort, the closed loop bandwidth could conceivably approach that of the sensor itself.

In the distributed flexibility case, the wave propagation time delays can effect both sensing and actuation. Disturbances at the distal (far) end of subsequent links will not effect the joint torque sensor until the traveling wave has run the length of the link. Thus, the sensing of disturbances is intrinsically delayed. Similarly, actuation through distributed flexibility is delayed by wave propagation, and cannot surmount this limit even with infinite control effort.

The possibility of doing feedforward compensation of planned torques on outboard links is a possible means to improve response. However, this can only help with planned trajectories, and the computational burden is even greater than feedforward for a rigid body manipulator, in itself no easy task. Unplanned disturbances, whether at the tip of the arm or along some link can only be controlled within the bandwidth imposed by wave propagation limits, even with ideal sensors and actuators. Multiple flexible link manipulators, with either direct or compliant drive are beyond the experimental scope of this research. However, a new facility for performing studies in this area is currently under design. This testbed will have a planar multi-link manipulator and will use air bearings to support the joints to remove the effects of friction, gravity, and torsional/bending coupling of modes.

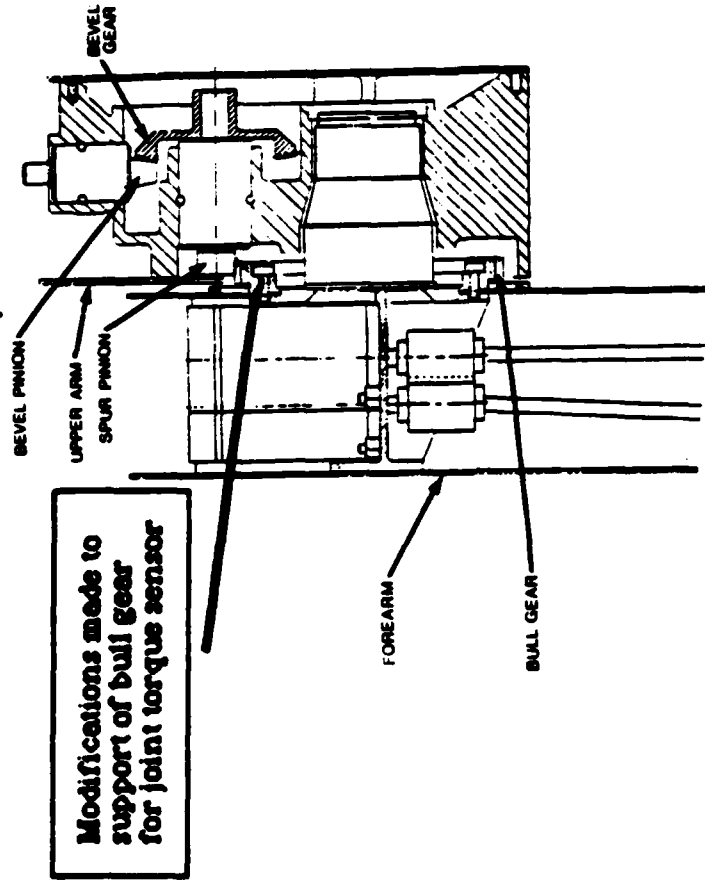
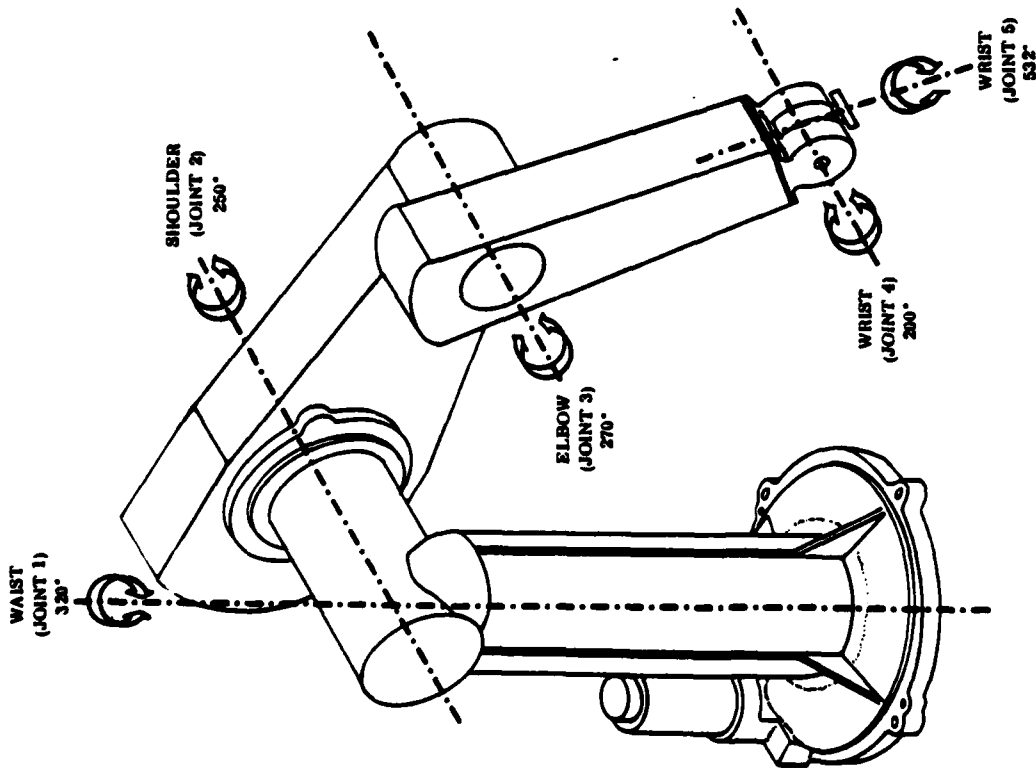


**Figure II-32. Drawing of the PUMA 500 series robot, with a detail of joint 3, which shows the location of the torque sensor and the bull gear it supports.**

## Experiments:

The experimental hardware was developed by two students in a Master's level mechanical design class. The project had industry sponsorship and was supervised by Unimation west (later ADEPT Technology) engineers as well as ME and CS faculty. A single joint of a Unimation PUMA 500 series robot was instrumented with a joint torque sensor on joint three (in PUMA parlance), see Figure II-32. The sensor was required to be a retrofit to the existing arm, causing minimal changes in robot performance. The design uses foil strain gauges, mounted on machined supports of a bull gear, to measure torque applied to the link. Despite the constraints on the design, the following performance characteristics were achieved:

Sensitivity: 0.0227 volts/os. (force referred to wrist)

Nonlinearity with respect to joint angle: 8.7% max. gain variation over joint range

Hysteresis: 1.0 Os. Max. with rated loads

These characteristics were measured both by the designers of the sensor, and were checked and found to be in good agreement in the course of control system design and experimentation in ARL. Usable bandwidth was found to be highly dependent on joint velocity. This effect is seen to be a consequence of the limitations due to the retrofit design. The sensor output is sensitive to the relative meshing of the final drive pinion against the bull gear (see Fig. II-32); the noise frequency from passing over the rough spots in the mesh depends on the speed at which the joint is driven over them, as does the amplitude. The worst case usable bandwidth of roughly 20 Hz. seems to be the principle limitation in performance, along with the related nonlinearity in angle. There is no fundamental reason why a sensor incorporated at the design phase could not overcome these problems. In fact, the flexible tendon drive currently used in our two link manipulator avoids the gear on gear forces which give rise to these problems.

The Unimation controller was found to be unsuitable for the type of experimentation we wished to do, so we used a transconductance (voltage to current) amplifier design (originally for the Z axis of the two link arm) to drive the motor. Amplifier Characteristics are as follows:

Sensitivity 2.27 volts input / ampere output

Max. current 4.0 Amp.

Max. voltage 22.0 volts

Bandwidth: 200 Hz.

This was adequate to test control algorithms, yet low enough power to prevent the initial stability problems during experimentation from being a hazard to experimentors or the robot. Some of the tests of the joint torque servo drove the amplifier into voltage saturation for large initial errors, thus showing lower performance than would otherwise be realized. Future experiments will use an amplifier better matched to the actuator.

Reliable data concerning the motor performance were not available, so the key parameters of the combined motor and geartrain were measured using the torque sensor, and a set of weights as a cross check:

**Sensitivity: 970 Oz./Amp. (referred to wrist)**

**Hysteresis: 0.07 Amp. (= 68 Oz. referred to the wrist)**

**Bandwidth:  $\approx$  50 Hz.**

It should be noted that the motor/geartrain friction was so great that the joint would not move due to gravity loads on the link, even with the link horizontal, until additional weight was added or the joint torque control loop was closed.

Using the same basic approach as Luh, Fisher, and Paul (Ref. 7) who had done similar work at Purdue, we used an analog compensator for the initial experiments with the arm. Since the first goal was to reduce the frictional effects of the arm drive while avoiding objectionable limit cycle behavior, simplicity and stability were favored over more complex designs. The principal nonlinearity in the PUMA robot we were experimenting with has a different principal nonlinearity than that described in later work at Purdue, and thus the form of the compensation is different. We employ a lag-lead network to counter Coulomb friction, where Paul et al uses phase lead compensation to counter backlash. (Interestingly, some of the Purdue work was done on a "Stanford" arm, a 6 degree of freedom manipulator originally designed for Stanford's Robotic laboratory.)

Figures II-33 and II-34 show a block diagram of the system and the form of the compensator. Since we were interested primarily in studying the effects of an inner force control loop, we did not close subsequent velocity or position loops. We let the gravity terms provide the error to drive the system, causing the servo to swing toward the vertical once released from horizontal. Without any compensation, the arm would not move with only the gravity term to force it. With the loop closed, the system approaches the vertical, with a residual force error that is only a few ounces. (2 - 3 s. this is near the resolution of the strip chart records.) See Figure II-35. A steady state error is to be expected of a system with no integral control and finite proportional gain. Integral control could be added, but this increases the order of both the inner control loop and complicates the task of the outer loop, which has to contend with another pole in the system response. Outer loops using tip position or tip force control (with an integration here) will drive the torque error to zero, because they contain integral terms forced by a sensor which encloses the error. Such control loops can be run at lower speed, (as appropriate given their complexity, from kinematics alone) and will regulate these errors using the sensor that really matters, the one at the working end of the robot.

The initial linear section of the angle trajectory on figure II-35 is a result of the amplifier's voltage saturation during this time. Thus, the response of the system with an amplifier correctly sized to the actuator should yield response that is significantly faster than that shown here, and should show a lightly damped pendulum oscillation rather than the modest overshoot shown here.

We intend to do more experiments with this robot, including a better characterization of its friction nonlinearities, a digital realization of more ambitious compensation, which may include a feedforward gravity term. Plans to incorporate similar sensing and control is discussed in the sections on new arm design and analysis.

**Impact:**

There are several aspects of the significance of this analysis and experimentation which

## Block Diagram

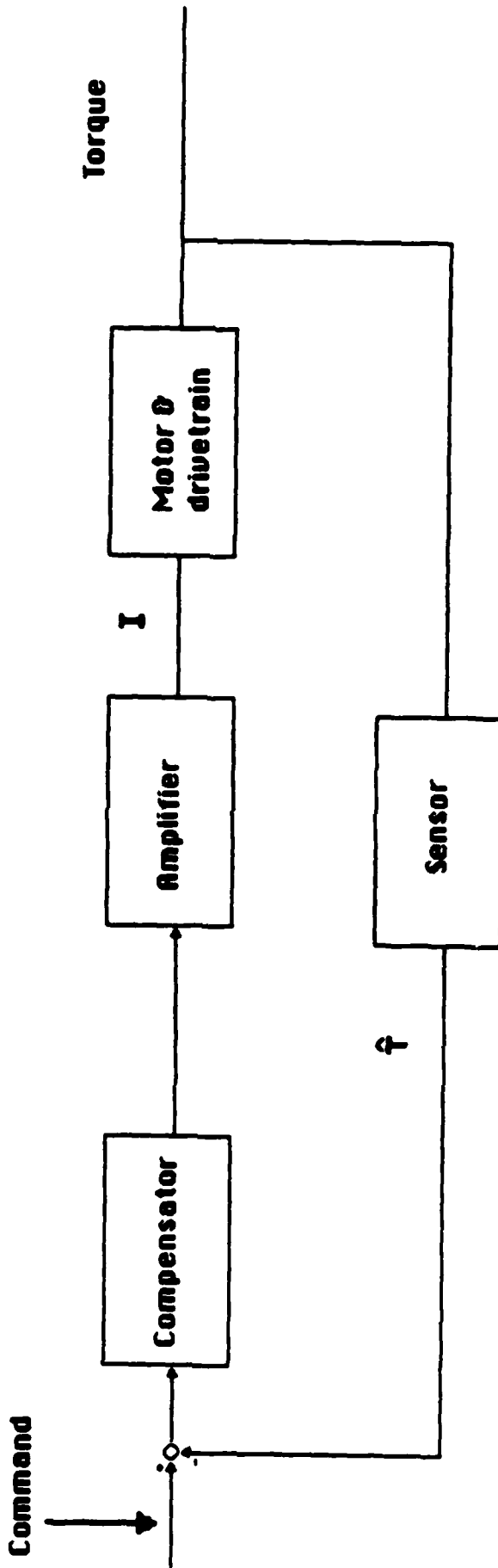
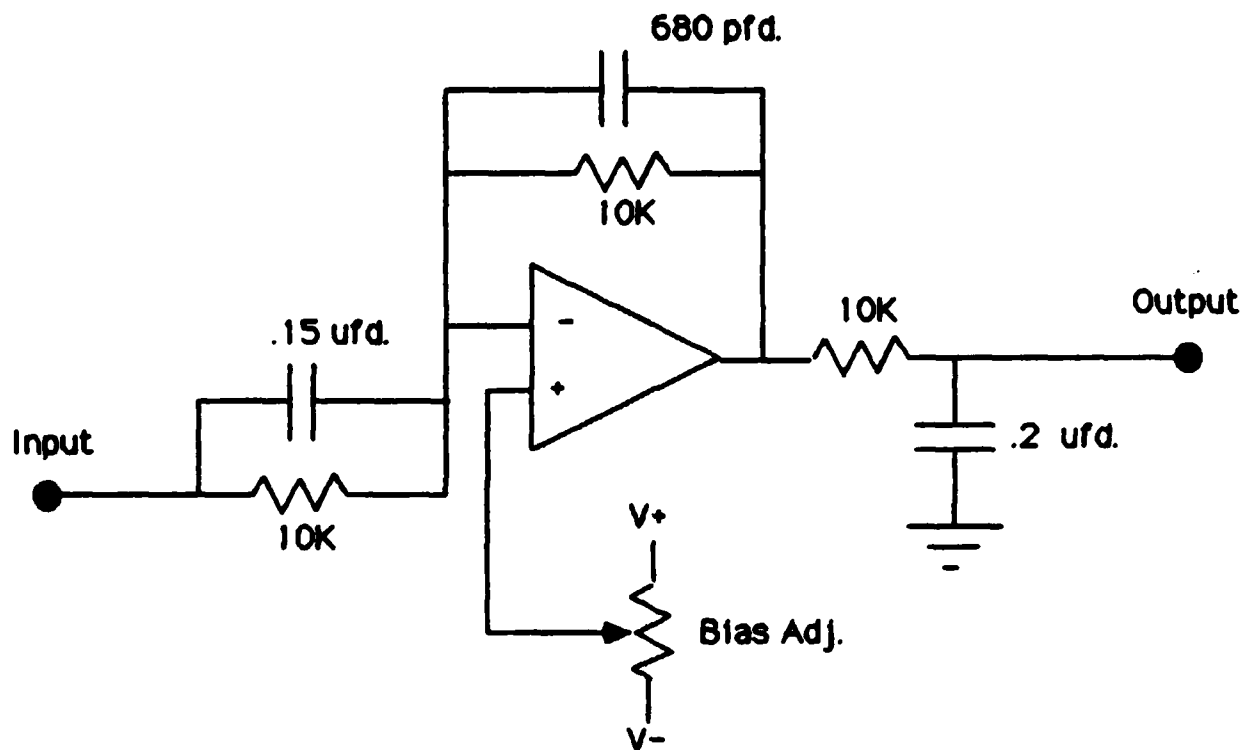
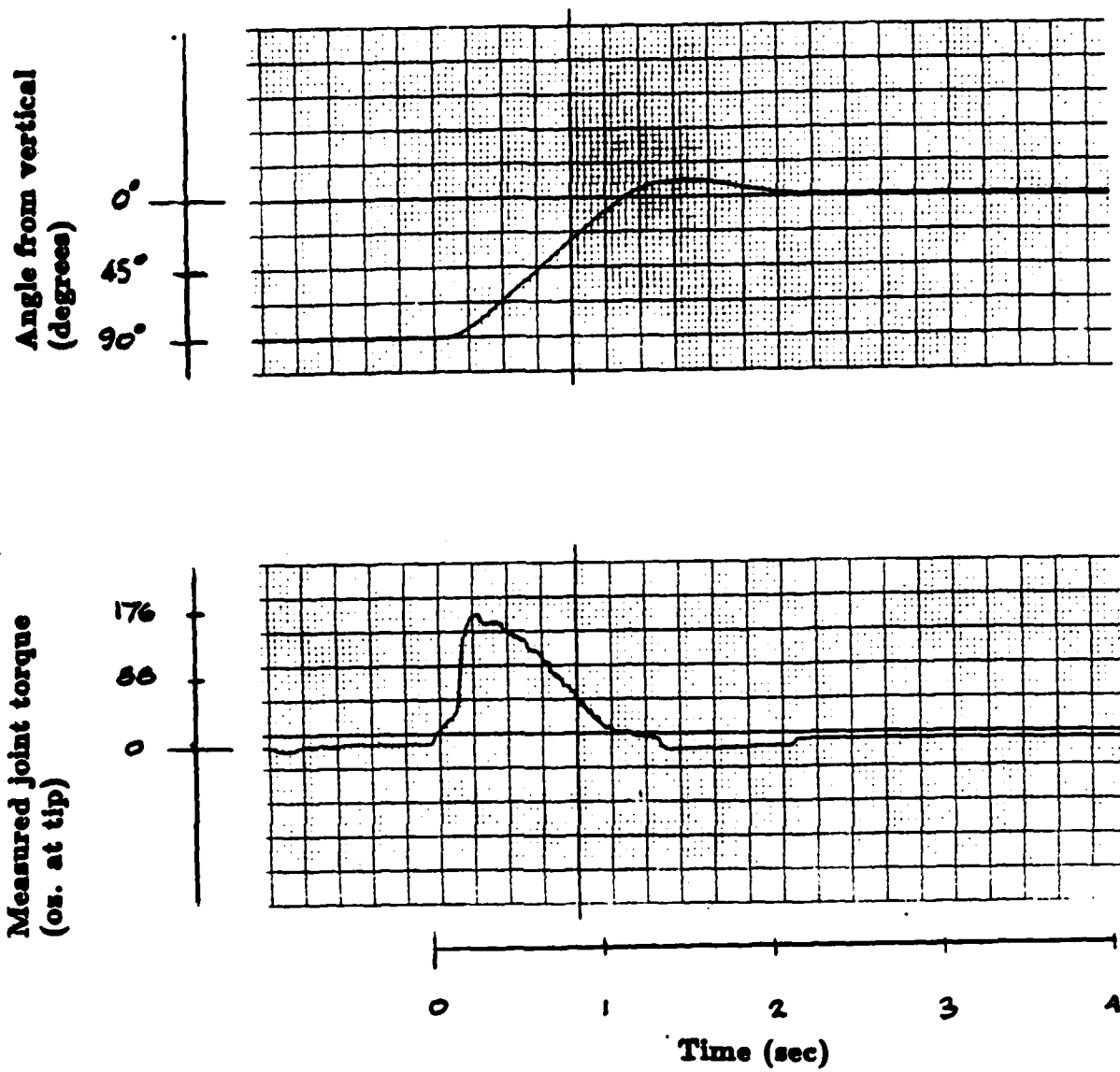


Figure II-33. Block diagram of joint torque feedback system. Note that the drivetrain separates the actuator (motor) from the sensor.



**Figure II-34. Lag-lead compensator schematic used for joint torque feedback on PUMA 500.**



**Figure II-35.** Time response of the experimental joint torque control system to a step change (sudden removal of hand supporting link 3 horizontally.) The system regulates the joint torque back toward zero, with a steady state error comparable to the sensor resolution. Note the initial linear trajectory of error angle, which indicates that voltage saturation was the limiting factor.

should be emphasized, because of their impact on future robotic control systems, especially those in which flexibility plays a role.

First, the individual sensors can be made to resolve torque about the axis of interest, and be insensitive to other loads, to a few percent, with available technology. Additionally, the sensor need not have the resolution or linearity required of an endpoint sensor in order to improve response significantly. Nor does the control system even need to attempt the decoupling of the small sensitivities to other loads. The outer position or force loops will correct for these imperfections, at small cost in performance. The acceptability of the approximate decoupling (which can easily be built into low cost sensors) is very important because it eases the implementation of fast inner loops. Being able to make good use of imperfect sensors means that simple strain gauge based sensors, with easily manufactured geometry can be employed; this is essential if we wish to apply this technique to a large number of joints. Being able to avoid resolving sensor data into joint axis components via software saves a tremendous amount of computation in a feedback loop whose main purpose is high bandwidth control. Resolving data into components about joint axes implies explicit matrix multiplication or equivalent calculation, in addition to forming the resolving matrix, which itself involves significant kinematics. Matrix multiplication, although a simple operation to represent in equations, takes the order of  $N^3$  operations, for  $N \times N$  matrices, the same, essentially as matrix inversion (Ref. 10). These reasons are the keys to the feasibility of using analog or fast digital inner joint torque control loops.

The analysis and the experimental results show that these techniques can dramatically improve the performance of existing robot control systems. The benefits are broader in scope than reduction in friction, although this is significant given the magnifying effect that gearing has on actuator friction. The inner loop can accommodate and stabilize drive train flexibility, as well as variations in actuator performance e.g., bias, drift, and ripple torque. These characteristics ease the restrictions on the design of outer control loops, permitting the designer to achieve greater performance without sacrificing stability or robustness. The overall impact is to make possible robotic systems with both increased ability and applicability.

## SECTION II-6: TECHNOLOGY ASSESSMENT

Section 4.1.8 calls for an assessment of the technology required to develop lightweight arms that use end-point control. That assessment is provided in this section, with additional material on the means to drive these technologies forward and induce industry to use them.

There are three basic technological areas that are crucial to the development of lightweight, high performance robots:

- Low mass, sensor based design.
- Dynamics and control techniques and tools.
- High speed computation.

These areas are broad in scope, ranging from analytical techniques to sensor hardware to computer software. Such diversity calls for differing approaches both to drive it forward and to induce industry to take full advantage thereof. These three areas, and approaches to accelerate their adoption, are presented in the order given above.

The current practice in robot and automated design reflects its origins in fixed automation and in CNC machine tools. An underlying philosophy of these fields has been to make the mechanism precise and to do little (if any) sensing and feedback. This approach has limited the abilities of today's robots and cannot serve as the basis for the high performance automation we need to develop. The next generation of robots must incorporate low mass, sensor based design. Sensor based design means a system approach that is based on the measurement of relevant physical quantities about the robot and the robot's environment. A sensor based robot can employ feedback principles to correct for changes in the robot's and the environment's behavior. Sensor based design and feedback control can achieve greater precision even when used with a flexible mechanism. This ability to work well with the compliance inherent in all mechanisms means that such designs can use lighter structure. Lightweight mechanisms can be faster, carry more payload, use less power, and be more deft.

The two driving forces behind low mass, sensor based design are clearly sensors and lightweight mechanisms. Sensor needs are assessed first:

Sensor based design requires the development and availability of sensors that measure the relevant physical quantities — not merely those quantities that are convenient to measure using traditional sensors and placements. Since the robot most often does its work with some tool(s) at its tip (endpoint), the relevant measurements are of endpoint quantities, such as position velocity, force, and proximity. There are two basic challenges that sensor technology must overcome: the geometric difficulties in endpoint sensing and the multi-dimensional (vs. scalar) nature of the measurements.

The geometric complexities of endpoint sensing are consequences of the same kinematic freedom and versatility that make robots useful. Position and velocity measurements usually require straight line access between the endpoint of the robot and some fixed reference points. The freedom of movement of the robot presents the sensor system with

occlusion, range and orientation problems that must be addressed by multiple reference points and intelligent use thereof. The principal quantities of interest (position/orientation and force/torque) are multidimensional quantities. With such vector measurements come the challenges of decoupling and calibration.

Position sensing may be accomplished by passive (vidicon or CCD camera) or by active (time-of-flight or relative orientation from active beacons). The passive approach — vision systems — shows great ultimate promise. Passive systems have the potential capability to recognize a variety of types of objects in addition to the robot, and measure the spatial relationships among the whole group. Vision systems do not yet operate at sufficient speed to be the sole endpoint position sensor for a robotic system. Advances in processing speed and in vision algorithms are needed. For basic endpoint sensing, only sparse position/orientation information is needed, rather than scene/object recognition; active sensing techniques can provide this. Thus the two techniques complement each other and should be developed in parallel.

### **Lightweight Mechanisms**

There must be fundamental changes in the design methodology of robotic mechanisms. Current attempts to build extremely stiff, perfectly repeatable, mechanisms will not significantly increase robotic accuracy on their own. Even advances such as composite materials will not remedy the situation without sensing. Backlash and play could not be completely removed from joints, bearings, or power transmissions even assuming infinitely stiff and strong materials. Robot designers must accept some level of flexibility (and backlash) and trade these characteristics off against mass, power, and speed. This compromise must be performed with endpoint sensing in mind, as sensor capability dictates how much mechanical imperfection can be compensated.

Sensor based design shines when the robot is designed to take full advantage of what it offers. A conventional mechanism, with its heavy structure, will still be limited in speed and payload, no matter what sensors and control system are retrofitted to it. New robots must use lightweight structural designs, more like aircraft than like locomotives. Thin walled shell structures, which achieve high stiffness to mass ratios (in bending and torsion) are essential. Constant strength designs, which place structural material only where it is needed, will be more efficient than simple, constant cross section structures.

Designs that use more of their finite amount of power to move payload and robot links as opposed to moving heavy actuators will show both higher speed and higher payload capacity for the same power and technology of actuation. Thus robots that can transmit power through their structures will be efficient in the cases where the transmissions are lightweight compared to the actuators they permit to be moved inboard. Mechanical transmissions to meet the requirements for robotics require advancement to meet these needs. Current robots are limited in many cases by the strength and durability limitations of existing mechanical transmissions. Alternatives or improvements to conventional gear technology must be sought. Harmonic drives, tensile tendons, and other transmissions that meet the load/speed requirements of robotics must be developed and made economically attractive alternatives.

Direct drive robots are attractive from the viewpoint of simplicity, but efficient actuators are crucial. Actuators with higher power/mass ratios are needed to make robots that do carry actuators around with them more efficient. This is an alternative to using transmissions to move actuators inboard. Some technologies, notably hydraulics and pneumatics are already at the point where they are efficiently deployed outboard. However, the difficulties of control and of managing the supply lines to such devices on an articulated mechanism remain. Semi-direct drive is a promising compromise for electric actuation. Motors designed for efficient operation in the low speed/high torque regimes require lower gear ratios to match them to typical robotic loads. A consequence of this is reduced costs of transmissions, lower forces on transmission elements near the actuator, and less performance degradation due to friction in the actuator. The new technologies of brushless servomotors show promise both in eliminating brush friction, and producing higher specific power ratios due to their superior heat dissipation properties. (Resistive heating is in the outer stator.) New materials are showing a dramatic effect on electric actuator technology. Improved magnetic materials, samarium-cobalt, and more recently, iron-neodymium compounds make possible motors with markedly better performance both in torque and power.

The fundamental advances in dynamics and controls are within sight. Powerful techniques for dynamics and control have recently been developed. These tools already address many of the key problems of endpoint control of robots, and their extension to the remaining problems is underway. Systematic, efficient techniques for deriving the dynamic models for rigid, articulated structures are now available. These include the iterative Newton-Euler method, operational space Lagrangian method, and the generalized speed, generalized force methods of Kane. Computer programs use these methods to derive (or assist in deriving) dynamic models have been developed, but are not yet widely available. These techniques are primarily systems of rigid bodies. As such, they force a user concerned with flexibility to use ad hoc methods to incorporate effects of compliance into the model. These algorithms need to be extended to model flexibility, as well as a wider class of mechanisms. In addition, these computer tools must be made available to designers.

Control theory has made great progress in the basic areas of interest to robotics. Multivariable, optimal, and discrete control theory have both a sound theoretical base and a rapidly growing community of practitioners. New work in robust and adaptive control techniques is underway. Computer tools for analysis, design, and simulation of such systems is experiencing a renaissance, fostered by powerful, tested software in the public domain, particularly the LINPACK and EISPACK libraries, and the OPTSYS/Sandy family developed at Stanford. Additional effort is needed to extend the theory, build the tools, and *disseminate* them.

The use of sophisticated sensors and control techniques requires the rapid accurate computation. There are three areas that are vital:

- Rapid, accurate computation of floating point arithmetic functions.
- Multiprocessing.
- Software development tools.

Robots require rapid arithmetic computations for sensor data interpretation (e.g.,

vision), coordinate transformations, trajectory planning, and for implementing control algorithms. High speed processing, with good accuracy and dynamic range are essential. Specialised hardware or RISC architectures are two differing approaches to these needs, both of which show impressive potential.

Multiprocessing (the use of many processing elements simultaneously) is needed to meet the speed demands of real time control. Multiprocessing can also provide benefits in robustness and growth by partitioning the problem into independent sub-systems that can be tested and/or improved independently. Robot control is particularly well suited to multiprocessing because of its basically linear structure both in time and information flow. This technology must be developed and made available in generic form in order for robot developers to use it.

Software tools are required to increase the productivity of robot developers and to increase the ultimate performance of robots. There are three areas to emphasize.

- High level languages for robotics.
- Real time software.
- Multiprocessing software.

Making these tools widely available will foster the development of high performance robots and automation. With access to these tools, techniques, and technologies, robot developers (and users) can work more productively on their real problems, rather than spending their time "reinventing the wheel."

## REFERENCES

1. Cannon, R. H. and Binford, T. O., "First Annual Report on End-Point Control of Flexible Manipulators," Stanford University, May 1983.
2. Craig, J. J., Introduction to Robotics: Mechanics and Control. Manuscript in preparation for publication. Mechanical Engineering Department, Stanford University.
3. Fearing, R. S., "Simplified Grasping and Manipulation with Dexterous Robot Hands", American Control Conference, San Diego, CA, June 1984.
4. Fearing, R. S. and Hollerbach, J. M., "Basic Solid Mechanics for Tactile Sensing", IEEE Robotics Conference, Atlanta, GA, March 1984.
5. Franklin, G. F. and Powell, J. D., Digital Control of Dynamic Systems. Addison-Wesley Publishing Co., Inc. Reading, Ma., 1980.
6. Katz, P., "Selection of Sampling Rate for Digital Control of Aircrafts," Ph.D. Thesis, Department of Aeronautics and Astronautics, Stanford University, SUDAAR No. 486, September 1974.
7. Luh, J. Y. S., Fisher, W. D. and Paul, R. P. C., "Joint Torque Control by a Direct Feedback for Industrial Robots," IEEE Transactions on Automatic Control, January 1983.
8. Maples, James, "Force Control of Robotic Manipulators with Structural Flexibility," Ph.D. Thesis, Department of Electrical Engineering, Stanford University, June 1985.
9. Schmits, E., "Experiments on the End-Point Position Control of a Very Flexible One-Link Manipulator," Ph.D. Thesis, Department of Aeronautics and Astronautics, Stanford University, SUDAAR No. 548, June 1985.
10. Strang, G., Linear Algebra and Its Applications, Academic Press, New York, 1976.

DATE 82 Jun 08

## APPENDIX A

## STATEMENT OF WORK

## End Point Control Flexible Robots

- 1.0 **OBJECTIVE:** The objectives of this program are two-fold: first, to significantly increase the speed and precision of performing "slew and touch" tasks by a flexible robot arm and second, to develop a universal robot end effector, capable of performing generic manipulation functions.
- 2.0 **SCOPE:** The Part I effort involves the development and integration of precision end point sensing and control techniques with advanced robot arm designs for greater speed and precision in accomplishing slew and touch tasks.

The Part II effort involves the development of an intelligent, dexterous hand. The hand shall be integrated with a robot arm and be able to perform the following: secure grasping, repositioning of objects, sensitive force control, and fine motion.

3.0 **BACKGROUND:**

- 3.1 Remote manipulator and robotic systems are rapidly emerging in many roles. Spurred by the dramatic decrease in computational costs, industrial robots are becoming commonplace in large-volume assembly lines and will be assuming more functions every year, as labor rates continue to increase. Versatile remote manipulators will be desperately needed for such hazardous-environment operations as ship-board nuclear power plants, undersea work, and operations in space.
- 3.2 Today's manipulator systems tend to be massive and ponderous: in industrial applications, manipulators weighing tons are required to transport and position parts and tools weighing a few pounds. Industrial robots are designed to be strong enough and stiff enough to ignore loads. They are therefore costly in the materials used to make them, the space they take up, the power they consume, and the time they require to do simple operations.
- 3.3 The underlying generic limitation of today's manipulators is that they effect position control by "dead reckoning": the computer is told the coordinates of the desired position, and the manipulator system is moved by controlling the angle of each link relative to the previous one. Dead reckoning requires that flexure in the structure of the manipulator and compliance in the drive trains be minimized. Consequently, the practice has been to make robotic arms much stiffer than required to merely support the payload--they must support it, even at full extensions, while not bending more than a few thousandths of an inch. Drive systems (gears or belts) must also be made very stiff. Of equal importance, dead reckoning cannot tolerate any inaccuracies in the placement of the parts to be handled. This gives rise to the need for very precise part fixtures for most tasks.

F33615-82-K-5108

PREVIOUS PAGE  
IS BLANK

- 3.4 In the few instances where some accommodation has been made for inexact part placement, the usual strategy is to slew to the area of the target and then continue at a low terminal velocity until contact is made. With today's ponderous and inflexible arm designs, this leads to large contact forces unless the terminal velocity is kept extremely low.
- 3.5 The required advancements will develop the technology for stable control of a flexible robot arm using end-point sensing. Current practices involve the application of torque at one end of a series of links, based upon feedback from the other end. Flex in the series tends to make the system inherently unstable.
- 3.6 To date, the growing computer power available for robots has been used to handle kinematic relations of increasing complexity, while problems of dynamics and flex have been solved by simply making the members extremely stiff and heavy. The ability to develop control techniques that tolerate flex in a manipulator's mechanical structure, will allow the use of such flexible arms and will have many desirable consequences: manipulators can be lighter and faster, safer to use, less prone to damage from collisions, require less power to run and cost less to construct.
- 3.7 An emerging requirement for applying robots cost effectively is the use of versatile, intelligent hands. One picture of the use of robots is that they will have a great variety of special end-effectors, hands in the form of special tools, and that they will function by quick-change of tools. This is the viewpoint of hard automation, relevant for volume production, but not adequate for the needs of general robot capabilities. Versatile grippers with sensing to grasp a variety of tools provide a capability to use simple, ordinary tools under sensory control. The tool-changing approach limits robots to expensive tools which must be engineered at considerable expense to include sensing and instrumentation, together with ingenious, effective, and reliable quick-change connectors. The time required for changing tools has been found to be an important parameter in test assemblies and in analyses of assembly.
- 3.8 End effectors able to perform generic, modular functional tasks can be integrated to span a broad spectrum of applications. These generic capabilities are: 1) tool using; 2) parts acquisition; 3) parts handling; and 4) parts mating. Research and Development has focused on six degree of freedom arms with hands of two parallel jaws without servo control. While arm designs require great future evolution in design, a pressing issue is to utilize current arms to their limits. Hands capable of great dexterity are important to fully realize this goal.

F33615-82-K-5108

**4.0 TECHNICAL REQUIREMENTS:****4.1 Part I. End Point Control of Flexible Robotic Arms.**

4.1.1 (Task 1). Develop a minimum-time algorithm for "slew and touch" which shall be capable of the following:

4.1.1.1 Directing a highly flexible (0.5 Hz), one degree of freedom, robotic arm, through a fast, large angle motion toward a target object.

4.1.1.2 Target object shall be contacted without pause in the motion of the robotic arm.

4.1.1.3 For a given allowable force level, the velocity with which the arm can contact the end-point will be increased by a factor of ten(10).

4.1.1.4 Tolerable time delays in system response shall be identified.

4.1.1.5 Required bandwidths for system components shall be defined.

4.1.2 (Task 2). Develop control system and precision end point sensor suitable for testing control system.

4.1.2.1 Position sensors, such as X-Y photodetectors, shall be developed to provide gross position determinations.

4.1.2.2 Force sensors, such as strain gauge equipped "fingers" shall be developed for fine position determinations. Possible use of proximity sensors shall be investigated.

4.1.2.3 The sensors shall be integrated into a control system and optimized to provide precision end-point sensing in conjunction with Task 1.

4.1.3 (Task 3). Investigate New Robotic Arm Designs.

4.1.3.1 New arm designs shall be optimized for decreased weight and increased terminal velocity.

✓ 4.1.3.1.1 An arm design with a minimum of two revolute joints shall be investigated.

4.1.3.1.2 Impulse forces imparted to the target object shall be minimized.

✓ 4.1.3.1.3 Methods of adding flexibility to the arm shall be investigated.

✓ 4.1.3.1.4 The impact of mass distribution on arm response shall be investigated.

F33615-82-K-5108

- Investigations shall be made of the implications of extending the arm design from paragraph 4.1.3.1.1 to have a minimum of three revolute joints such that the arm achieves cartesian positions within its spherical envelope.
- 4.1.3.1.5
- 4.1.3.2 Inherent limits to operation time for performing a "slew and touch" task shall be investigated and characterized.
- 4.1.4 (Task 4). Develop Control Algorithms.
- 4.1.4.1 Algorithms shall be developed to allow for smooth switching between control modes, (i.e., gross control vs. fine control), while the arm is in motion.
- 4.1.4.2 The algorithms shall be capable of sophisticated slew and and touch control of the arm designs from Task 3.
- 4.1.5 (Task 5). Task Integration.
- 4.1.5.1 Develop a demonstration plan for Government approval in accordance with Sequence 7 of Atch #L DD Form 1423. The plan shall include a schedule and an outline of the necessary tasks for demonstrating that the system fulfills the performance goals of the program.
- 4.1.5.2 Develop task software that will coordinate the position/force data with control algorithms to execute the Demonstration Plan.
- 4.1.6 (Task 6). Functional Assessment.
- 4.1.6.1 The feasibility of integrating the developed end-point control system with a robotic arm shall be demonstrated.
- 4.1.6.2 Apply control system in functional tasks. Assess results and correct problem areas.
- 4.1.7 (Task 7). System Demonstration.
- 4.1.7.1 Set-up and conduct the approved demonstration plan, from Task 5, with the integrated end-point control system. The demonstration shall include, but not be limited to, the following:
- 4.1.7.1.1 Increased speed of robot arm in performing "slew and touch" tasks.
- 4.1.7.1.2 Increased positional precision over "dead reckoning" controlled arm.

F33615-82-K-5108

4.1.7.1.3 Capability for performing "slew and touch" tasks with delicate and heavy objects.

4.1.8 (Task 8). Assess the technology required for developing light weight robotic arms, requiring less power to operate, and utilizing the developed end-point control system.

4.2 Phase II. Skilled Hand Development.

4.2.1 (Task 1). Design, construct and implement a three finger, nine degree of freedom robot hand.

4.2.1.1 Hand design shall concentrate on performance and dexterity.

4.2.1.2 The hand shall be able to perform the following generic manipulations:

4.2.1.2.1 Secure grasping

4.2.1.2.2 Repositioning of objects (translation and rotation)

4.2.1.2.3 Sensitive force control

4.2.1.2.4 Fine motion

4.2.1.3 The hand shall be readily interfasciable with a robot arm and control system.

4.2.2 (Task 2). Develop and implement tendon motor control loops.

4.2.2.1 Feedback shall be provided by tendon force sensors which shall determine the torque at joints and the forces on the bearing at each joint.

4.2.2.2 Tendon controller shall ~~include feedthrough terms~~ to remove steady state errors due to friction, and to compensate for dynamic forces or nonlinear effects, such as Coulomb Friction.

4.2.3 (Task 3). Implement existing force and tactile sensors, and/or develop new sensors for use on fingertips, inside of fingers and on the palm.

4.2.4 (Task 4). Develop and implement preliminary single finger control subsystem.

4.2.4.1 Subsystem shall transform target fingertip position/force data into desired fingertip force control signals.

- ✓ 4.2.4.2 A demonstration of the single finger control subsystem shall be performed at the contractors facility.
- 4.2.4.2.1 Demonstration shall show capability of controlling finger stiffness and force.
  - 4.2.4.2.2 An assessment of control subsystem performance shall be made and problem areas corrected.
- 4.2.5 (Task 5). Develop and implement interactive finger(hand) control subsystem.
- 4.2.5.1 The coupled control of finger shall be mathematically represented.
    - 4.2.5.1.1 The representation shall relate finger-tip forces to external forces on the object and internal grasp forces. The representation is specified by the relationship between object grasp points and desired center of compliance, and shall be computed at least once for a given grasp.
  - 4.2.5.2 Develop a simplified object model.
    - 4.2.5.2.1 This model shall be able to estimate, from data provided by sensors integral with the hand, both local surface curvature and orientation and gross surface curvature and orientation.
  - 4.2.5.3 Subsystem shall use the grasp representation and a simplified object model to compute (the interdependent) desired fingertip control signals from specified object position and compliance.
  - 4.2.5.4 Demonstrate the developed hand.
    - 4.2.5.4.1 Demonstration shall show the capability of the hand to perform simple grasping tasks and the ability to control individual finger stiffness and force.
    - 4.2.5.4.2 An assessment of the hand performance shall be made and problem areas corrected.
- 4.2.6 (Task 6). Investigate technology required to extend hand capabilities beyond tip pretension manipulation.
- 4.2.6.1 Investigation shall focus on the ability of the hand to reorientate grasped objects.

F33615-82-K-5108

4.2.6.2 Kinematics of hand design shall be optimized.

4.2.7 (Task 7). Software development.

4.2.7.1 Software shall be developed in a manipulator language for programming and describing hand tasks.

4.2.7.2 Develop performance goals and task specifications, representative of sensor estimates, as geometric constraints and manipulation rules in a system such as ACRONYM.

4.2.8 (Task 8). Integration with vision and range sensing.

4.2.8.1 Techniques shall be incorporated into the developed robot hand system which allows the use of wavelength and reflectivity properties of object surfaces, to achieve vision range sensing.

4.2.8.2 Constant categorization of the sensed image shall be maintained under different ambient illuminations.

4.2.9 (Task 9). System integration and demonstration.

4.2.9.1 Develop a demonstration plan for government approval in accordance with Sequence 8 Atch #1 of the DD Form 1423. Upon approval, the plan shall be implemented and clearly demonstrate that the integrated system of a nine degree of freedom intelligent hand fulfills the performance objectives of Phase II.

4.2.9.2 Assess the technology required to integrate the developed intelligent dexterous hand system to a commercially available robot arm.

## 5.0 ADDITIONAL REQUIREMENTS:

5.1 Environmental Impact. The contractor shall assess the environmental consequences of the technology being developed from the standpoint of the project itself and from the standpoint of potential future scale-up to production size quantities. If the technology turns out to have adverse environmental consequences, the contractor shall provide suggestions for making the technology environmentally acceptable and indicate what impact the suggestions shall have on technology from an economic standpoint.

5.2 Reports, Data and Deliverables as described in Section C, SOW, and the DD Form 1423. All data shall be reported in both English and Metric (SI) units. The English units shall be in parentheses, adjacent to the corresponding Metric (SI) units.

END

10-86

DTIC